# THE BEHAVIOUR OF IONS IN THE PRESENCE OF THE LIQUID-VAPOUR INTERFACE IN HELIUM

Stuart G. Kennedy

A Thesis Submitted for the Degree of PhD
at the
University of St Andrews

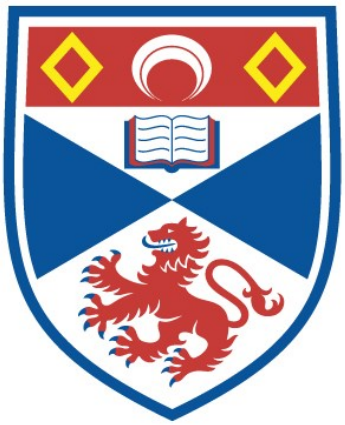

1972

# THE BEHAVIOUR OF IONS IN THE PRESENCE OF THE LIQUID-VAPOUR INTERFACE IN HELIUM

A thesis presented by

Stuart G. Kennedy, B. Sc.,

to the University of St. Andrews

in application for the degree of

Doctor of Philosphy.

## DECLARATION

I hereby certify that this thesis has been composed by me, and is a record of work done by me, and has not previously been presented for a Higher Degree.

The research was carried out in the School of Physical Sciences in the University of St. Andrews, under the supervision of Professor J. F. Allen, F.R.S.

Stuart G. Kennedy

CERTIFICATE

I certify that Stuart G. Kennedy, B. Sc., has spent nine terms at research work in the School of Physical Sciences in the University of St. Andrews under my direction, that he has fulfilled the conditions of the Resolution of the University Court, 1967, No. 1, and that he is qualified to submit the accompanying thesis in application for the Degree of Doctor of Philosophy.

Research Supervisor

ACKNOWLEDGEMENTS

I should firstly like to express my thanks to Professor J. F. Allen for his interest and encouragement while supervising this work.

My thanks are also due to Mr. J. G. M. Armitage for suggesting the project, and for his valuable assistance throughout.

I appreciated the many helpful discussions with members of the Physics Department at St. Andrews, in particular, Dr. P. W. F. Gribbon and Mr. C. S. M. Doake.

I am indebted to Dr. E. M. Wray for designing the circuit of the capacitance level indicator.

Mr. J. McNab was extremely helpful during the design and subsequent construction of the cryostat, and Mr. R. H. Mitchell is to be thanked for providing an ample supply of liquid Helium.

## PERSONAL PREFACE

From 1964 till 1967 I studied at Paisley College of Technology for an external degree from London University. In 1967 I obtained an upper Second Class B. Sc. Honours in Special Physics.

In October, 1968, following the award of an S.R.C. Research Studentship, I started research in the School of Physical Sciences, University of St. Andrews, under the supervision of Professor J. F. Allen. At the same time I was admitted as a research student under Ordnance General No. 12, and in October 1969 I was admitted as a candidate for the degree of Ph. D.

And if the world were black or white entirely
And all the charts were plain
Instead of a mad weir of tigerish waters,
A prism of delight and pain,
We might be surer where we wished to go
Or again we might be merely
Bored but in brute reality there is no
Road that is right entirely.

LOUIS MacNEICE

CONTENTS

ABSTRACT

The thesis is concerned with some of the properties of positive and negative ions in liquid Helium, and in particular with the passage of ions, which are generated inside the liquid, through the free liquid surface into vapour. It was found, for negative ions, that this process was inhibited by an energy barrier, in agreement with other workers who have examined this problem, although there is considerable disagreement as to the magnitude of the barrier. It has been observed in the present work that the energy barrier depends upon the field, the position of the liquid surface in an ion cell, and the nature of the ion cell itself. The dependence of the barrier on these three parameters probably explains why diverse values for it have been reported.

It was originally intended to use the ions as probes to examine dissipation mechanisms in the mobile superfluid Helium film. It had been reliably reported that ions preferentially travelled in the film. This was observed not to be the case however. The negative ion currents in the film were found to be extremely small, when they existed at all, and no real positive ion currents in the film could be detected. This has been interpreted as being due to the combination of the large image potential binding the ion to the substrate, and the intrinsic roughness of the substrate.

The present work has revealed that what appears at first sight to be a current of positive ions crossing the liquid surface can be attributed to a current of photoelectrons due to photoelectric emission from the surface of the collector. Such photoemission can arise from the uv radiation produced largely by ionic recombination in the region close to the α-emitting source. Screening the collector from the direct view of the α-source greatly reduced the photoelectron current.

In order to extend the temperature range available for the study of ion currents, a vortex refrigerator was designed and constructed. This enabled measurements to be extended down to 0.8K. Since there has been only one publication on the vortex refrigerator, which appeared during the building of the present one, its properties and operation with various design parameters were studied in detail.

# INTRODUCTION

The present work began initially as part of an extensive programme on the properties of superfluid Helium films, and in particular the study of dissipation mechanisms in such films. There is growing evidence that dissipation is concerned with the generation of quantised vorticity in films. There was also apparently well-founded evidence that the film could carry quite strong ion currents. Since ions can be trapped by vorticity, it was hoped by this means to determine the location of the vorticity in the films so as to learn more both about ion-vortex interactions and also about how the vorticity is generated and its extent and duration in films.

As the work progressed, it became evident that ions preferred not to travel in films, for reasons which have become reasonably clear. The work therefore changed to a more general study of the mechanism of ion passage across liquid-vapour interfaces.

In order to extend the temperature range available for the study of ion currents, a vortex refrigerator was designed and constructed, which enabled measurements to be extended down to 0.8K. The properties and mode of operation of the vortex refrigerator were studied in considerable detail.

# CHAPTER 1

# THE PROPERTIES OF HELIUM 11

## 1 Introduction

The superfluid nature of liquid Helium 11 was first observed during attempts to measure its viscosity via narrow channel flow by Kapitza (1938) and independently by Allen and Misener (1938). Both investigations found that the flow was extremely non-classical, with a rate of flow largely independent of the driving pressure. If there was a "viscosity" then it must have been less than $10^{-9}$ poise. These observations were at variance with that of Keesom and MacWood (1938) who employed the method of the damping of an oscillating disc immersed in the fluid. They found a strictly classical viscosity, with a value of about $10^{-5}$ poise, or $10^{4}$ times greater than the $10^{-9}$ poise found by Kapitza and by Allen and Misener. Since both observations appeared correct and yet were completely at variance, this posed a serious dilemma. It was suggested by Tisza (1938), and later by Landau (1941) that liquid Helium 11 would have to be described by some fundamentally new hydrodynamics if the dilemma was to be resolved.

## 2 The Two Fluid Model

The similarity between the liquid Helium lambda transition and the phenomenon of Bose-Einstein condensation in an ideal Bose gas was first pointed out by F. London (1938). In an ideal Bose gas, below a certain critical temperature, a finite macroscopic fraction $\alpha$ of the particles condenses into the zero momentum state. This fraction $\alpha(T)$ increases from zero at the critical temperature to

unity at the absolute zero. The condensation process is accompanied by an anomaly in the specific heat, whose shape is not unlike that of the lambda transition in liquid Helium. Furthermore, the condensation temperature for Helium treated as a Bose gas has been calculated to be 3.09 K, which is close to the lambda temperature for liquid Helium of 2.18 K.

Since Helium is even-numbered in the nucleus, the gas should obey Bose-Einstein statistics, and although the liquid state must depart from the condition of an ideal Bose gas, nevertheless the striking similarity between the two specific heat curves and the closeness of the critical temperatures, led London to consider it plausible to assume that the lambda transition in the liquid represented Bose-Einstein condensation.

Tisza (1938) suggested that in the liquid below the transition temperature, the viscosity should be due entirely to the atoms in excited states, while that fraction of the liquid which has condensed into the ground state should show zero viscosity. Such a regime of properties could then explain the apparent discrepancy in viscosity measurements. The appearance of real viscosity in Keesom and MacWood's logarithmically-damped oscillating disc would be due to the "excited" fraction of the liquid, while the pressure independent flow in capillaries would be due to the flow of the inviscid ground state fraction.

Landau (1941) pointed out that in a degenerate Bose gas, since there is no energy gap between the ground state and the lowest excited states, nothing could prevent the ground state atoms from colliding with excited atoms and therefore from experiencing friction. Landau approached the Helium problem more directly by considering that at absolute zero Helium is a quantum liquid devoid of

excitations. At finite temperatures, excitations in the fluid will exist and be characterised by a unique spectrum (which will be described later), which accounts for the superfluid behaviour of the liquid.

Landau suggested that liquid Helium II can behave as an intimate mixture of two fluids, the normal fluid, which contains the excitations, and the background superfluid. The superfluid has density $\rho_s$, velocity $v_s$, viscosity zero, and carries no entropy, while the normal fluid has density $\rho_n$, velocity $v_n$, viscosity $\eta_n$, and carries all of the entropy. The total liquid density $\rho$ is then given by

$$\rho = \rho_n + \rho_s,$$

and the total momentum density J is given by

$$J = \rho_s v_s + \rho_n v_n.$$

The relative density of the normal fluid $\rho_n/\rho$ decreases from unity at the lambda point to zero at the absolute zero, while that of the superfluid increases from zero at the lambda point to unity at the absolute zero.

The contradiction in viscosity is thus understandable by noting that in the narrow channel flow, the normal fluid with finite viscosity will be locked to the walls, while the superfluid fraction can flow without friction; whereas in the oscillating viscometer, the disc will experience a drag due to the presence of the normal fluid .

Although Landau has stated that "liquid Helium has nothing to do with an ideal gas", it appears well established that the lambda

transition in liquid Helium 4 is some form of Bose-Einstein condensation. This is convincingly demonstrated by comparing the liquid with Helium 3, which obeys Fermie-Dirac statistics, and which shows no comparable transition. Penrose and Onsager (1956) have shown that even in an interacting Bose gas, a condensation still occurs, but the fraction $\alpha(T)$ no longer tends to unity at the absolute zero. The fraction can be quite small if the interactions are strong, and in liquid Helium it is probably about 0.1. It is therefore not strictly correct to equate $\rho_s$ with $\alpha(T)$.

Landau has stressed that the two fluid model is no more than a convenient method for describing phenomena occurring in liquid Helium 11, and has emphasized there can be no real division of the liquid into two parts.

## 3 The Excitation Spectrum

The dispersion relation (energy E versus momentum p) for the elementary excitations in liquid Helium 11 was predicted by Landau (1941 and 1947). He considered that the low lying excited states, where the wavelength of the excitations is greater than the interatomic spacing, represent collective motions of the atoms of the liquid. Such excitations represent sound waves or phonons, with energy $E = pc$.

At higher energies, where the wavelength of the excitation is of the order of the interatomic spacing, the dispersion curve exhibits a characteristic minimum. Excitations in the region of this minimum were given the name of rotons by Landau after a suggestion by I. E. Tamm. In this region the energy is given by

$$E = \Delta + \frac{(p-p_o)^2}{2\mu},$$

where $\Delta$ is the roton excitation energy and $\mu$ the effective roton mass. Since it requires a non-vanishing energy of $\Delta$ to create a roton, and since this energy is greater than kT for superfluid Helium, the number of rotons per unit volume $n_r$, will be given by the Boltzmann factor

$$n_r \propto e^{-\frac{\Delta}{kT}} \qquad (1)$$

The number of phonons per unit volume $n_p$, at a temperature T, is given by

$$n_p \propto T^3.$$

A theoretical approach to the excitation spectrum has been given by Feynman (1954 and 1955). From a series of physical arguments relating to the microscopic motion of the particles of the liquid, he has shown that the only low lying excited states must be phonons, in agreement with Landau, and has deduced a trial wavefunction for the excited states. From this wavefunction Feynman has been able to express the energy of the system as

$$E(k) = \frac{\hbar^2 k^2}{2m\, S_o(k)},$$

where the function $S_o(k)$ is the liquid structure factor. (The liquid structure factor is the Fourier transform of the ground-state function). Thus from an empirical knowledge of $S_o(k)$, obtained from X-ray or neutron scattering, Feynman has derived the form of the excitation spectrum proposed by Landau, though with not very satisfactory numerical agreement in the region of the minimum.

Feynman's wavefunction for the excitations has the flaw that it prescribes that all the particles move in the same direction and lacks the return flow required to conserve current.

Feynman and Cohen (1956) found that the introduction of backflow results in a reduction of the energy of an excitation, and were able to construct a trial wavefunction which does conserve current, and from which the excitation spectrum could be deduced. The form of this spectrum is in good agreement with that proposed by Landau. Feynman and Cohen suggested that it should be possible to detect the presence of elementary excitations and the form of the excitation spectrum in Helium 11, by experiments on the inelastic scattering of slow neutrons in the liquid. The experiment has been carried out by several groups of workers (see Wilks 1967 Chapter 5), all of whom have verified the spectrum given by Landau (1947). The parameters characterizing the minimum in the curve are found to be

$$\frac{\Delta}{k} = 8.65 \text{ K} \qquad \frac{p_o}{\hbar} = 1.91 \text{ Å}^{-1}.$$

4 Superfluidity

According to Landau (1941), superfluidity and the concept of "critical velocity" result from the form of the dispersion relation via the following argument.

If the fluid at T = 0K. moves with some velocity v, then it can only slow down by the creation of elementary excitations at the walls, and this is only possible if

$$v > \left|\frac{E}{p}\right|_{\text{min.}}$$

Now in a free particle spectrum, where $E = p^2/_{2m}$, the value of $\left|\frac{E}{p}\right|$ min. is vanishingly small, while in liquid Helium II the Landau spectrum gives a value of $\left|\frac{E}{p}\right|$ min. of about 200 m. $sec^{-1}$ for phonon creation, or 60 m. $sec^{-1}$ for roton creation. This implies a superfluid critical velocity of at least 60 m. $sec^{-1}$. The observed critical velocities, however, are considerably smaller than this, being a few 10's of cm. $sec^{-1}$ at most. To account for such low velocities another type of excitation must be sought.

It was first suggested by Onsager (1949) and later independently by Feynman (1955) that macroscopic vortex excitations with low energy and large momentum might exist in Helium II in addition to the phonons and rotons proposed by Landau, and that the vortex circulation should be quantized in units of h/m. Feynman has shown that the quantization condition follows from the form of the wavefunction for the flowing superfluid at absolute zero. This will be described later. Feynman has pointed out that while a nonviscous classical fluid will flow turbulently at any finite velocity this is not possible in liquid Helium II. This is because in order for turbulence to appear in the superfluid its velocity must give rise to sufficient kinetic energy to create one quantum of vorticity. Feynman has calculated the minimum velocity which will create one quantum of vorticity in a channel diameter of $10^{-5}$ cm. and has obtained the value of 100 cm $sec^{-1}$. This result is only about a factor of two greater than the observed critical velocity in such a channel.

## 5 The Condensate

The characteristic feature of all superfluids is the macroscopic occupation of a single quantum state. The resulting condensate part

of the superfluid can then be described by a wavefunction $\psi$, where

$$\psi(r,t) = a\,(r,t)\; e^{\,i\,\phi\,(r,t)} \qquad (2)$$

The amplitude a and phase $\phi$ are real functions of position, and the condensate is in the state with momentum $\hbar\,\nabla\phi$. If this momentum does not vary too quickly with position, then the superfluid velocity $v_s$ will be given by

$$v_s = \frac{\hbar\,\nabla\phi}{m} \qquad (3)$$

This is not a rigorous definition of $v_s$ since it has not been shown to be a real particle velocity. However if the flow is uniform then $v_s$ will be given by (3) as the whole condensate will be in a state with particle momentum $mv_s$. The irrotational flow of the superfluid then follows from (3).

In superfluid Helium, $\psi$ is often referred to as the Order Parameter. ("An order parameter is the symmetry element characterising a second order phase transition" - Keller 1969 chapter 7.) It is to be noted that $\psi$ is complex, and since the condensate wave function must be single-valued, the phase of the order parameter can only change by some multiple of $2\pi$ when one returns to the same point in the superfluid; that is

$$\oint (\nabla\phi)\cdot dr = n\,2\pi\,.$$

$$\text{or} \quad \oint v_s \cdot dr = n \cdot \frac{h}{m}, \qquad (4)$$

and we have the condition that the circulation is quantized in units

of $h/_m$, as suggested by Onsager (1949) and shown by Feynman (1955).

Evidence for the validity of the quantization of circulation in Helium II has come from the experiments of Vinen (1961) and Whitmore and Zimmerman (1968), where the circulation about a thin wire, stretched along the axis of a rotating cylinder in the liquid, has been directly measured.

The quantization of circulation has also been convincingly demonstrated from the experiments of Rayfield and Reif (1963), who measured the dependence of the velocity on the energy of charged vortex rings in the liquid at low temperatures. They found that the vortex rings which had trapped an ion in their cores had a circulation equal to $h/_m$.

# CHAPTER 2

# IONS IN LIQUID HELIUM

## 1 Introduction

Ions were first produced in liquid Helium by Gerritsen (1948) in order to test the theory of Kramers (1952) on the ionization and extraction of ions from α particle tracks. Williams (1957) was first to measure the ionic mobility, though his results are for very high field strengths and he found the mobility to vary approximately as $E^{-1/2}$. Meyer and Reif (1958) performed the first measurements of the low field mobility, and found it to be field-independent for fields up to about 200 v/cm. They confirmed that below the lambda point the ions are scattered by the normal excitations of the fluid, and showed that the mobility of the positive ion is about 50% greater than that of the negative ion.

In the past decade considerable work has been done on the properties of ions in superfluid Helium, notably the behaviour of ions in rotating Helium II where the interaction of ions and vortices can be studied, (see Donnelly (1967) chapter 6). It is found that, unlike the positive ion, the negative ion can be easily trapped by vortex lines, and that the binding energy of the negative ion to the vortex line is much greater than that for the positive ion.

Mobility measurements of ions in Helium II under pressure reveal that as the pressure is increased, the positive ion mobility falls, while that of the negative ion initially rises until it reaches almost the positive ion mobility, and then falls again, like the positive mobility.

It might be expected, since both the positive and negative ions

are different from the uncharged $He^4$ atoms, that they should behave in a similar way as $He^3$ solute atoms, but the differing properties of the two ions do not confirm this expectation. This caused considerable initial speculation regarding the structure of the two ions. The currently accepted models are fairly well confirmed, although the magnitudes of the two important parameters, namely the radius and the effective mass, have not yet been directly measured.

## 2 Structure

### (a) The Positive Ion

Atkins (1959) has shown that the diffusion coefficient of the positive ion is about 100 times smaller than the diffusion coefficient of $He^3$ in dilute mixtures of $He^3$ in $He^4$. There must therefore be a fundamental difference between the positive ion and a $He^3$ atom. Atkins has also shown that the strong electric field due to the charge of the ion polarizes the liquid in its vicinity, and the resultant polarized atoms experience a net force directed towards the ion, such that the immediate liquid is compressed round the ion.

Assuming that the liquid may be treated as a continuum down to microscopic size, and that macroscopic relations such as the equation of state are valid at this level, Atkins has calculated the liquid density as a function of distance from the charge, and has shown that there should be a solid core to the ion with a radius of 6.3 Å at 1.25 K, and an excess density outside this core falling off as $r^{-4}$.

The effective mass of this "snowball" model is then the sum of;

(a) the mass of the solid spherical core of compressed liquid,

(b) the mass due to the excess density outside the core, and

(c) the hydrodynamic mass (i.e. half the mass of liquid which is displaced by the sphere).

The sum gives an effective mass of about 100 Helium atoms.

(b) The Negative ion

Due to the Pauli exclusion principle, which prevents overlap of the electron with the saturated closed electronic shell of the Helium atom, there is a strong, short range repulsion between an electron and a Helium atom. Sommer (1964) and Woolf and Rayfield (1965) have measured this repulsive barrier to be about 1.1 ev. That is, an electron must acquire an energy greater than this in order to enter the conduction band of the liquid.

An electron which finds itself immersed in the liquid can effectively eliminate its large repulsive energy with the liquid if it surrounds itself with a cavity from which the liquid is excluded. This "bubble" model has been shown by Jortner, Kestner, Rice, and Cohen (1965) on theoretical grounds, to be much more stable at liquid densities than any delocalized state, (i.e. free electron), and that as the density is lowered, a transition should occur from the localized bubble state to the free electron state. Mobility measurements in helium vapour by Levine and Sanders (1967), and more recently by Harrison and Springett (1971), have shown that such a transition does occur.

The radius of the bubble may be estimated by minimizing the total energy of the bubble with respect to the radius. The total energy of the ion may be written as the sum of;

(a) the kinetic energy of the electron confined in a spherical square well of depth $V_o$, (where $V_o$ = 1.1 ev.),

(b) the surface energy of the bubble, ( $\gamma$ is the surface tension), and

(c) the volume work required to form the bubble against the surrounding pressure P.

Thus $$E = \frac{h^2k^2}{2m_e} + 4\pi R^2\gamma + \frac{4}{3}\pi R^3 P.$$

where k is the solution of $k \cot kR = -(k_o^2 - k^2)^{1/2}$, and R may be estimated from $\partial E/\partial R = 0$.

The radius so obtained is found to be approximately 16 Å, and this model also has an effective mass of about 100 Helium atoms.

# CHAPTER 3

## THE VORTEX REFRIGERATOR

### 1 Introduction

Following the discovery of the fountain, or thermomechanical effect by Allen and Jones (1938), where a temperature gradient along a narrow channel gives rise to a flow of liquid towards the warmer end, Tisza (1938) predicted the inverse effect, where forced flow through a narrow channel should cause heating at the entrance and cooling at the exit. This is the mechano-caloric effect, and was first observed by Daunt and Mendelssohn (1939) and later by Kapitza (1941).

A thermodynamic explanation of the thermomechanical effect was first advanced by H. London (1938) who deduced a relation between the pressure difference $\Delta P$ arising from a temperature difference $\Delta T$ along a narrow channel. The relation is,

$$\Delta P = \rho S \Delta T, \qquad (1)$$

where $\rho$ is the liquid density and S is the entropy per unit mass of the liquid. Equation (1) is only valid when the channel is so narrow that only the nonviscous superfluid fraction, carrying zero entropy, can flow in it; that is, when the narrow channel is what is known as a superleak.

Kapitza (1941) carried out extensive measurements on the mechano-caloric effect, and observed that for a given pressure head, the temperature difference obtained across a superleak increases as the bath temperature falls. He suggested that considerable temperature differences should be obtainable in this way, and that

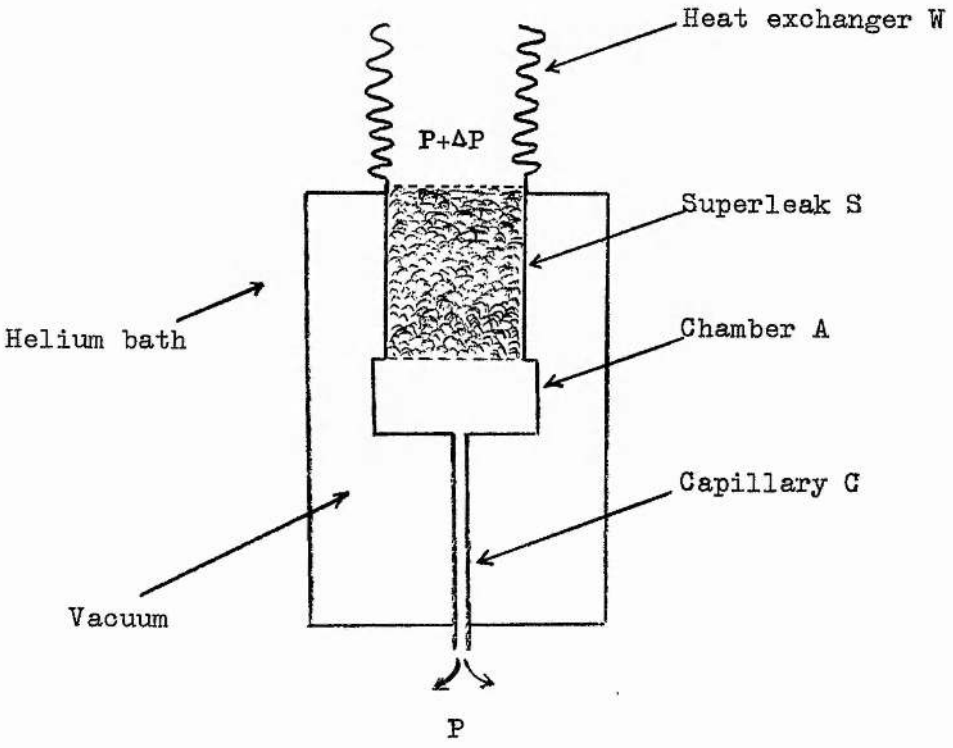


Heat exchanger, superleak, chamber and capillary arranged in series.

FIGURE 3.1

the limitations in the method were the attainment of sufficiently low bath temperatures and the efficient pumping of the liquid through the superleak. He further suggested that the mechano-caloric effect should make it possible "to approach infinitely near to absolute zero".

It was pointed out by Simon (1950), however, that such a cooling system would require a very large number of narrow channels, perhaps as large as $10^{10}$, for the cooling capacity to be comparable with magnetic cooling. This is because the entropy and heat capacity of liquid Helium below 0.1 K are very small compared with the magnetic entropy and energy of a paramagnetic salt.

Although millidegrees might be unobtainable, it was nevertheless interesting to consider that by forcing Helium II through a superleak into a chamber, and possibly recirculating it via a capillary, one might produce and maintain temperatures considerably below 1 K.

Olijhoek, Van Alphen, De Bruyn Ouboter and Taconis (1967) first experimented on the combination of a superleak, chamber, and capillary arranged in series, as shown schematically in figure 3.1. At this time they were interested in the mechanism of superfluid flow and dissipation, and were not concerned to produce a refrigerating device. In figure 3.1, an overpressure $\Delta P$ at the top end of the superleak S, causes superfluid to flow through the superleak into the chamber A below, and out through the capillary C. Since the normal fluid is retained in the top chamber W, the temperature there tends to rise. This rise is obviated by keeping it in thermal contact with the bath.

Olijhoek et al measured the temperatures of the chamber, capillary centre, and capillary end next to the bath, as a function of the applied pressure head $\Delta P$ for various bath temperatures.

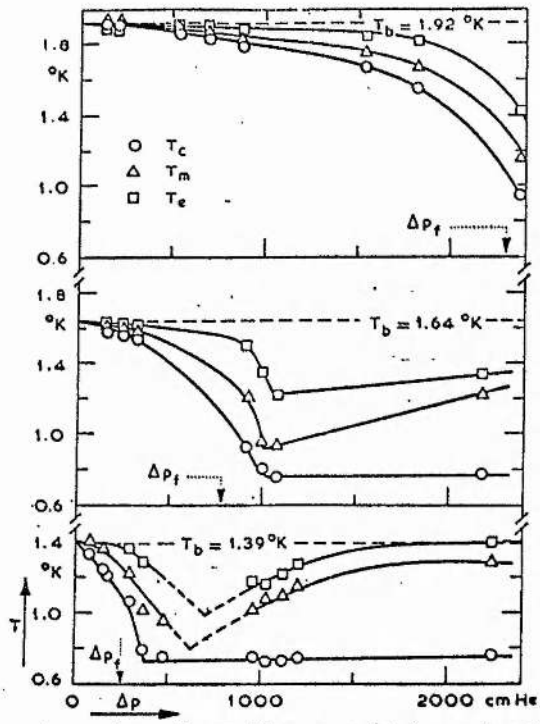


Fig. 2. The temperatures along the capillary measured as a function of the applied pressure.

The results of Olijhoek, Van Alphen, De Bruyn Ouboter and Taconis (1967)

$T_c$ = chamber temperature

$T_m$ = capillary centre temperature

$T_e$ = capillary end temperature

Capillary diameter 0.1 mm

$$\Delta P_f = \int_0^{T_b} \rho S \cdot dT = \text{Total fountain pressure}$$

FIGURE 3. 2

Their results are shown in figure 3.2. It may be seen that the three temperatures initially fell with increasing flow through the system, and that thereafter the chamber temperature remained at a low value while the two capillary temperatures rose again. The largest temperature differences between the bath and the chamber were obtained at the highest bath temperatures, but this required relatively large pressure heads $\Delta P$. The lowest temperature which they obtained in the cooling chamber was 0.73 K, with the bath temperature at 1.39 K, the lowest bath temperature at which they worked.

If the bath temperature is $T_b$ and the chamber temperature is $T_c$, then the temperature difference is determined by

$$\int_{T_c}^{T_b} \rho \, S \, dT = \Delta P - (\Delta p_d + \tfrac{1}{2} \rho_s \, v_s^2) \, . \qquad (2)$$

The left hand side of equation (2) is the fountain pressure due to the temperature difference over the capillary. The term $\frac{1}{2} \rho_s \, v_s^2$ is the Bernoulli pressure which may be neglected. $\Delta p_d$ is the difference between the applied pressure $\Delta P$ and the fountain pressure across the capillary, and is due to dissipation in the capillary caused by the superfluid having exceeded its critical velocity.

It was shown by Vermeer et al (1965) and by Van Alphen et al (1966) that the rate of energy dissipation $\dot{E}$ is given by the product of mass transfer and the difference in chemical potential over the capillary:

$$\dot{E} = \pi r^2 \rho_s \, v_s \, \Delta \mu = \pi r^2 \, v_s \, \Delta P \, . \qquad (3)$$

Dissipation in the capillary must create normal excitations, and

these must be drained away in the turbulent flow due to the pressure difference $\Delta p_d$. That is,

$$\dot{E} = \pi r^2 \rho s T v_n \qquad (4)$$

where $v_n$ is the velocity of the entropy-carrying normal fluid.

From measurements of the flow velocity through the capillary, taken simultaneously with temperature, pressure head $\Delta P$, and equations (3) and (4), Olijhoek et al estimated $v_n$, and then calculated the pressure $\Delta p_d$ required to establish $v_n$ in a capillary of radius r, from the empirical equation of Blasius, which is,

$$Re_p = 4{\cdot}94 \times 10^{-3} Re_v^{7/4} , \qquad (5)$$

where the two Reynolds numbers are given by:

$$Re_p = \frac{\rho r^3}{4\eta_n^2} \overline{\text{grad } P} \qquad (6)$$

$$Re_v = \frac{\rho 2r}{\eta_n} \bar{v}_n$$

Staas, Taconis and Van Alphen (1961) give plausible reasons for using $v_n$ in $Re_v$, and ignoring $v_s$.

Olijhoek et al found that the values of $\Delta p_d$ calculated in this way were in good agreement with the experimental values of the difference between the applied pressure $\Delta P$ and the fountain pressure.

They employed the calculated values of $\Delta p_d$ in equation (2) to calculate the chamber temperature $T_c$ for a given bath temperature $T_b$ and pressure head $\Delta P$, again finding good agreement between experiment and calculation, and concluding that the energy dissipation

(a)

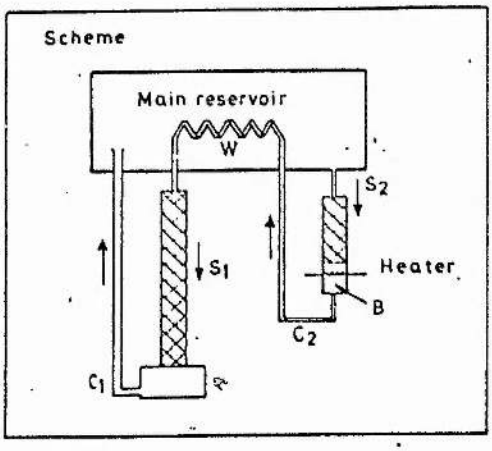


Figure 3. Cooling device without moving parts

(b)

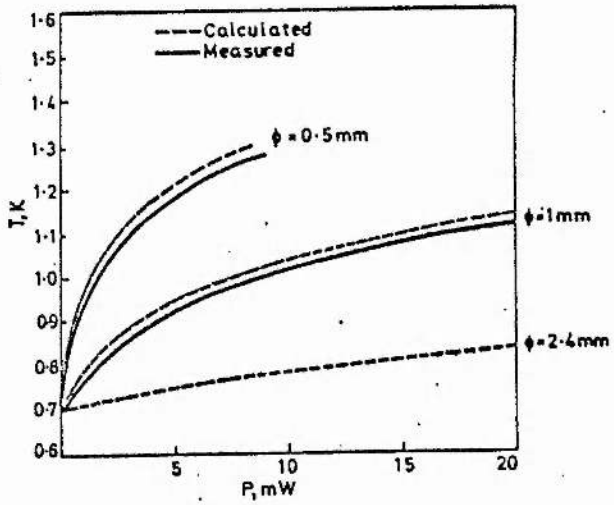


Figure 4. Temperature of chamber A versus heat load in chamber A

The refrigerator and cooling capacity of Staas and Severijns (I969)

FIGURE 3. 3

is uniform along the capillary.

## 2 The Vortex Refrigerator

The extension of the experimental arrangement of Olijhoek et al shown in figure 3.1 into a refrigerating device is due to Staas (private communication) and Staas and Severijns (1969). Staas has called the device a "vortex refrigerator" because it relies for its operation on the creation of vorticity in the capillary C, and the consequent coupling (mutual friction) between the superfluid and normal fluid, such that the normal fluid is drained from the cooling chamber A.

Staas and Severijns, in different versions of the device, employed a mechanical pump of the centrifugal type, and a fountain pump to create continuous flow through the device. The schematic diagram of their refrigerator employing a fountain pump is shown in figure 3.3 (a). It may be seen that applying heat to the chamber B causes a flow of superfluid from the main reservoir or bath through the superleak S2 into this chamber, and a flow of normal and superfluid out of it via the capillary $C_2$, to the heat exchanger W, where the temperature of this high pressure chamber above the superleak S1 is returned to the bath temperature. The pressure difference $\Delta P$ and thus the circulation through the combination of the superleak S1, cooling chamber A, and capillary $C_1$ may therefore be varied simply by varying the amount of heat supplied to the pumping chamber B.

Staas and Severijns have measured the cooling capacity of the fridge chamber A for two fridge capillaries C, of 0.5 and 1.0 mm diameter. The cooling capacity may be defined as the amount of heat that the fridge chamber A can absorb at any given temperature and still be able to hold that temperature. Their results are shown in

figure 3.3 (b). The form of the curves 3.3 (b) and the theoretical operation of the device will be discussed in the next section.

## 3 Theory

Staas and Severijns have shown that the Anderson equation, which relates the gradient of the thermodynamic potential to the motion of vortices, is the important equation describing the operation of the device.

The phase $\phi$ of the order parameter $\psi$ in Helium 11, given by 1 (2), is related to the chemical potential $\mu$ by

$$-\hbar \frac{d\phi}{dt} = \frac{\partial E}{\partial N} = \mu \qquad (7)$$

Anderson (1966) has considered equation (7) to be essential in the understanding of superfluidity because two important contributions may be drawn from it; namely,

(a) If the state of the superfluid is constant in time, then the chemical potential $\mu$ will be constant everywhere.

(b) If there is a finite potential difference $\mu_1 - \mu_2$ between two elements in the superfluid, then $\phi_1 - \phi_2$ must change in time.

Anderson has shown that if there are two points, 1 and 2, in the superfluid with chemical potentials $\mu_1$ and $\mu_2$ then,

$$\overline{\mu_1 - \mu_2} = h \frac{d\bar{n}}{dt}, \qquad (8)$$

where $\overline{\quad}$ is the time average, and $\frac{d\bar{n}}{dt}$ is the average rate of motion of vortices across a path from 1 to 2. Equation (8) is the Anderson relation and implies that a difference in chemical potential, involves

a motion of vortices.

Now the dissipation in a channel is proportional to the number of vortices produced per unit time, and does not depend on the channel diameter, (Keller 1969 chapter 8), therefore the chemical potential will be the crucial quantity in determining the dissipative processes in the superfluid.

Staas and Severijns have considered the equation of motion of the fluid in the light of the Anderson relation as

$$-\nabla\mu = \frac{1}{\rho}\nabla P - S\nabla T - \frac{\rho n}{2\rho}\nabla(\bar{v}_n - \bar{v}_s)^2 + \frac{1}{2}\nabla \bar{v}_s^{\,2} \,.$$

$$= N\,\bar{v}_L \times K \,, \qquad (9)$$

where $\bar{v}_s$, $\bar{v}_n$, and $\bar{v}_L$ (the velocity of the created vortex lines) are averaged over a small volume. N is the number of lines per unit area, and is given by

$$\text{curl } v_s = N\,\underline{K} \,,$$

where $\underline{K}$ is a vector in the direction of the vortex line, and of magnitude $h/_m$. The kinetic terms involving the square of the velocities to the right of equation (9) are small in the flow direction, and may be neglected.

The fountain pump in the refrigerator creates a pressure difference at constant temperature, that is, it creates a difference in chemical potential along the combination of superleak $S_1$, cooling chamber A, and fridge capillary $C_1$. Now the chemical potential is constant along a superleak because there is no motion of vortices therein (by equation (8)), and there can be no dissipation in a

superleak (Van Alphen et al 1966). Therefore, the difference in chemical potential is felt only across the chamber and the capillary, and has the initial effect of driving away the viscous fluid $\rho_n$ through the capillary $C_1$ from the chamber A. That is, in equation (9), since $\nabla T$ is initially zero and the kinetic terms may be neglected, the gradient of the chemical potential is given by $\nabla\mu = \frac{1}{\rho} \nabla P$. However, as soon as normal fluid is being driven from the fridge chamber A, a difference in temperature appears, this is because the entropy per unit volume in the chamber has fallen.

As long as the pumping power is unaltered (and the bath temperature does not vary too much) the difference in chemical potential will be unaltered. Therefore, while a temperature difference gradually establishes itself across the capillary, the pressure difference across it gradually falls; and the fall of $\Delta P$ across the capillary equals the increase of $\Delta P$ (fountain pressure) across the superleak. Eventually the gradient of chemical potential in (9) manifests itself mainly as a temperature difference along the capillary.

The lowest temperature which is obtainable with the device obviously depends on the inevitable heat leak present (see figure 3.3b), but it should not be expected to cool much below 0.7 K, since the motion of vortices in the capillary by equation (8) essentially scatter rotons out of the fridge chamber, and the roton density, given by equation 1 (1), becomes extremely small below about 0.7 K.

Staas and Severijns have calculated the cooling capacity Q for their refrigerator. Q may be described as the heat flow up the capillary from the chamber A which is at a temperature T.

$$Q = \pi r^2 \dot{q} \ , \qquad (10)$$

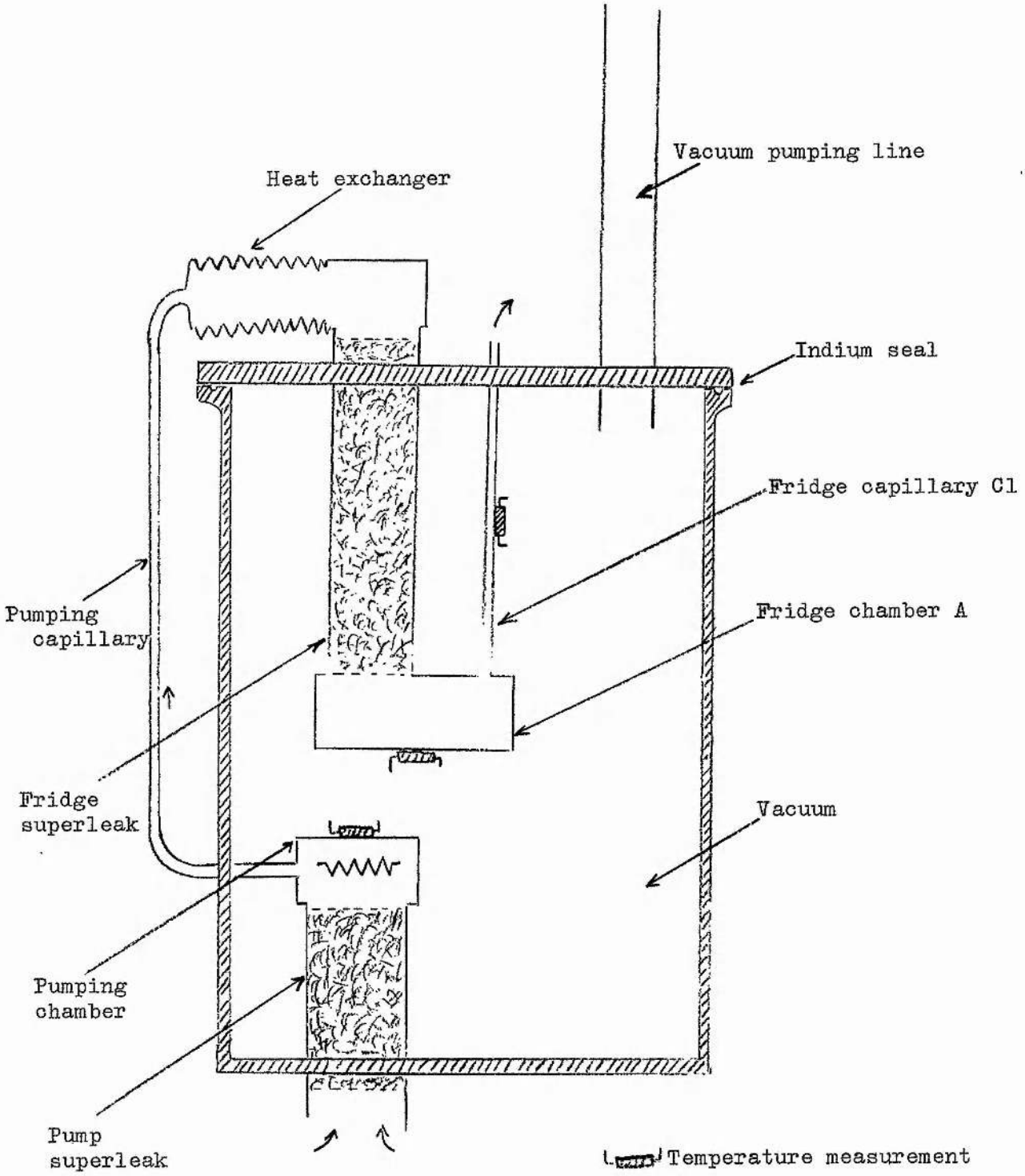


The vortex refrigerator used in the present work.

FIGURE 3. 4

where $\dot{q}$ is the heat flow density in the capillary of radius r; and since entropy is only carried by the normal fluid,

$$\dot{q} = \rho \, s \, T \, v_n \, . \tag{11}$$

For turbulent flow in a capillary, we may describe the dependence of the velocity on the pressure gradient by the empirical equation of Blasius given by (5) and (6), and where grad P in equation (6) is given by

$$\text{grad } P = \rho \int_{T_c}^{T} S \, dT \, , \tag{12}$$

where $T_c$ is the lowest temperature obtainable with zero heat input, that is when $Q = 0$.

Using equations (5), (6), (10), (11) and (12), Staas and Severijns have shown that the cooling capacity Q is given by the equation

$$\frac{\rho^2 r^3}{4\eta_n^2} \int_{T_c}^{T} S \, dT = 4.94 \times 10^{-3} \left( \frac{2Q}{\pi r \, \eta_n S T} \right)^{7/4} , \tag{13}$$

and assuming $T_c = 0.70$ K, they have calculated Q between the temperatures of the bath and 0.70 K, and have recovered the experimentally measured form of the curves shown in figure 3.3 (b).

## 4 Experimental

In the version of the vortex fridge employed in the present work, the operation of the combination of a superleak S1, chamber A and capillary $C_1$, as shown in figure 3.4, was studied with various sizes of refrigerator capillary $C_1$. Flow through this combination was

Poiseuille's Law. The velocity of flow through a cylindrical tube, radius $a$, length $L$, is given by $V = \frac{\pi P a^4}{8\eta L}$ where $P$ is the pressure difference and $V$ the flow (volume per second). If kinetic energy of the emergent fluid is allowed for by putting the effective pressure drop

$$p = P - \rho V^2 / \pi a^4.$$

1. The energy spectrum is such that He-II consists of a "background" phase (superfluid) plus an excited (higher-energy) phase (normal fluid). At the absolute zero the entire liquid is superfluid; as the temperature is raised, excitations appear, the density of which depends only on temperature. Formally we can describe these two phases and normal phase respectively. If the "ordinary" density of the liquid is $\rho$, then

$$\rho_s + \rho_n = \rho$$

Also $\rho_s = \rho$ $\rho_n = 0$ $T = 0°K$

$\rho_s = 0$ $\rho_n = \rho$ $T = \lambda$ point $(T_\lambda)$

Apart from these limits, the exact form of $\rho_n/\rho$ or $\rho_s/\rho$ as a function of temperature remains, at the moment, undetermined

2. The viscosity of superfluid is zero. It is also energetically at absolute zero, i.e its entropy is also zero. Contrariwise, the normal fluid possesses both viscosity and entropy.

If we consider the flow to possess no irreversibilities and hence are able to apply the second law, then the heat current will be

$$\dot{q} = \rho S T v_n \qquad \text{cal/cm}^2\text{sec}$$

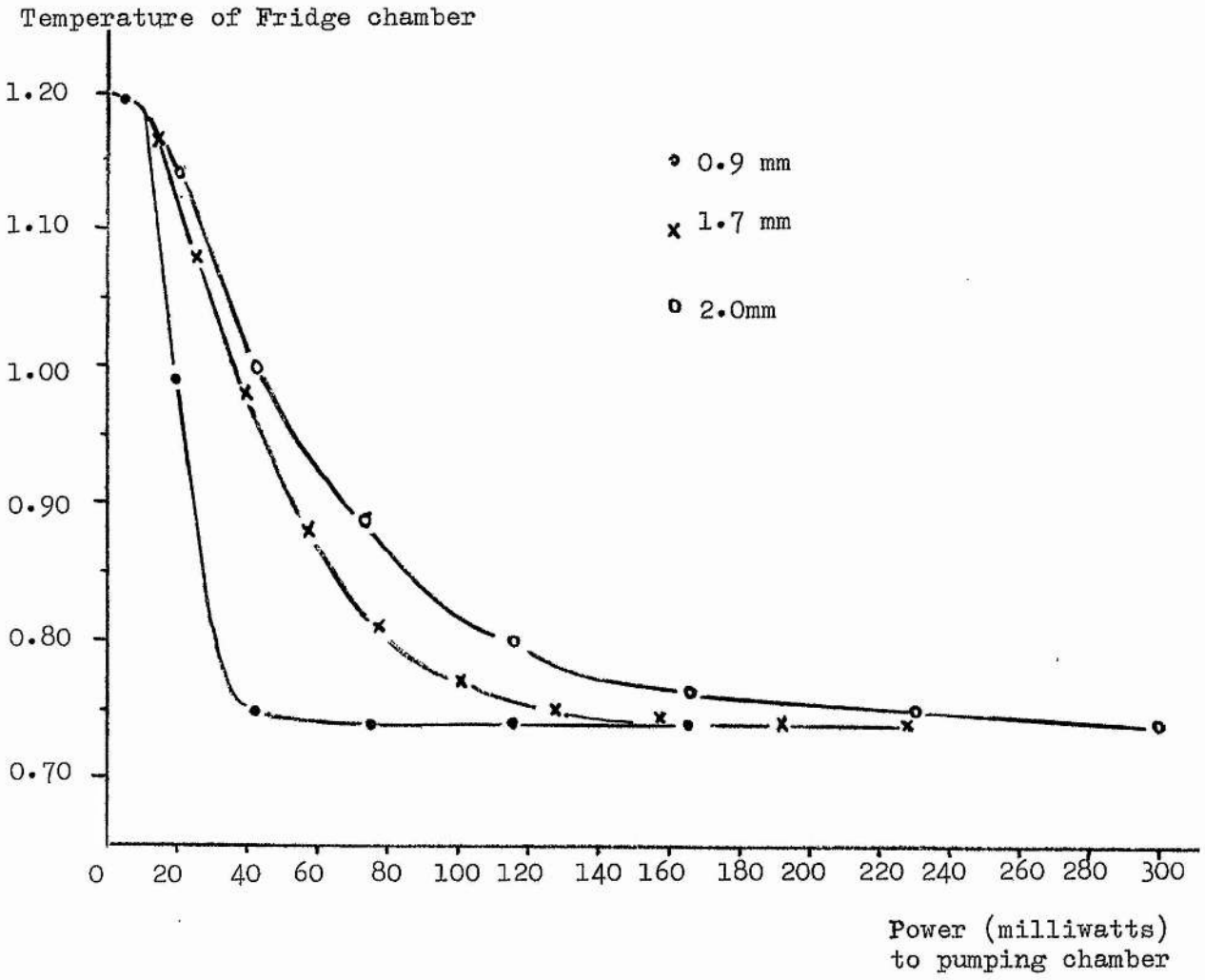


Fridge temperature versus pumping power for various fridge capillary diameters.

FIGURE 3. 5

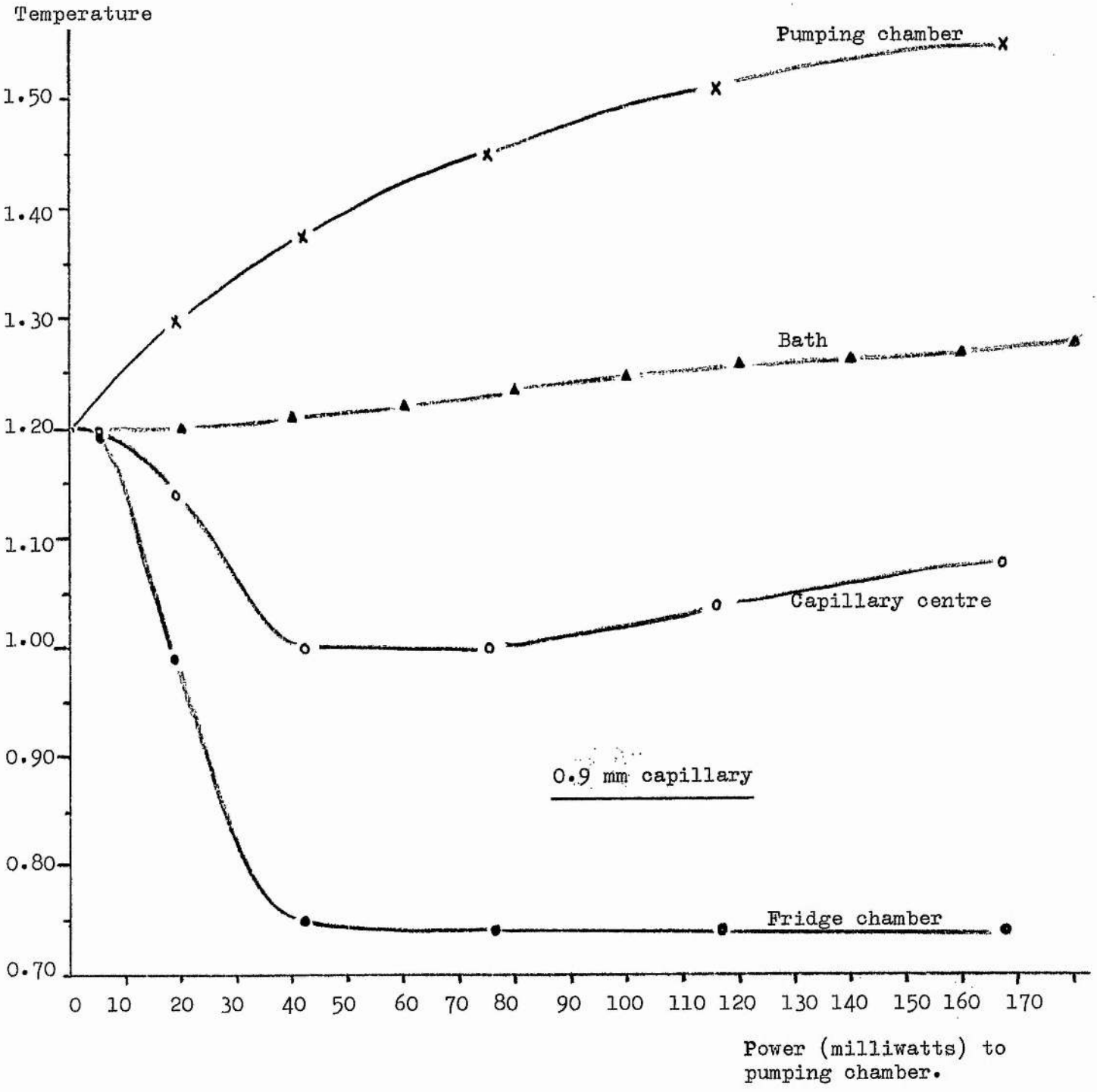


Temperatures at various points in the refrigerator versus pumping power.

FIGURE 3. 6

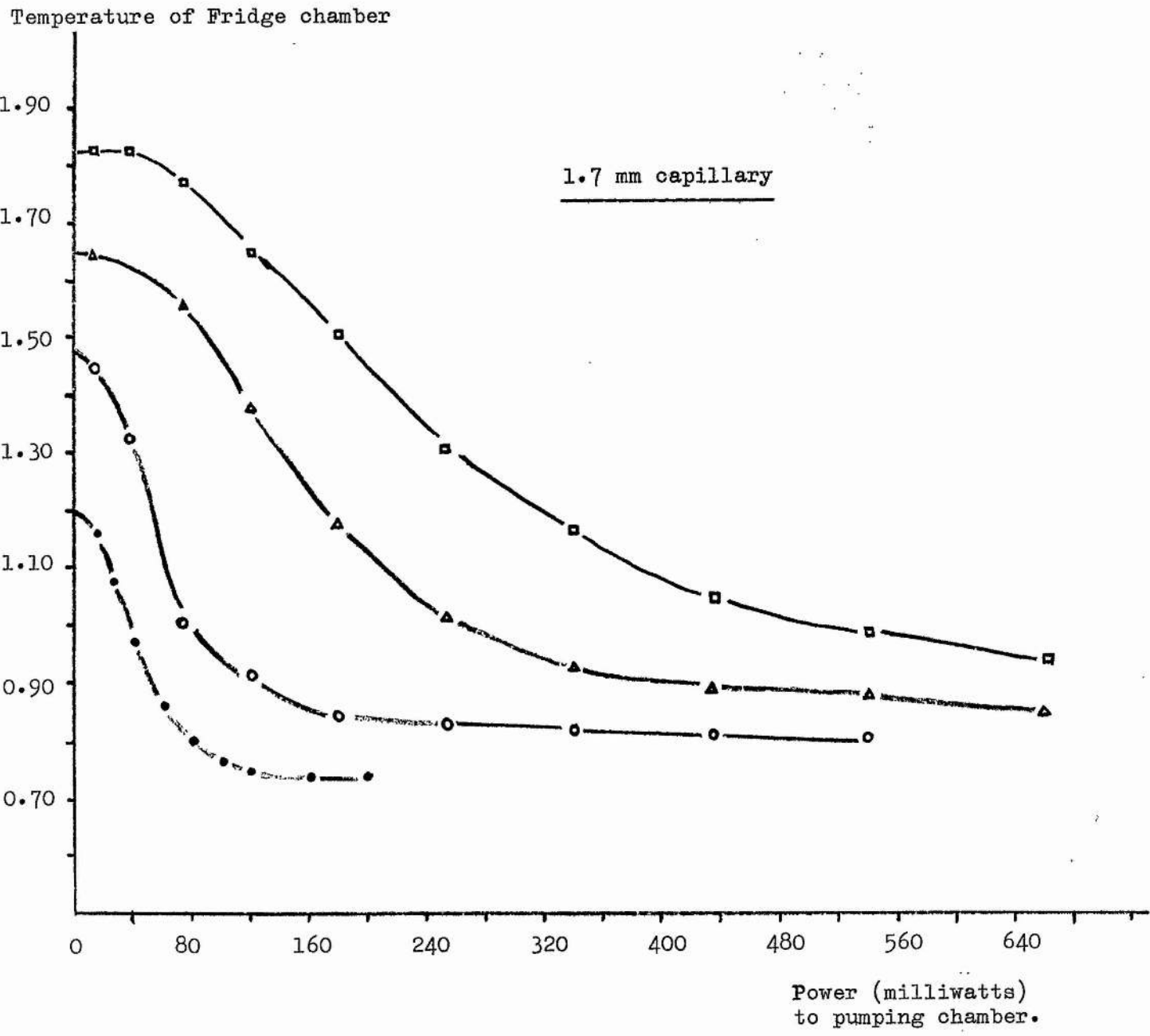


Fridge chamber temperature versus pumping power at various constant bath temperatures.

FIGURE 3. 7

effected by fountain-pumping from another superleak and capillary as shown.

The temperature of the fridge chamber as a function of the power input to the pump, is shown in figure 3.5 for three different capillary sizes, with the bath temperature held at 1.20 K. It may be seen that the lowest temperature reached by the fridge chamber is almost the same for all three capillaries, but that greater pumping powers are required to produce this as the capillary size increases.

The temperatures of the fridge chamber, capillary centre, pump, and bath, were also measured as a function of the power input to the pump chamber, and the results for the 0.9 mm diameter capillary at the bath temperature of 1.20 K are shown in figure 3.6. It may be seen that the variations of temperature of the fridge chamber and capillary centre, are in good qualitative agreement with those of Olijhoek et al, as shown in figure 3.2.

It can be seen in figure 3.6 that the bath temperature increased slightly with increasing pump power. This was because 1.20 K, the starting temperature in figure 3.6, was the lowest temperature to which the bath could be reduced with the large backing pump in the absence of fountain pump heating; consequently, when heat was applied to the pump chamber and dissipated in the heat exchanger, the bath temperature rose slightly, due to the backing pump's inability to cope with it.

Figure 3.7 shows the fridge chamber temperature as a function of the power input to the pump for various constant bath temperatures, for the 1.7 mm diameter capillary. These results are also in good qualitative agreement with those of Olijhoek et al, in figure 3.2. In the present apparatus, the final temperature reached by the fridge chamber for the higher bath temperatures of 1.83 K and 1.65 K, was

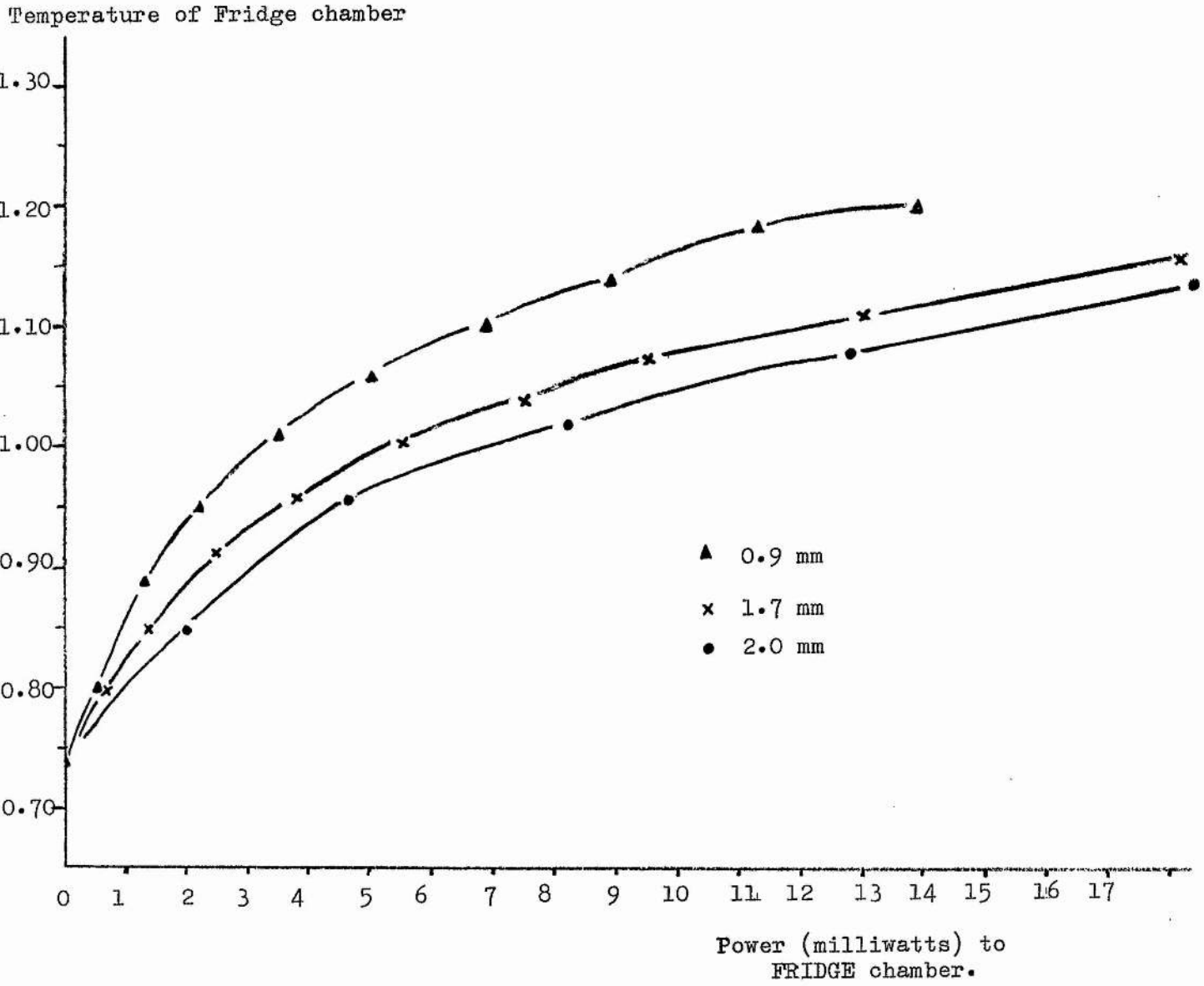


Cooling capacity of the refrigerator.

FIGURE 3. 8

somewhat unstable, while at the lower bath temperatures it was not. From the point of view of stability rather than temperature drop, one can say that the device is more efficient at the lowest bath temperatures.

The cooling capacity of the fridge chamber has been measured for different capillaries. This was done by applying sufficient power to the pump chamber for the fridge chamber to reach its lowest temperature, then applying heat to the fridge chamber and observing its subsequent rise in temperature. The results are shown in figure 3.8, and are in qualitative agreement with those of Staas and Severijns shown in figure 3.3 (b). The latter researchers would appear to have made a more efficient device than the present one, in that the cooling power of their fridge for a comparable capillary size is better.

At a given temperature between that of the bath and the lowest attainable temperature of the fridge, the greatest cooling capacity is obtained with the largest diameter capillary. However, as is seen in figure 3.5, the larger capillaries required larger pumping powers, and in terms of experimental usefulness, e.g. run duration, this is undesirable. For the device to be practical, therefore, a balance must be sought between the heat pumped into the bath, and the cooling capacity demanded of the refrigerator. For this reason, the 1.7 mm diameter capillary was used in the present research. The more detailed geometry and experimental techniques will be described in the next chapter.

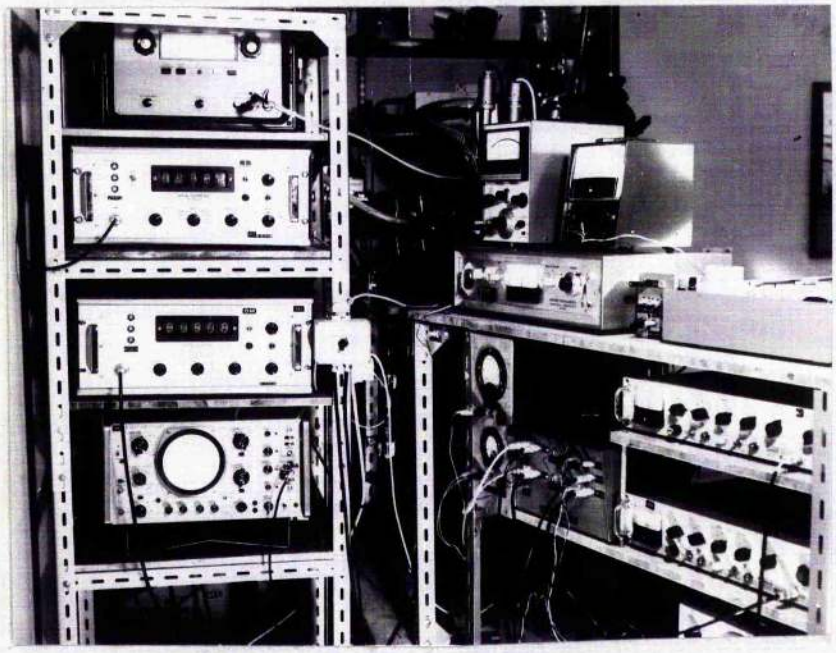

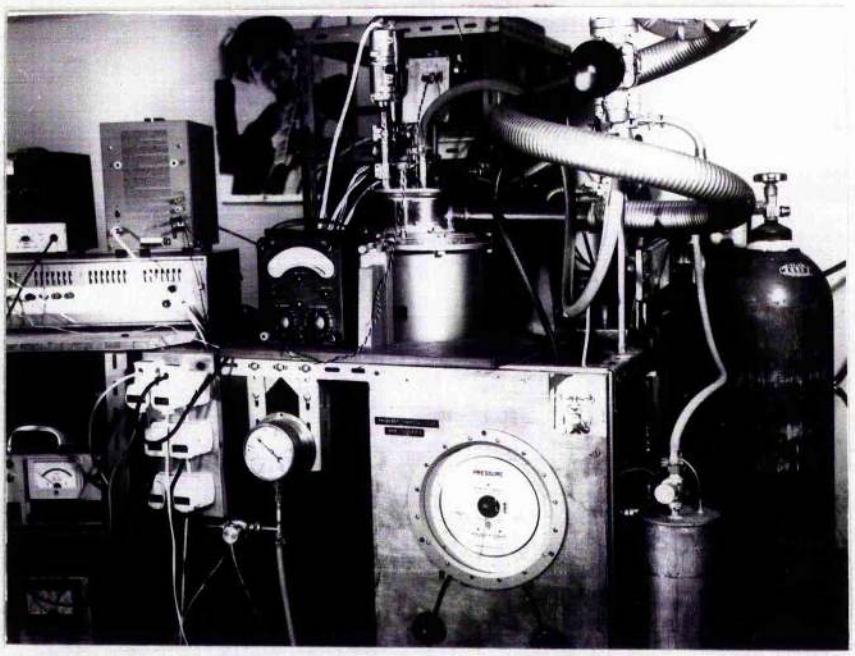

FIGURE 4.1 (a)

# CHAPTER 4

# THE APPARATUS

## 1 The Cryostat Assembly

The cryogenic part of the apparatus was housed in an Oxford Instruments stainless steel dewar mounted on a concrete antivibration mounting. The cryostat was capable of holding about 15 litres of liquid Helium and, with a boil-off rate of about 0.2 litre $hr^{-1}$, was thus able to hold the experimental region at temperatures below the lambda point for more than two days.

A photograph of the apparatus is shown in figure 4.1 (a).

## 2 The Vortex Refrigerator

The mode of operation of the refrigerator has already been described. The arrangement of fridge and ion chamber which was used in the present work is shown in figure 4.1.

The fridge capillary was of stainless steel, 1.7 mm in diameter, while the pumping capillary was 2.0 mm in diameter. The diameter of the pump capillary is not critical so long as the pump can supply the flow rates demanded by the fridge capillary.

The geometry of the refrigerator was such that the pump drew in Helium from the bottom of the dewar. This gave the longest possible running time of the fridge, and it also allowed the superfluid trapped between the superleaks to empty by gravity back through the pump superleak at the end of a run.

The fridge and pump superleaks were made from 14 mm and 16 mm diameter stainless steel tubes respectively. The length of the pump superleak is not important, but the length of the fridge

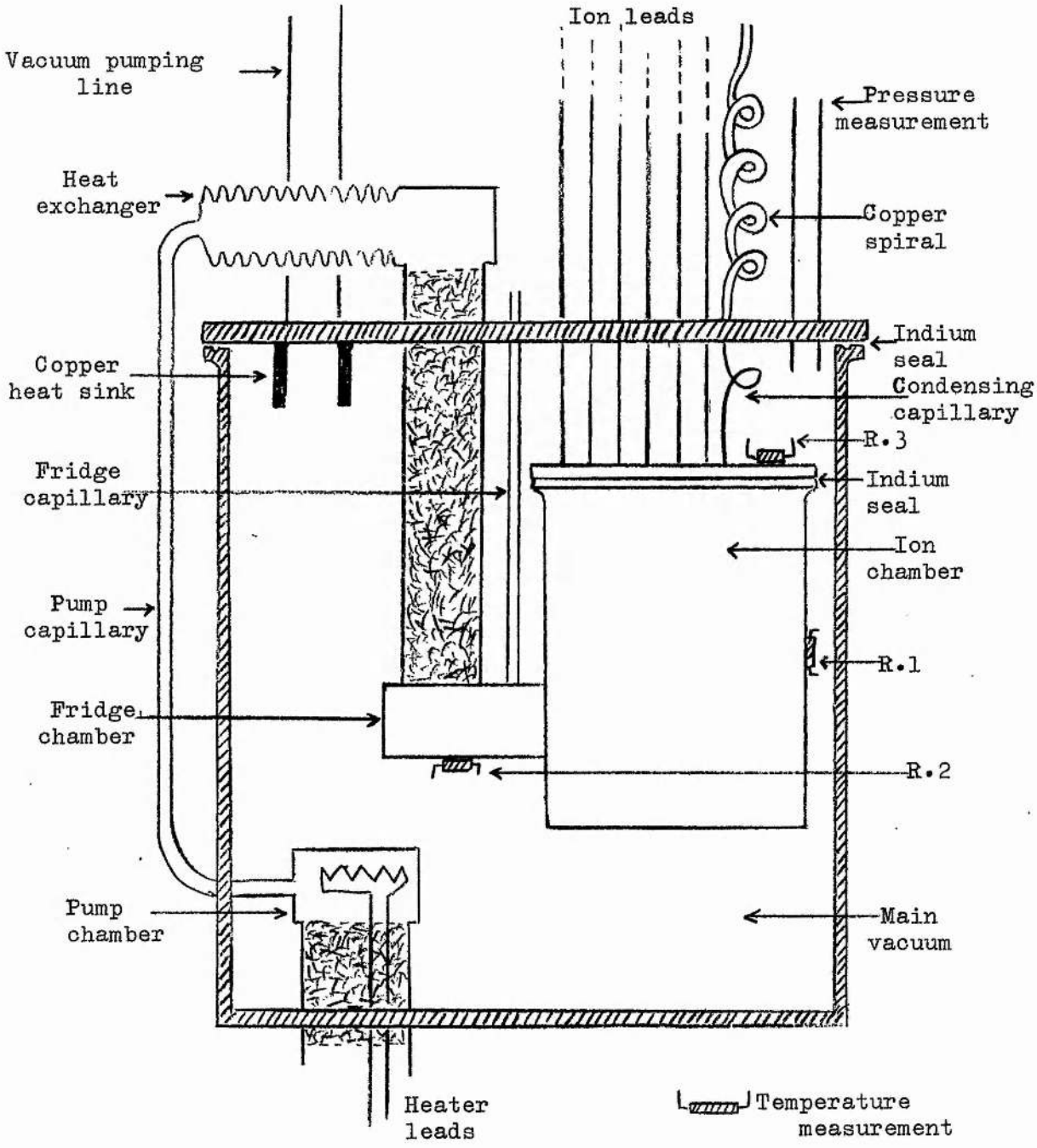


The cryogenic part of the apparatus.

FIGURE 4. 1

superleak, 10 cm, must be such that the heat conduction through the stainless steel walls and the material of the superleak to the fridge chamber is small.

The material of the superleaks was jeweller's rouge. Some carborundum powders were tried during the early work with the fridge but were not very satisfactory. Rouge binds very strongly to the tube into which it is hammered, and thus prevents normal leakage. Flow rates were measured through various grades of jeweller's rouge, (obtained from Canning Ltd., Glasgow), but no difference was observed.

The method of applying heat to the pump chamber to produce circulation was found to be fairly critical. When the pump heater (48 s.w.g. eureka wire) was contained inside the pump chamber, the device was much more stable, reached lower temperatures, and gave greater cooling capacity, than if the heater wire was simply wound round and varnished to the outside of the chamber. The heater leads were brought out through the rouge in the pump superleak without affecting its operation.

Several large and complicated heat exchangers were used in the early experiments, but these were abandoned in favour of a simple, thin-walled brass bellows, which proved to be entirely satisfactory.

The fridge chamber used in the ion experiment was machined from solid copper, specially shaped so as to fit against the ion chamber. Following several unsuccessful methods of fastening the ion chamber to the fridge chamber, the two chambers were soft soldered together. This gave good thermal contact, but it did have the disadvantage that two Rose's metal joints had to be broken and remade each time the ion chamber had to be modified.

The pressure in the vacuum chamber which housed the fridge and ion chamber was monitored by means of a Penning gauge connected to

the chamber by a vacuum line separate from the vacuum pumping line.

3 Temperature measurement

Temperatures at various points in the fridge and ion chamber were measured with Speer 220 ohm carbon resistors on an Oxford Instruments resistance thermometer bridge. This instrument has a power dissipation in the sensor of about $10^{-11}$ watts, which was sufficiently small to avoid raising the temperature of the sensor significantly.

In order to prevent heat being conducted down the leads to the sensors, the following proceedure was adopted. The leads were brought down the main vacuum chamber pumping line from a room temperature glass/metal seal on the cryostat top. They were bound with low temperature varnish (Oxford Instruments G varnish) to a copper post which was at the bath temperature. They were then wound round and sealed with varnish to the ion chamber. In this way the heat conduction from room temperature was absorbed by the bath, while the small heat leak from the bath to the ion chamber and fridge, present when the fridge was in operation, was absorbed by the ion chamber and extracted by the fridge.

The resistors R1 and R2 shown in figure 4.1 were sealed with G varnish into small copper cylinders which had previously been soldered in position. The resistor R3 was held in position by varnish and a metal belt. The resistor R4 rested in the bottom of the dewar.

Mercury manometers were used to measure the temperature of the bath from the N. B. P. to about 1.20 K, the lowest bath temperature.

Initially the Speer 220 ohm resistors were calibrated from the N. B. P. down to 1.20 K using the mercury manometers. Below 1.20 K

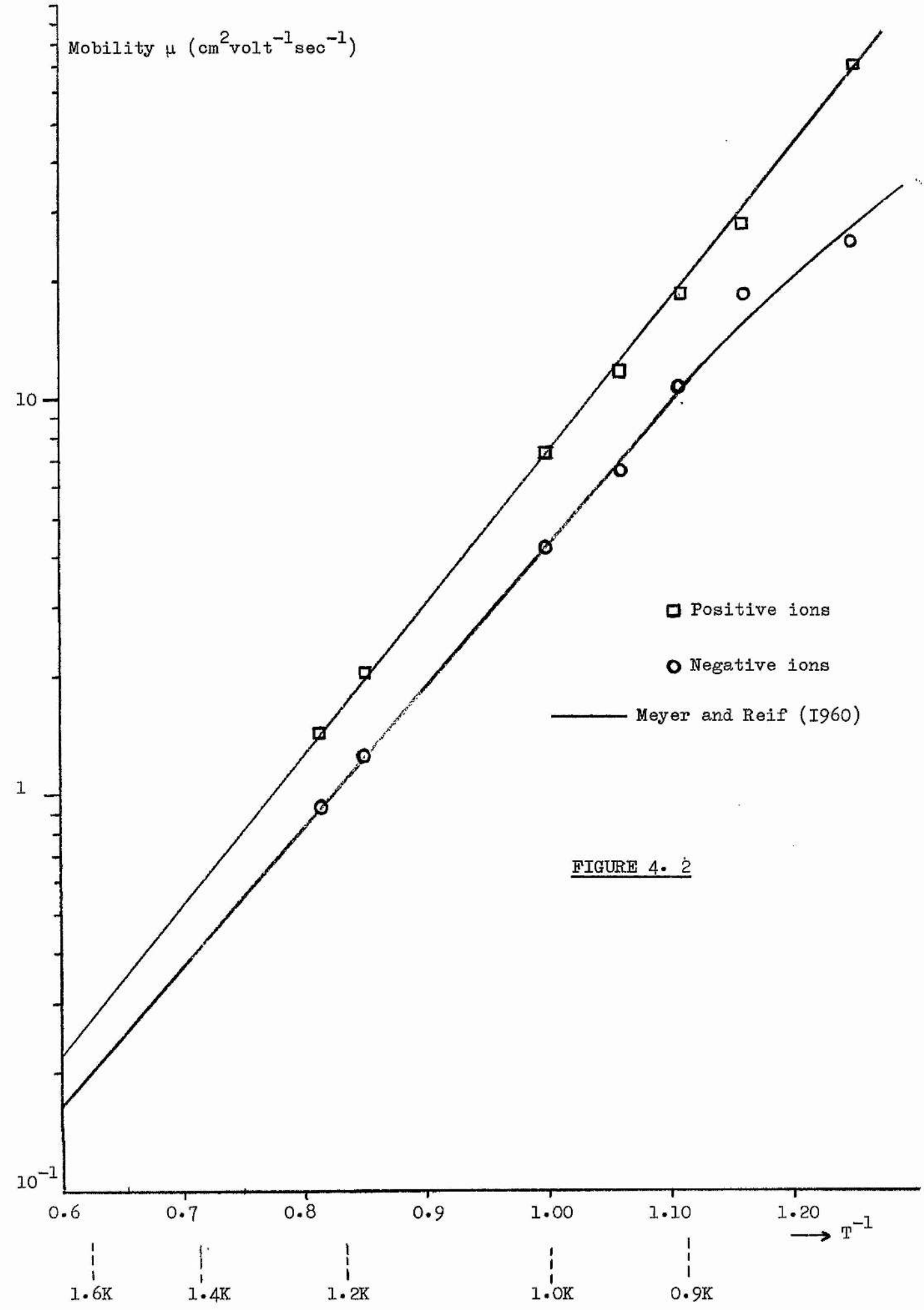
Mobility μ (cm²volt⁻¹sec⁻¹)
10
1
10⁻¹
Positive ions
Negative ions
Meyer and Reif (I960)
0.6
0.7
0.8
0.9
1.00
1.10
1.20
T⁻¹
1.6K
1.4K
1.2K
1.0K
0.9K

FIGURE 4. 2

the interpolation formula of Hetzler and Walton (1968),

$$\frac{1}{T} = A + BR + CR^{1/2},$$

was used, where A, B, and C were chosen to fit a set of calibration points. However, discrepancies were found in the temperatures below 1.20 K when measured by different resistors calibrated in this way.

Finally, a calibrated Speer resistance thermometer R1 was obtained from Oxford Instruments, and two other resistors, R2 and R3, whose characteristics were known to be fairly reproducible from run to run, were attached with it to the fridge chamber and calibrated from it.

After the ion chamber had been permanently soldered to the fridge chamber, the resistors R1, R2, and R3, were always found to read the same temperature which showed that there were no temperature gradients in the ion chamber itself.

An interesting method of checking the calibration of the resistors was by means of ion mobility. The mobilities of positive and negative ions in Helium 11 were measured at different temperatures, and compared with the data of Meyer and Reif (1960). The comparison is shown in figure 4.2, in which it is seen that agreement was satisfactory. It was hoped to develope this novel method further, but time did not permit this.

The characteristics of the resistors were checked during each run from the N. B. P. to about 1.20 K using the manometers. It was found that the resistors were always reproducible to within 20 millidegrees, which was the error in measuring absolute temperature from the calibration curve for R1 supplied by Oxford Instruments.

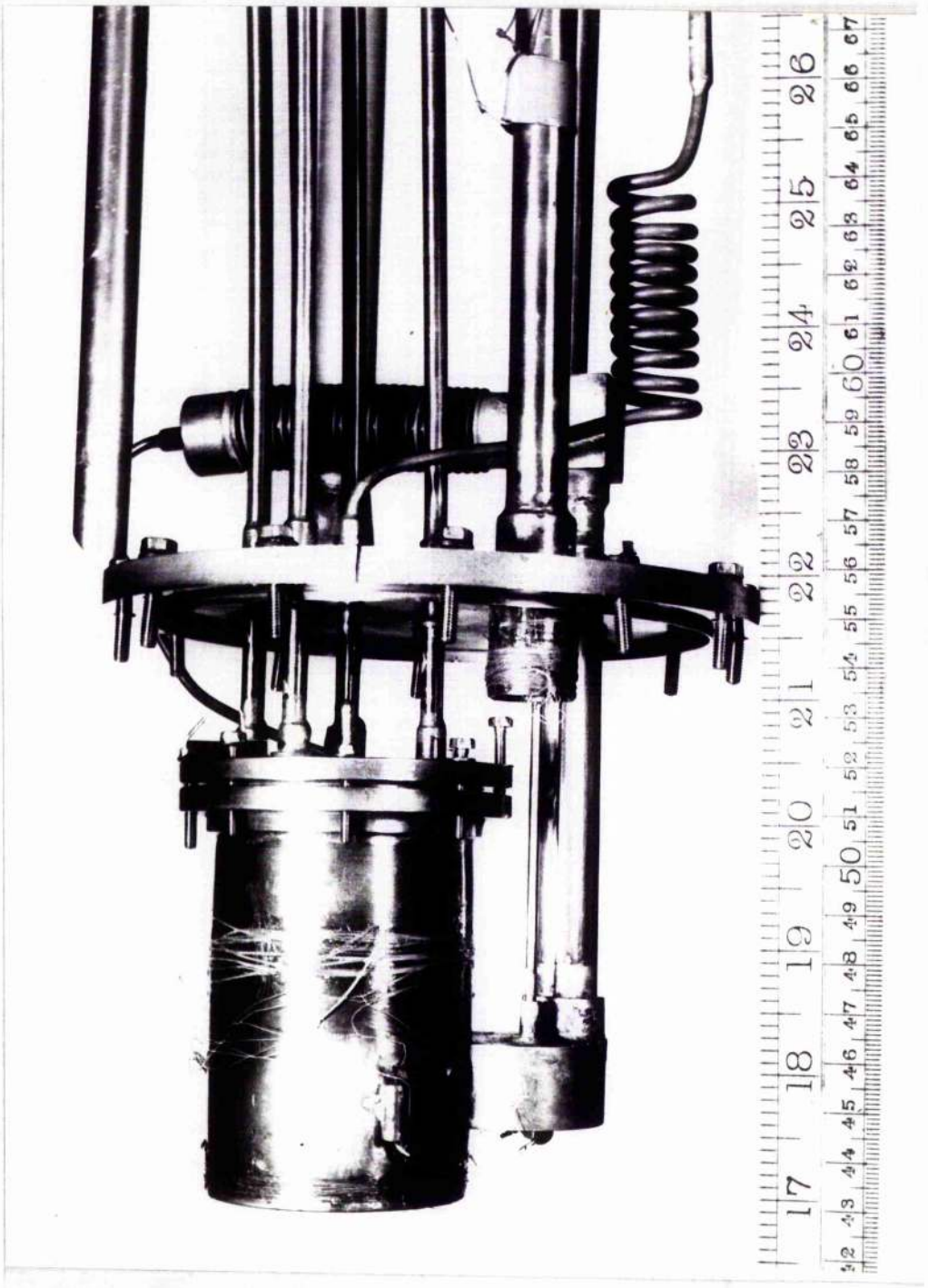

Tha Fridge and Ion Chambers

FIGURE 4.3(a)

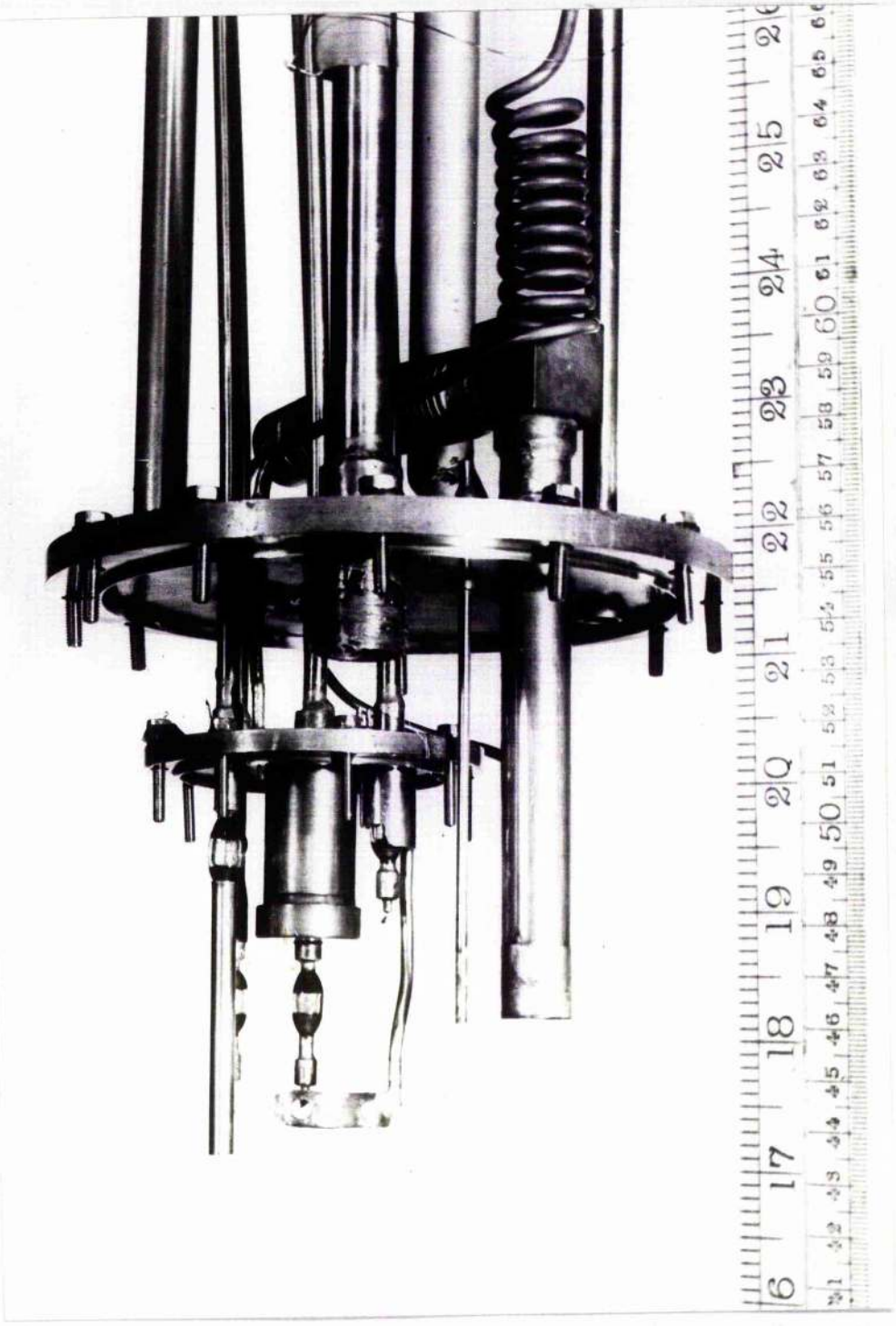

The Experimental Region

FIGURE 4.3(b)

4 Temperature control

Suitable adjustment of the fine and coarse valves on the main pumping line provided adequate control of temperatures between the N. B. P. and about 1.20 K. Temperatures below 1.20 K with the fridge were controlled by varying the amount of power supplied to the pump chamber. Because of the sensitivity of the resistance bridge, the temperature could be held constant to within 3 millidegrees, although its absolute temperature was not known to that accuracy.

5 The Ion Chamber

A photograph of the arrangement of fridge and ion chambers is shown in figure 4.3 (a), and the photograph 4.3 (b) shows the experimental region with these chambers removed.

The body of the experimental ion chamber was machined from copper tube while the ends were brass. The inside of the chamber was gold plated for cleanliness. Before pre-cooling at the start of a run, the chamber was pumped and flushed out with Helium gas several times. After the cryostat had been filled with liquid Helium, the chamber itself was filled by condensing Helium gas from a storage cylinder, first through a liquid nitrogen cooled charcoal trap, then through a stainless steel tube to a copper spiral, and finally through a fine stainless steel capillary, the condensing capillary shown in figure 4.3. The copper spiral had the twofold advantage both of providing a good thermal contact with the main bath, in order to remove the specific and latent heats of the condensing gas, and also of being a further agent in the purification process.

From the results shown in figure 3.8, it was important that if the fridge and ion chambers were to cool sufficiently, then the heat

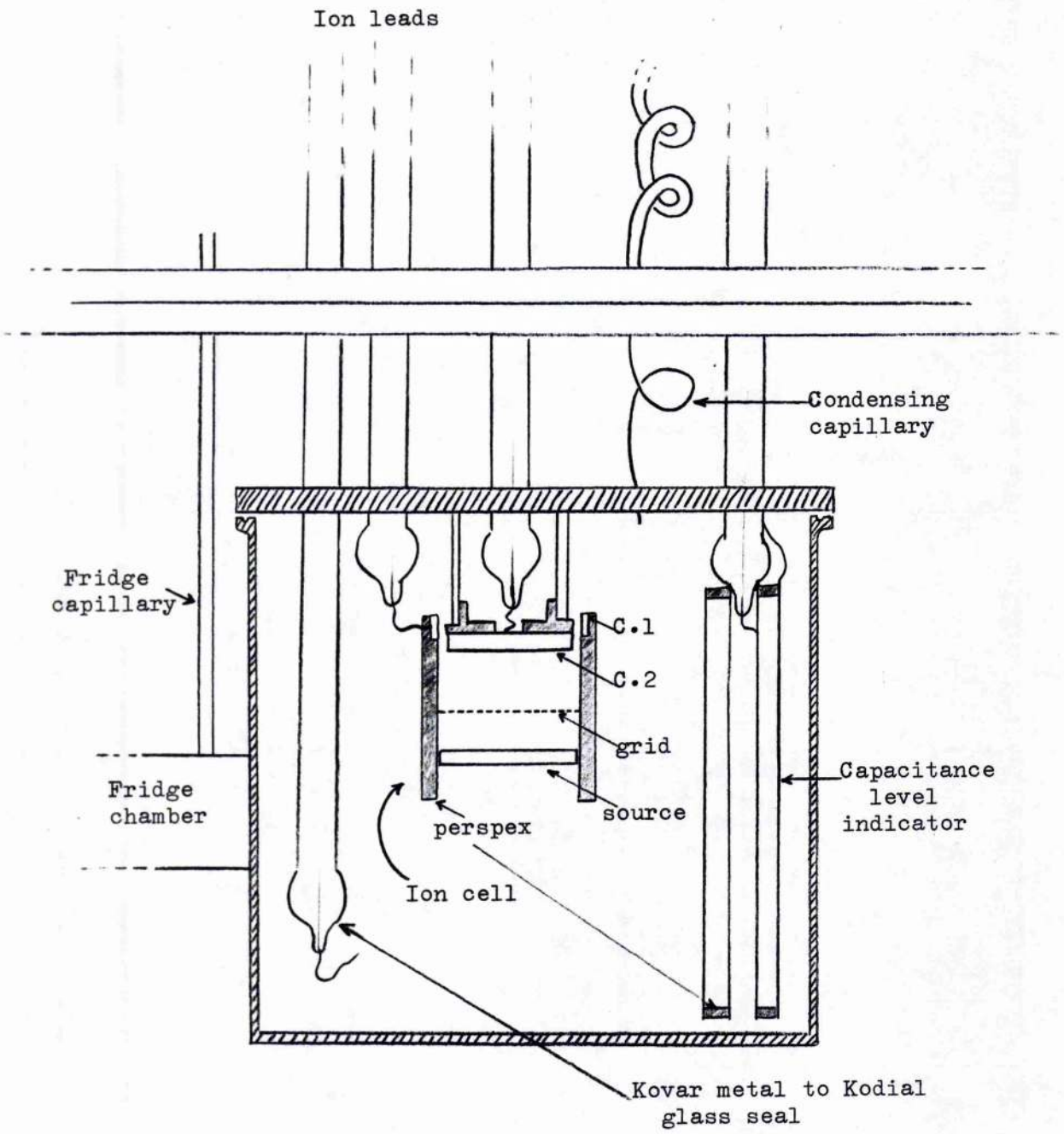


The experimental chamber.

FIGURE 4. 3

leak reaching them would have to be small. Bertman and Kitchens (1967) have shown that even quite small capillaries, filled with superfluid Helium, provide a very large heat leak between two baths at different temperatures. Care was therefore taken to ensure that the ion chamber was never completely filled with liquid, so that the only heat path available to the superfluid in the ion chamber was via the film on the inside of the condensing capillary. Heat transfer via the film in the 0.5 mm diameter capillary was a small fraction of a milliwatt, which was small enough to be tolerable.

Other sources of heat leak into the ion chamber were the 5 mm diameter stainless steel tubes used to bring in the leads to the ion cell. Each tube contained a length of 40 s.w.g. eureka wire, insulated by glass tubing, running from a Kovar-Kodial metal-glass seal in the ion chamber, to a normal glass-metal seal on the cryostat top, where it was connected to the appropriate piece of electronics. Experimenting with ions in liquid Helium demands very high insulation resistance, in $10^{12}\Omega$ , and these lead tubes were therefore pumped and their pressure continuously monitored. The insulation resistance was measured on a Norma Teraohmeter.

The ion chamber is shown in figure 4.3 with a typical triode ion cell in position. Although there are in fact four electrodes, because there are two collectors, the use of the term triode is more appropriate. The collector C2 was made from brass and was gold plated to avoid oxidised insulating layers. The collector C1 was either a gold plated brass ring, or a gold ring evaporated on to a glass cylinder or beaker.

All the grids used were made from Nickel mesh, 60 lines per inch.

The lowest temperature reached during any one run with the ion experiment was not always the same, but generally ranged between

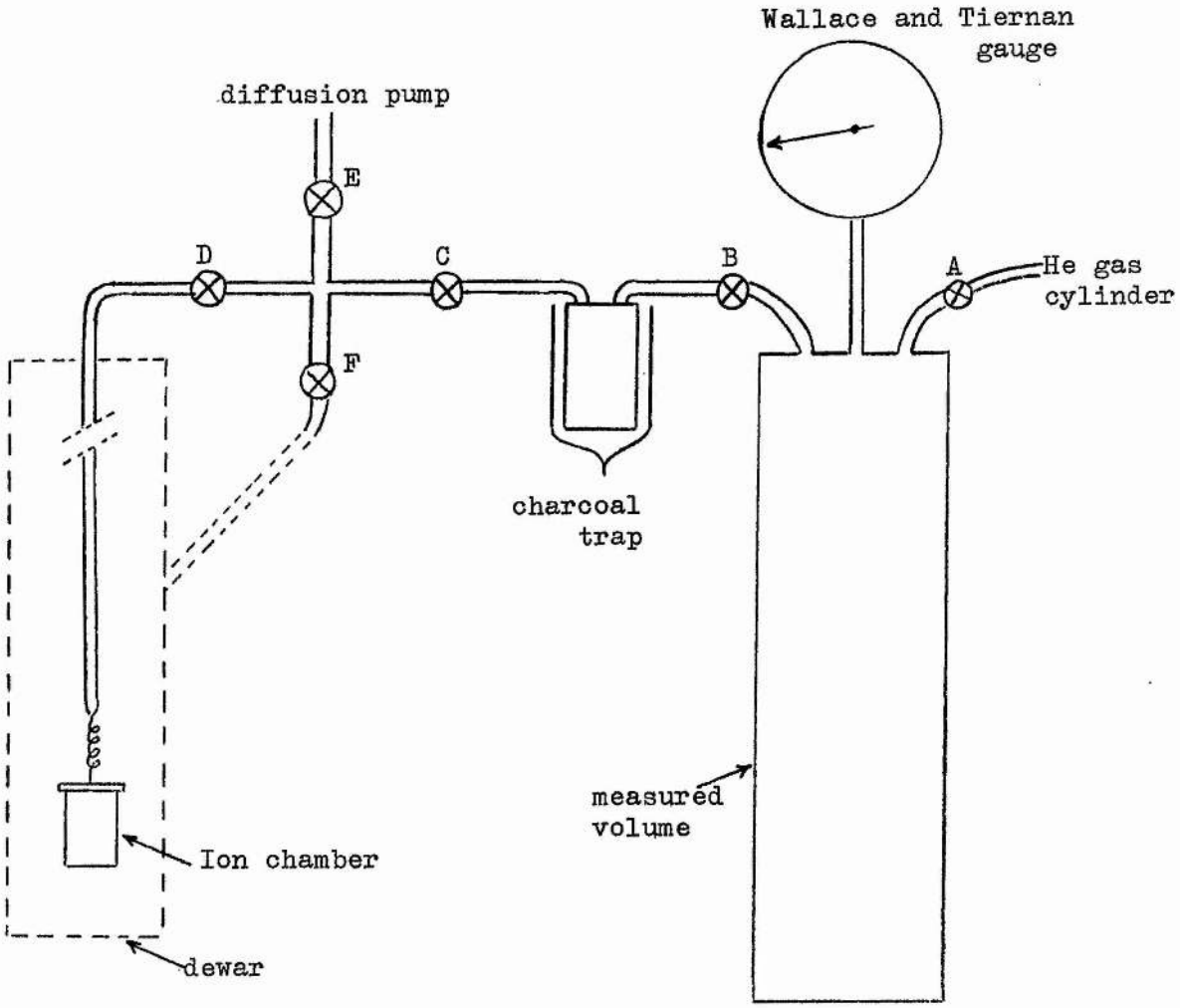


Condensing circuit

FIGURE 4. 4

0.80 K and 0.88 K, while the lowest temperature with an empty ion chamber ranged between 0.75 K and 0.80 K. The run to run variation appeared to be due mainly to the dependence of the lowest bath temperature upon the volume of liquid in the main bath. It was shown in figure 3.7 that the bath temperature affected the lowest temperature reached by the fridge.

6 The Control of the liquid level in the ion chamber

Each time the ion cell was replaced by one of a different design, the variation of liquid level in the ion chamber with the volume of liquid condensed had to be freshly determined. This was done, prior to fitting the cryostat into the dewar, by fitting a glass beaker, which was made with the same dimensions as the ion chamber, on to the apparatus in the position of the ion chamber. Known volumes of a liquid (e.g. Carbon tetrachloride) were then added from a burette and the resulting liquid level measured with a cathetometer. In this way it was known where the level in the ion chamber would be if the same volume of liquid Helium was added. The accuracy of this method was about $\pm$ 2 mm.

In order to condense a known volume of liquid Helium from the gas storage cylinder, the condensing circuit shown in figure 4.4 was used. With valve B closed the cylinder V, whose volume was measured to be 10.02 litres, was pressurised to a measured value P, on the Wallace and Tiernan gauge, through valve A. Closing valves A, F, and E, and opening B, C, and D, allowed the gas in the cylinder to condense into the ion chamber.

Since the volume of the gas prior to condensation was known to be 10 litres at about $20^{\circ}$ c, a relation was obtained between its pressure P, and the volume of liquid Vcc, below the lambda point,

Capacitance Level Indicator FIGURE 4. 5

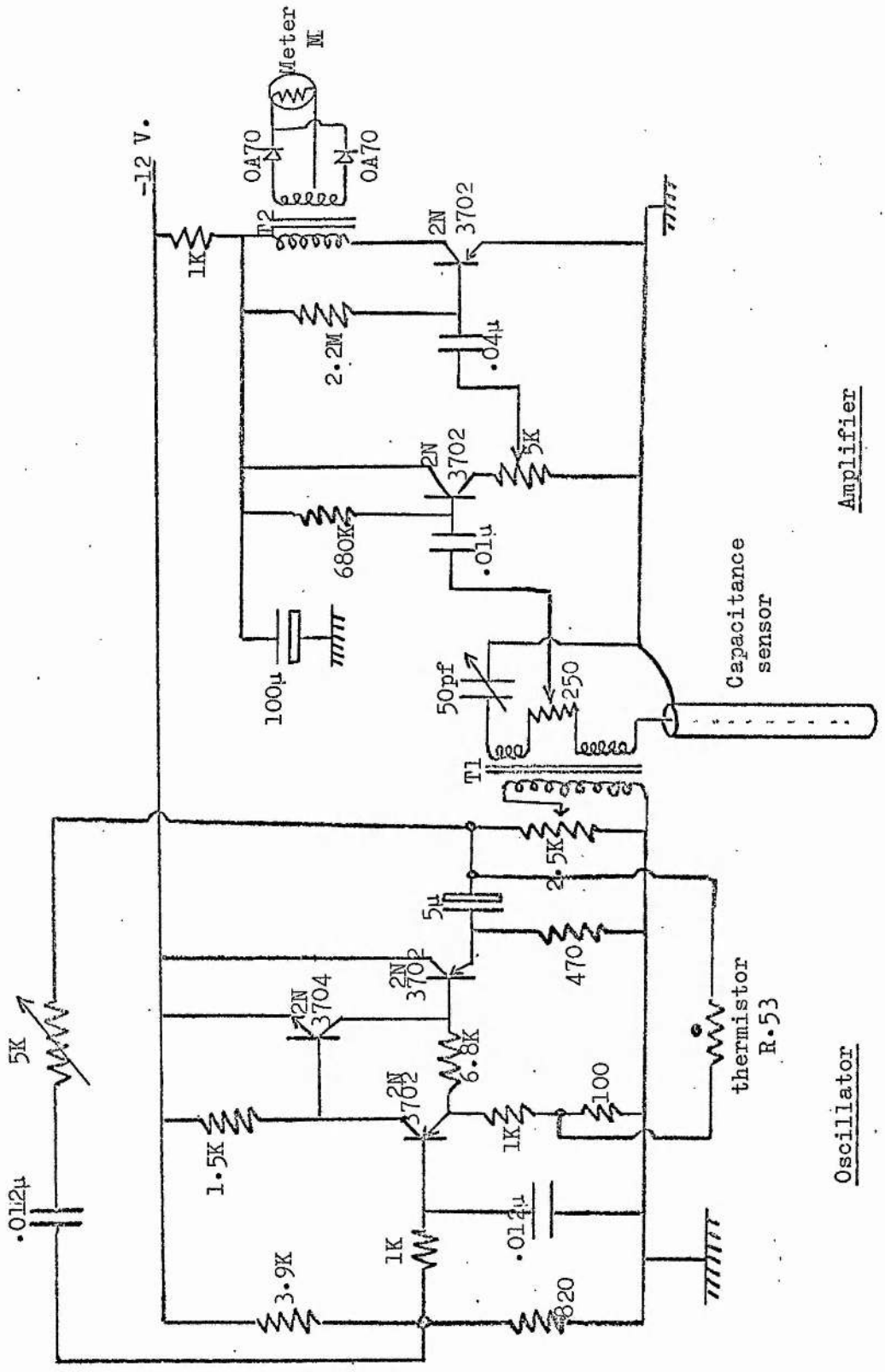

into which it will condense. This working relation is,

$$P = 6.61\ V \text{ cm Hg.}$$

7 Capacitance level indication

In order to confirm the estimate of the level by the method of condensing a known gas volume, a capacitance level indicator was used. The capacitance sensor consisted of two coaxial stainless steel cylinders. Since there is a difference of about 5% in dielectric constant between liquid Helium and the vapour above it, the value of the capacitance will change by about 5% when liquid fills the annulus between the cylinders of the sensor. The absolute value of the capacitance was only a few picofarads, which was much smaller than the capacitance of the lead to it; consequently, the sensitivity and stability of the detection circuit was very important.

Considerable time was spent on the Clapp oscillator circuit of Sequin and Leonard (1966), where the change in capacitance is measured by the change in frequency of the oscillator which uses the capacitance sensor in the frequency-determining part of the feedback circuit. However, the circuit was found to suffer from such short term instability that it was abandoned.

The circuit shown in figure 4.5 was much more successful. The oscillator of this circuit drives the transformer $T_1$, whose secondaries are arranged to give 1 : 4 + 4. The capacitance sensor and a variable capacitance are arranged in the form of a bridge in the secondary circuit. The 250 ohm potentiometer provides the resistive balance. When the sensing capacitance was empty, that is

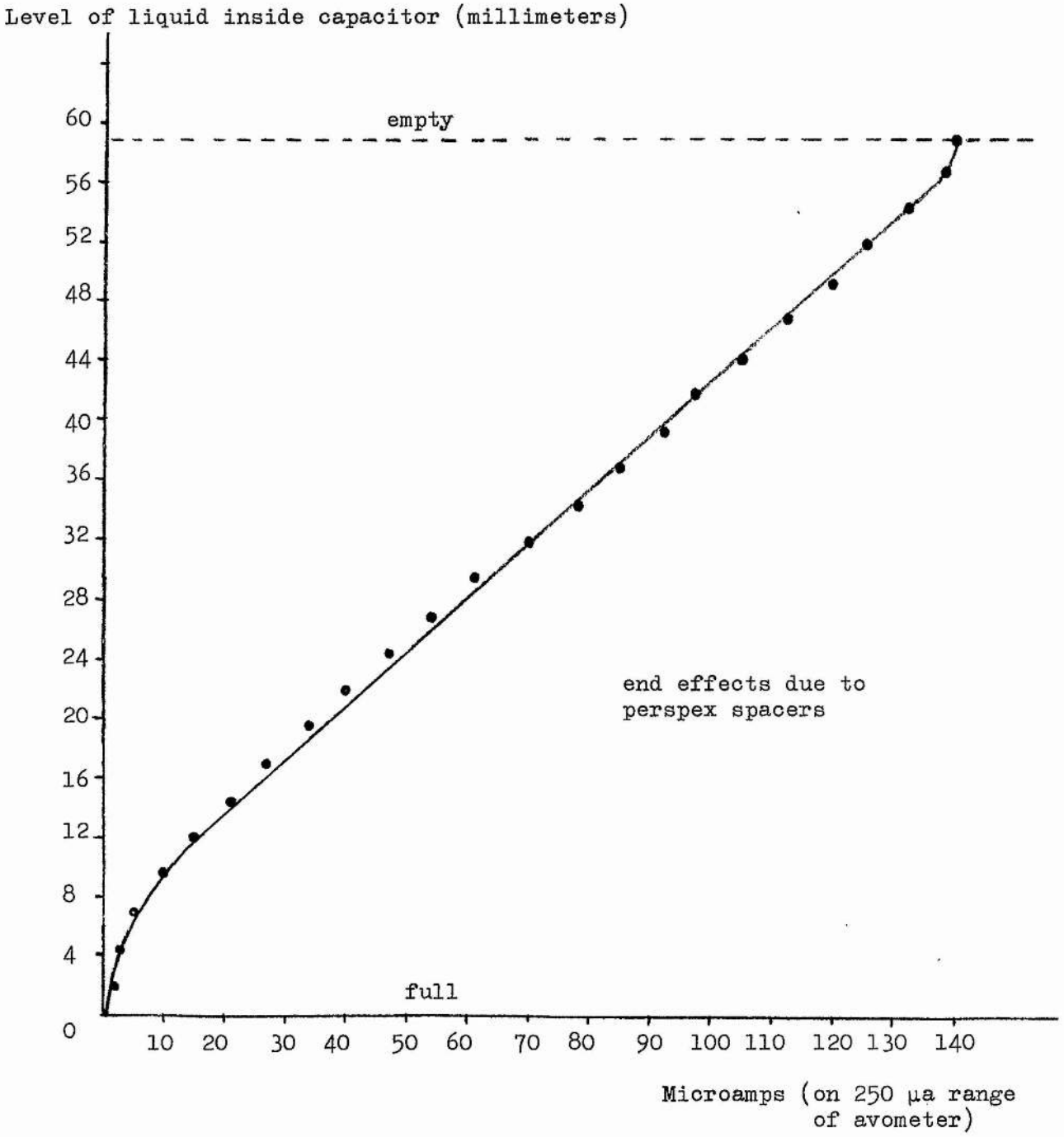


Displacement of indicator meter versus liquid level inside capacitor, shown in figure 3.

FIGURE 4. 6

with no liquid in the ion chamber, the bridge was balanced with the variable capacitance so that no signal reached the amplifier, giving a zero reading on the meter M. As liquid Helium began to fill the annulus its capacitance changed, and the resultant out of balance signal was amplified and displayed on M. M was an avometer on its 250 μ amp range, in which state its impedance of 2 K ohms is just the matching impedance necessary for the secondary of the output transformer $T_2$.

In order to calibrate M against liquid level, a capacitance sensor, of the same geometry and of similar lead capacitance to that used in the apparatus, was inserted in a glass dewar system so that the operation of the level indicator could be observed visually. The result is shown in figure 4.6. The sensitivity is approximately 30 μA/cm, which gave a resolution of about $\pm$ 1 mm. This circuit suffered from some long term instability, which may have been caused by varying temperature gradients in the long lead down the dewar to the sensor during the course of long runs.

## 8 Production of Ions

The ions were produced by alpha particles from a radioactive source. The two sources used were either Americium 241 (obtained from the Radiochemical centre, Amersham), or Polonium 210 (obtained from Nuclear Radiation Developments Inc., Grand Island, New York). The strength of the sources used was between 100 and 200 microcuries, and this introduced about 1 microwatt into the ion chamber.

## 9 Electronics for Ion measurement

The block circuit diagram for a typical ion cell is shown in

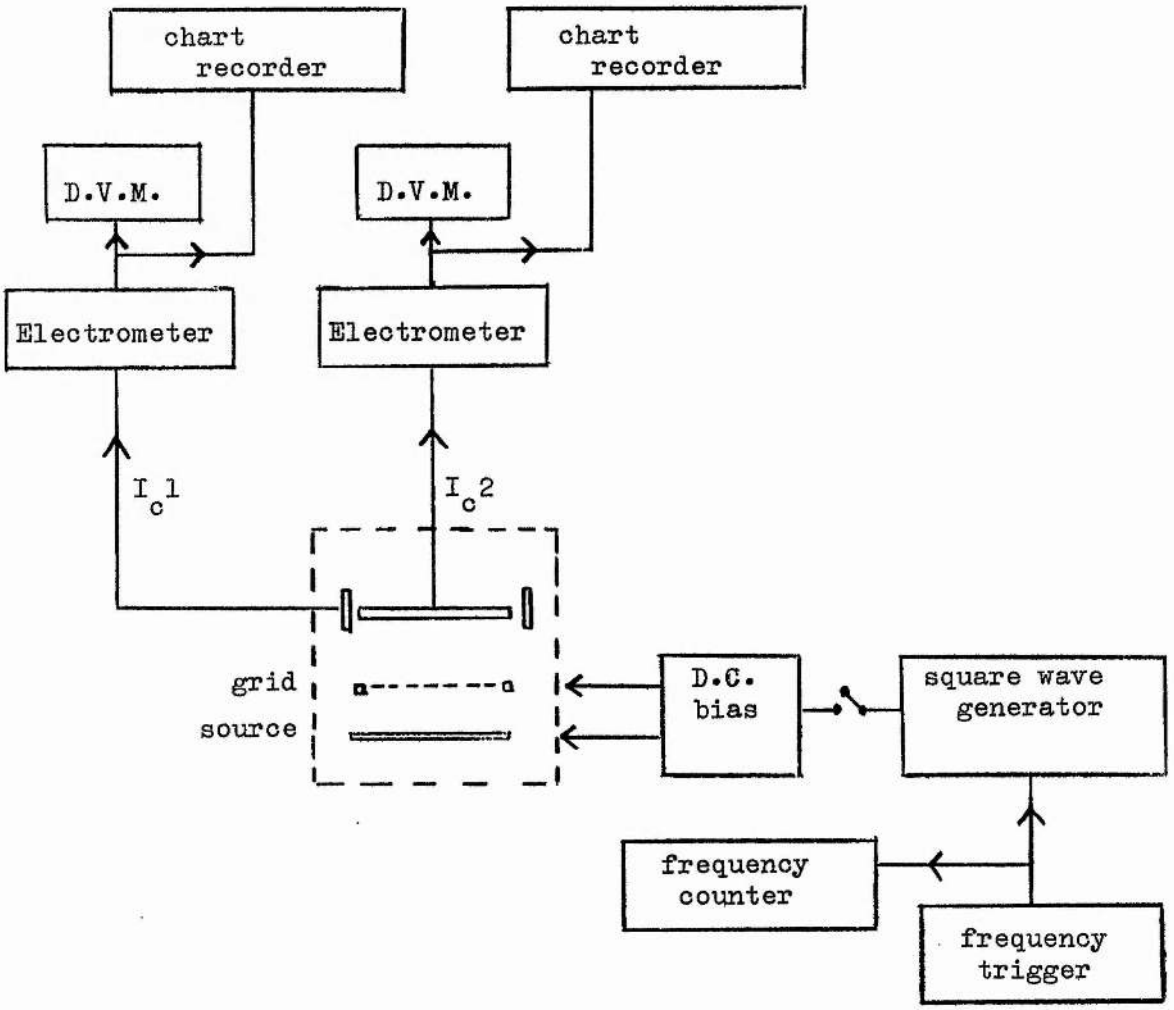


Block circuit diagram.

FIGURE 4. 7

Square Wave Generator

FIGURE 4. 8

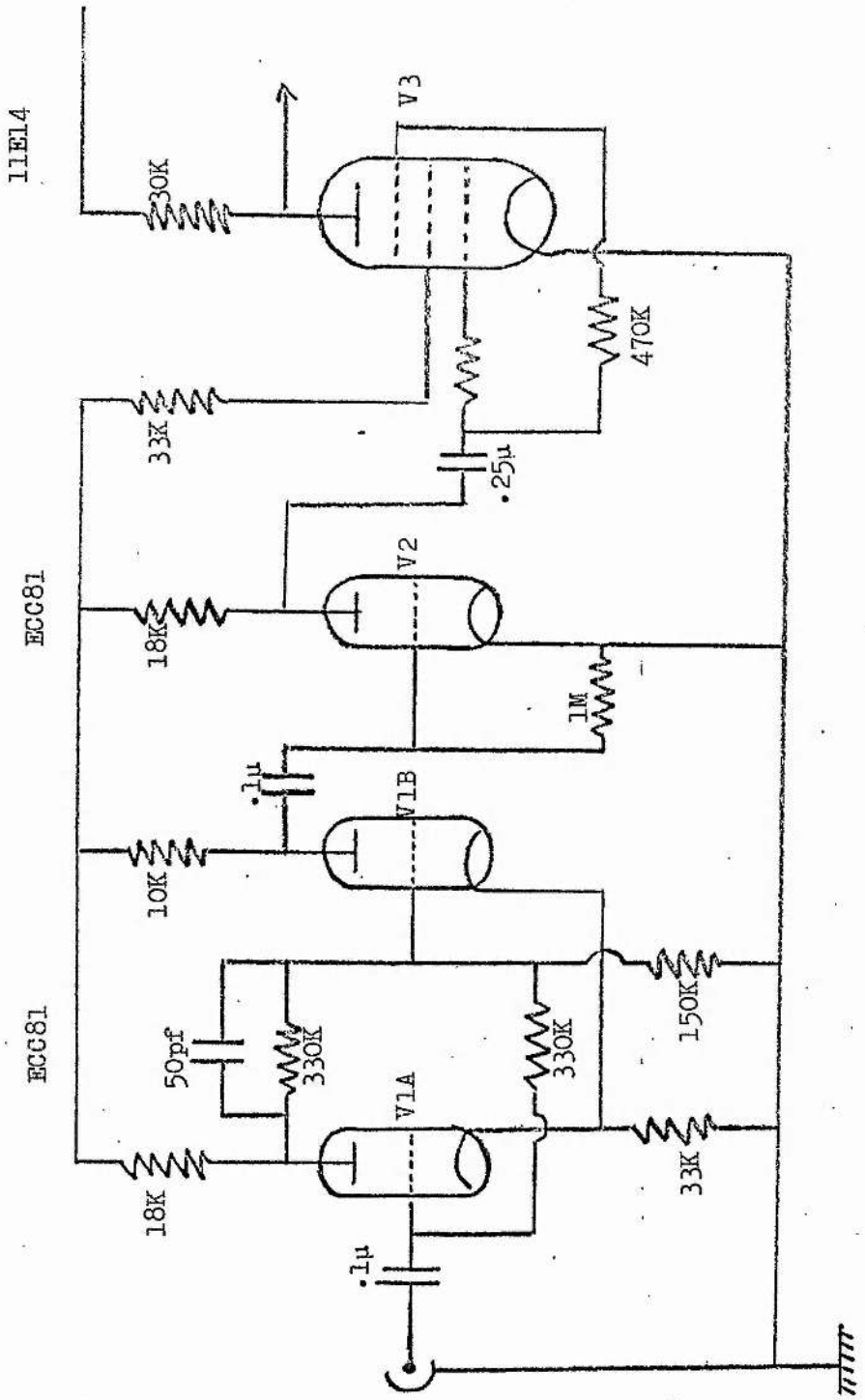

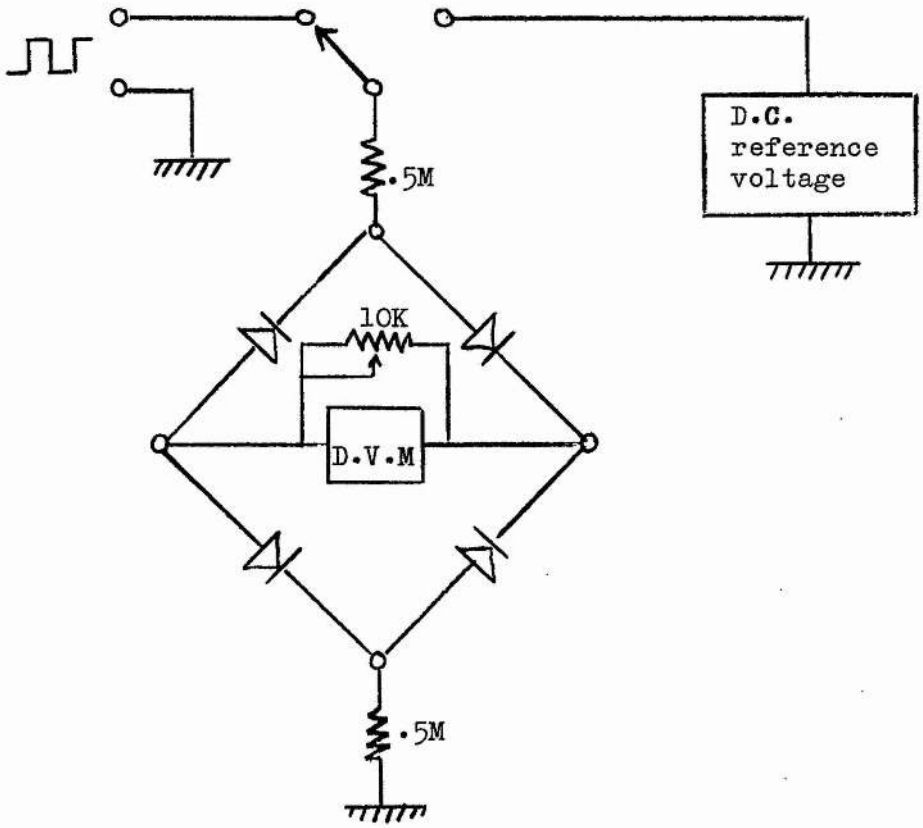


Bridge for measuring square wave amplitude, from Bruschi, Mazzoldi and Santini (1968)

FIGURE 4. 9

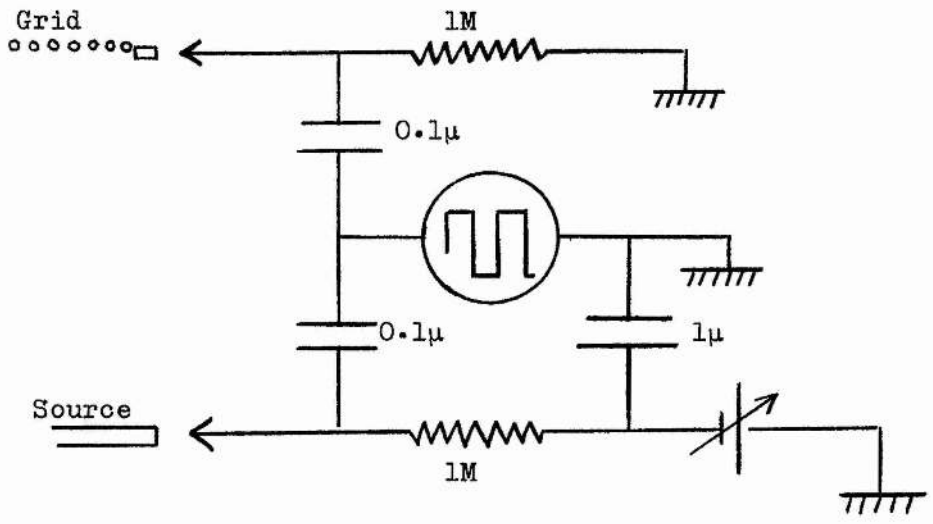


Application of square wave

FIGURE 4. 10

figure 4.7. The ionic currents reaching the collectors $C_1$ and $C_2$ were measured on a Keithley 602 and a Wayne Kerr electrometer respectively. The Keithley 602 has a great range of input resistors, and can measure a range of current of fourteen orders of magnitude down to its zero current of about $5 \times 10^{-15}$ amp. The Wayne Kerr has only one input resistor of $10^{10}$ ohms, giving it a range from $10^{-9}$ to about $10^{-14}$ amp. On both electrometers, currents below $10^{-14}$ amp were neglected. Each electrometer has a one volt, full scale deflection, output, and these outputs were fed into two Dynamco digital voltmeters to allow much better resoltuion of the electrometer scales. The electrometer outputs were displayed on two Servoscribe chart recorders in order to note any interesting variation of the currents with time.

The D.C. biases for the source and grid were supplied by Fluke high voltage power supplies.

10 Measurement of Ionic Mobility

The mobility was measured by the square wave technique of Cunsolo (1961), in which a square wave electric field applied to the grid of a triode causes ions to be drawn towards the collector during one half cycle, and to be drawn back towards the grid during the reverse half cycle. The collected current is measured as a function of the frequency of the square wave until the time of flight of the ion from the grid to the collector is greater than the half cycle period of the square wave. The equation for the collected current is

$$I = Io \left(\frac{1}{2} - \frac{df}{v_d}\right) , \qquad (1)$$

where f is the frequency, d the grid-collector distance, and $v_d$ is the drift velocity. $v_d = \mu E$, where $\mu$ is the mobility in the field E. If $f_c$ is the frequency where the straight line of equation (1) cuts the frequency axis I = 0, then $v_d = 2\ d\ f_c$, and thus

$$\mu = \frac{2\ d\ f_c}{E}\ .$$

The square wave generator shown in figure 4.8 was made for the experiments. A low voltage square wave (trigger) was applied to the Schmidt trigger, and the output amplified and fed to the grid of the high voltage beam tetrode 11E14. The output was at anode potential when this valve was non-conducting, and was at zero potential when the valve was conducting. The output therefore, at the frequency of the trigger, alternates between zero and approximately the value of the power supply voltage delivering the anode potential. The amplitude of the square wave was measured on a four diode bridge, similar to that of Bruschi, Mazzoldi and Santini (1966), shown in figure 4.9. The D.C. reference which gives the same reading on the D.V.M. as the square wave, is one half of the square wave amplitude.

The frequency of the square wave was measured on a Hewlett Packard 5233L electronic counter.

The square wave was applied simultaneously to the grid and source via the large capacitors shown in figure 4.10, so that the mean voltage was brought down to zero for the grid, and to the value of the D.C. bias for the source. In this way the ion mobility was measured in the grid-collector space.

# CHAPTER 5

## THE EXTRACTION OF IONS FROM A RADIOACTIVE SOURCE IN LIQUID HELIUM

### 1 Introduction

Ions have been produced in liquid Helium by a variety of different methods by different workers. Negative ions have been produced by tunnel junctions, heated Tungsten filaments, and photoelectric emission, while both negative and positive ions have been produced by X-rays, field emission from a Tungsten tip, a Promethium 147 β source, but most commonly of all by the extraction from the region of intense ionization produced close to the source by the α particles from either Polonium 210 or Americium 241.

The mechanism and temperature dependence of the low field extraction of ions from the ionized layer in front of a radioactive source immersed in liquid Helium is not completely understood. A review of the work which has been carried out on this subject will be given, together with the results of experiments carried out during the course of the present research.

### 2 The Theories of Jaffé and Kramers

A modification of the theory of Jaffé (1913) on the extraction of ions from the ionized column produced by α particles in a gas, was presented by Kramers (1952) to account for the results of Gerritsen (1948), who carried out extensive measurements on the field dependence of the current extracted from a Polonium α source immersed in liquefied gases at low temperatures.

Both Jaffé and Kramers assumed that all the ions which are created by an α particle are contained in a characteristic cylinder of radius b, around the path of the particle. They introduced an

initial linear ionic density $N_o$ along the axis of the cylinder (assumed to be the z axis), and assumed a Gaussian distribution of the number $n_o$ of ions per $cm^3$. That is,

$$n_o = \frac{N_o}{\pi b^2} \; e^{-\left[\frac{x^2 + y^2}{b^2}\right]} \qquad (1)$$

Now the initial distribution of the ions will be modified by,

(a) the recombination between ions of different sign in the cylinder, tending to reduce the ionic density,

(b) the diffusion of the ions tending to spread the ions apart, and

(c) the applied electric field which tries to separate ions of different sign.

The object of the theory was to obtain the fraction of the initial number of ions which, per unit length of the column in the course of time, was extractable by the applied field. The equation describing this process is

$$\frac{\partial n_{\pm}}{\partial t} = \mp \mu_{\pm} E \operatorname{Sin} \phi \frac{\partial n_{\pm}}{\partial x} + D \nabla^2 n_{\pm} - \alpha n_+ n_- , \qquad (2)$$

where the term on the left gives the variation of ion density with time, and assumes $n_+ = n_-$ and $= n_o$ at $t = o$, where $n_o$ is given by (1), $\mu_+$ and $\mu_-$ are the mobilities of the positive and negative ions respectively in the electric field E, which is assumed to be in the x, z plane, the angle between its direction and the z axis being $\phi$. D is the diffusion coefficient, given by the Einstein relation

$$D = \mu \, k \, T/e,$$

and $\alpha$ is the recombination coefficient, given by the Langevin expression

$$\alpha = 4\pi e ( \mu_+ + \mu_- ) .$$

Both Jaffé and Kramers realized that an exact mathematical solution of equation (2) was not possible. By neglecting the recombination term, Jaffé solved equation (2) and then took recombination into account by replacing $N_o$ by a function $N(t)$ of time, which was assumed to satisfy the equation which followed from (2). It was pointed out by Kramers, however, that such a procedure would only be valid in low density gases, where the effect of recombination would be much smaller than that of diffusion or electric field; in liquids, especially at low temperatures, the diffusion effect should be small, and recombination should be the dominant process governing the evolution of the ionic density.

Kramers introduced a new time variable $t'$ such that $t' = \mu t/e$, and introduced it into equation (2), keeping D and $\alpha$ as before and considering the ionic mobilities to be the same. Thus,

$$\frac{\partial n^{\pm}}{\partial t'} = \mp e E \operatorname{Sin}\phi \frac{\partial n^{\pm}}{\partial x} + kT \nabla^2 n^{\pm} - 8\pi e^2 n_+ n_- \qquad (3)$$

$$= (e) + (d) + (r) ,$$

where the symbols (e), (d), and (r) stand for the field term, the diffusion term, and the recombination term respectively. Assuming the distribution (1), Kramers estimated the order of magnitude of these terms at $t = o$.

$$(e)_o = \frac{e\,E\,N_o}{\pi\, b^3}$$

$$(d)_o = \frac{kT\,N_o}{\pi\, b^4} \qquad (4)$$

$$(r)_o = \frac{8e^2 N_o^{\,2}}{\pi\, b^4}$$

From the set of equations (4) there then follows the ratio, and hence the relative importance, of any two of these terms.

$$\text{e.g.}\ \frac{(d)_o}{(e)_o} = \frac{kT}{eEb},$$

hence the diffusion effect will be small compared with the field effect if

$$E >> \frac{kT}{eb} \qquad (5)$$

That is, if the field E is greater than about 100 T volts $cm^{-1}$, assuming b in liquids $\sim 10^{-6}$ cm, then the diffusion effect will be small in comparison to it.

In this way, Kramers showed that in liquids at low temperatures, recombination is by far the most important process, even for applied fields as high as $10^6$ volts $cm^{-1}$.

Kramers first obtained a solution of (3) by omitting the diffusion term and afterwards correcting for its influence. His solution in the absence of diffusion, which is applicable in very high field strengths (of order hundreds of kilovolts $cm^{-1}$) is,

$$p = 1 - \sqrt{2\pi}\,\frac{e\,N_o}{b}\,\frac{1}{E\,\text{Sin}\,\phi},$$

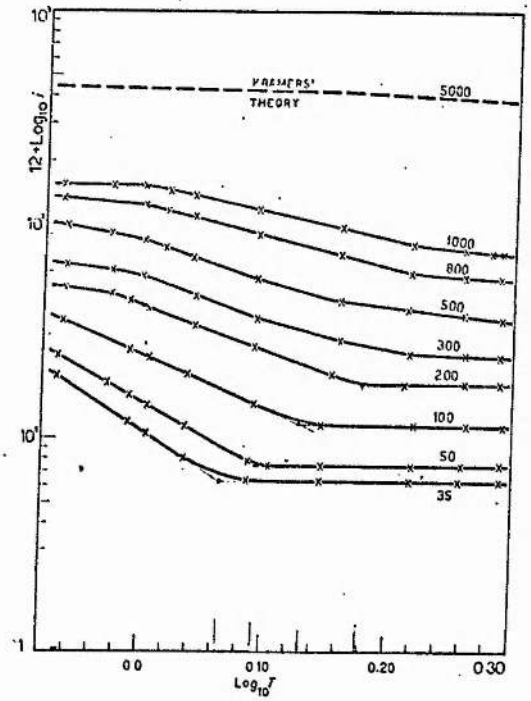


Fig. 9. The current versus temperature in a diode ionized by $\alpha$ particles; the curves are labelled according to the constant value of the field, in V/cm.

The results of Careri (I96I)

FIGURE 5. 1

where p is the ratio of the number of ions set free by the field per unit time to that produced per unit time.

In weak fields, Kramers obtained the approximate solution

$$p^* = \frac{b \sin \phi}{3N_o \pi e} \left( \ln \frac{8\theta\, e^2 N_o}{kT} \right)^{3/2} E + p_d \,, \qquad (6)$$

where $p^*$ is the same ratio as p above, and where $p_d$ is the correction term accounting for the influence of diffusion, and is given by

$$p_d = \frac{kT}{8\theta e^2 N_o} \ln \left( \frac{8\theta e^2 N_o}{kT} \right) \,,$$

and $\theta$ is a number between 1 and 5. Equation (6) predicts that for small fields, the current $p^*$ should depend linearly on field, since all other parameters are fairly constant. However, the "small" fields implied, and used by Gerritsen to test the theory, are of the order of kilo volts $cm^{-1}$. That is, the theory is not valid for fields of the order of tens of volts $cm^{-1}$.

In his experiments on liquid Helium, Gerritsen found that the Kramers theory did not quantitatively explain the results, and he suggested that the assumption of an initial Gaussian distribution of the densities of the ions along the path of the $\alpha$ particle was inadequate. He also found no temperature dependence of the extracted currents between 4.0K and 1.3K, although an irregularity at the lambda point was noted.

3 Careri's Diode Experiment

Careri (1961) first reported the temperature dependence of the low field extracted current from an $\alpha$ source immersed in liquid Helium. His results are shown in figure 5.1, and correspond to the

(a)

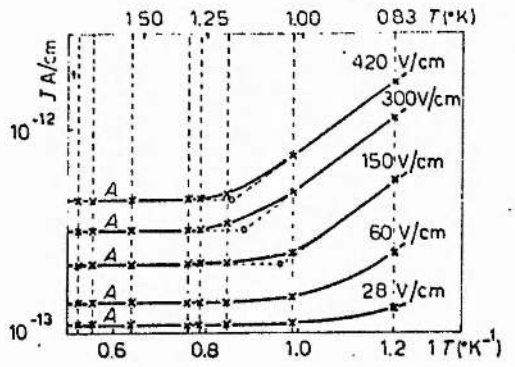


Fig. 4 – Ionic current densities *vs.* reciprocal of temperature. Each curve is drawn at constant field intensity. All these data have been obtained with cell « *A* ».

(b)

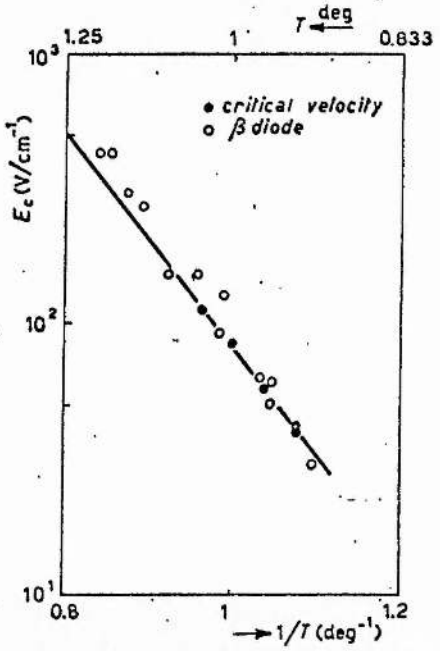


Fig. 5. – Field *vs.* reciprocal of temperature plot of the bending points obtained extending the rectilinear portions of the $J(1/T)$ curves. (Full line and dots from the mobility experiments): ● critical velocity, ○ β diode.

The results of Gaeta (I962)

FIGURE 5. 2

variation of current in a diode with temperature in a constant extracting field. The constant fields used by Careri varied between 35 and 1000 volts $cm^{-1}$. Also shown in figure 5.1 is the almost temperature independent solution of the Kramers theory for E = 5000 volts $cm^{-1}$.

It is to be seen from figure 5.1 that at low fields and high temperatures the results display a horizontal temperature-independent region, while at low temperatures a transition has occurred to a temperature-dependent region, this transition being less well defined for the higher fields, and occurring at higher temperatures for the higher field strengths. The gradient of the temperature-dependent increase is greater for the lower fields, and a current saturation effect is observed for the higher fields at low temperatures.

4 Gaeta's Diode Experiment

Gaeta (1962) performed an experiment on the field and temperature dependence of the extracted ion current from a Promethium 147 β source deposited on one of the plates of a diode immersed in liquid Helium, the extracted current being collected on the opposite plate. His results are shown in figure 5.2 (a), where it may be seen that at first glance the characteristics appear to be very similar to those of Careri. However, upon close inspection several differences can be observed. These are,

(a) the transition from the temperature-independent to the temperature-dependent region, for an equivalent field strength, occurs at lower temperatures in Gaeta's β diode experiment.

(b) the gradient of the temperature-dependent increase is greater for the larger fields in Gaeta's experiment which is opposite

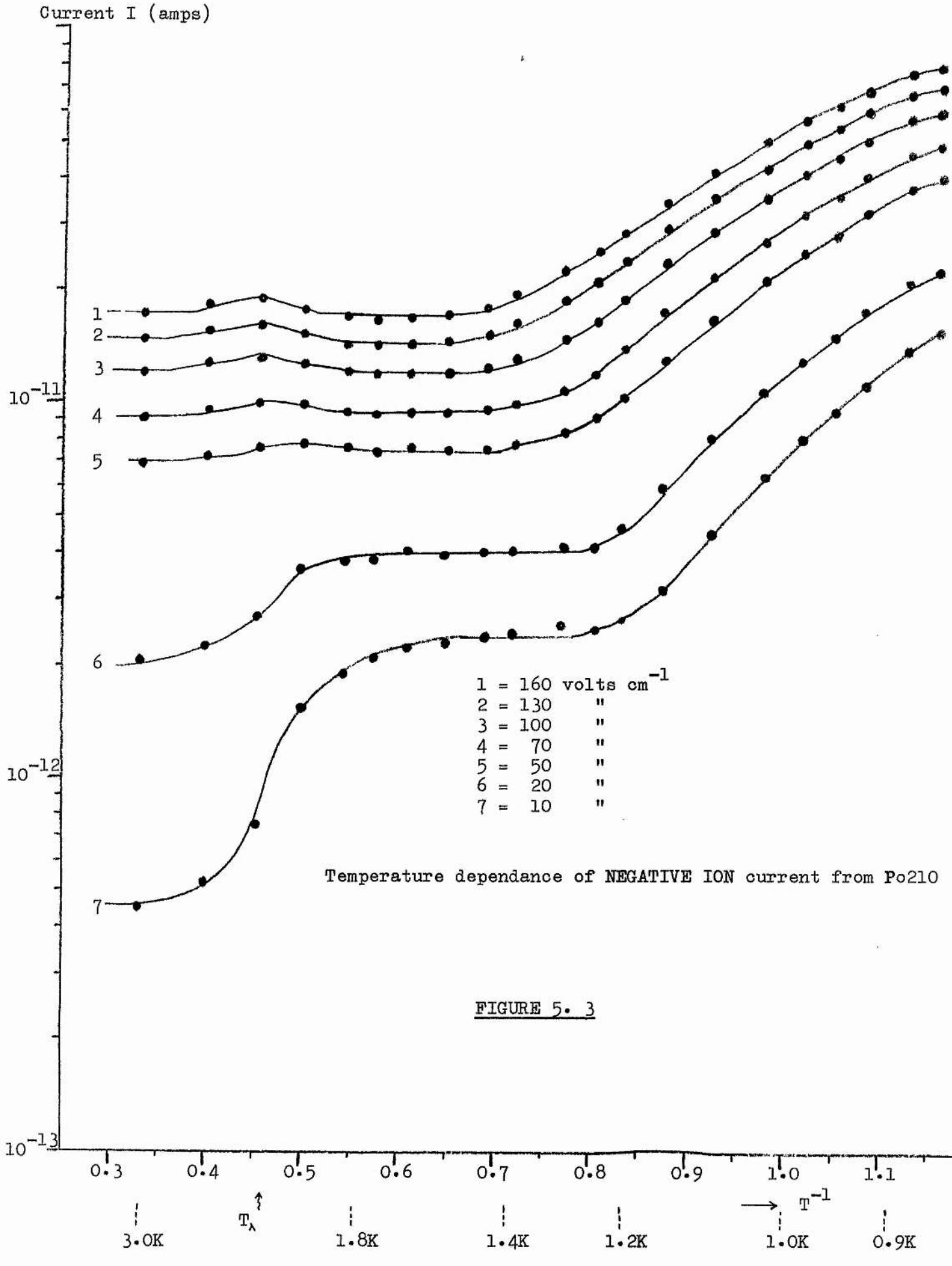


Temperature dependance of NEGATIVE ION current from Po210

FIGURE 5. 3

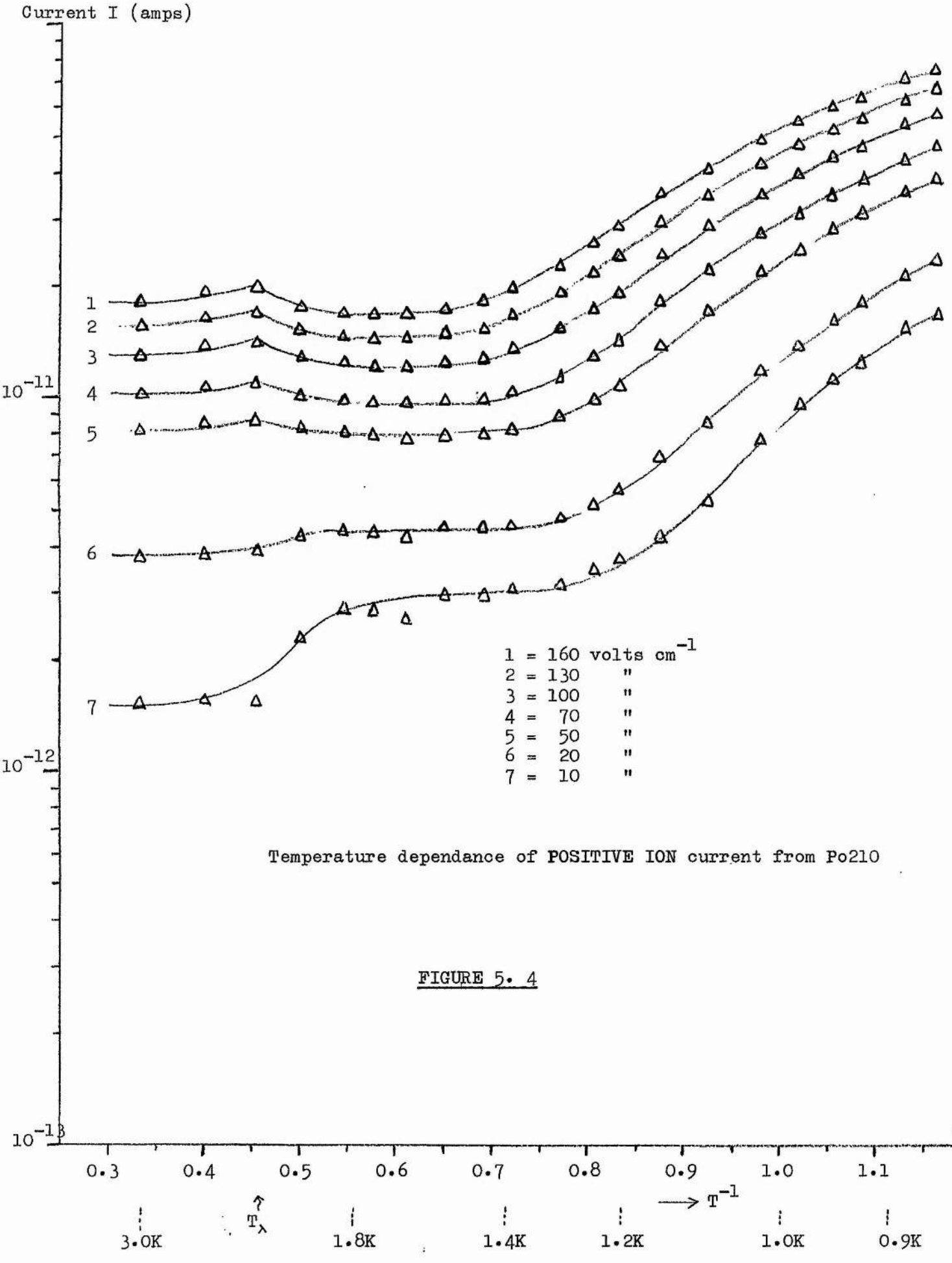


Temperature dependance of POSITIVE ION current from Po210

FIGURE 5. 4

to the effect observed by Careri.

(c) there appears to be no suggestion of a low temperature, high field, current saturation effect in Gaeta's results.

The observations of Careri and Gaeta, together with the results of experiments carried out during the course of the present work will be discussed in section 5.6.

## 5 Present Experimental Results

The temperature dependence of the positive and negative ion currents, extracted in a constant field from an α source, have been measured for both Americium 241 and Polonium 210. Although the absolute magnitude of the extracted current for a given field and temperature was not the same in both cases, since the sources were of different strengths, there was no qualitative difference in characteristics observed.

Figures 5.3 and 5.4 show the variation of current with temperature in a constant extracting field for a diode immersed in liquid Helium, using Polonium 210 as the α source. Below 2K the agreement with Careri's result is very good. It may be seen from the figures that for fields between 50 and 100 volts $cm^{-1}$, there is a slight hump in the current at about the lambda point. For the lowest fields of 10 and 20 volts $cm^{-1}$, however, a large increase in current begins at about 2.8 K and ends at about 1.7 K, below which the extracted current remains constant until the temperature-dependent region is reached.

A recent calculation by Armitage (private communication) is of interest in the interpretation of the 10 volts $cm^{-1}$ characteristics of figures 5.3 and 5.4. He has obtained the variation of ionic current in a diode immersed in liquid Helium, as a function of the ionic mobility and therefore of temperature. Starting from Poisson's

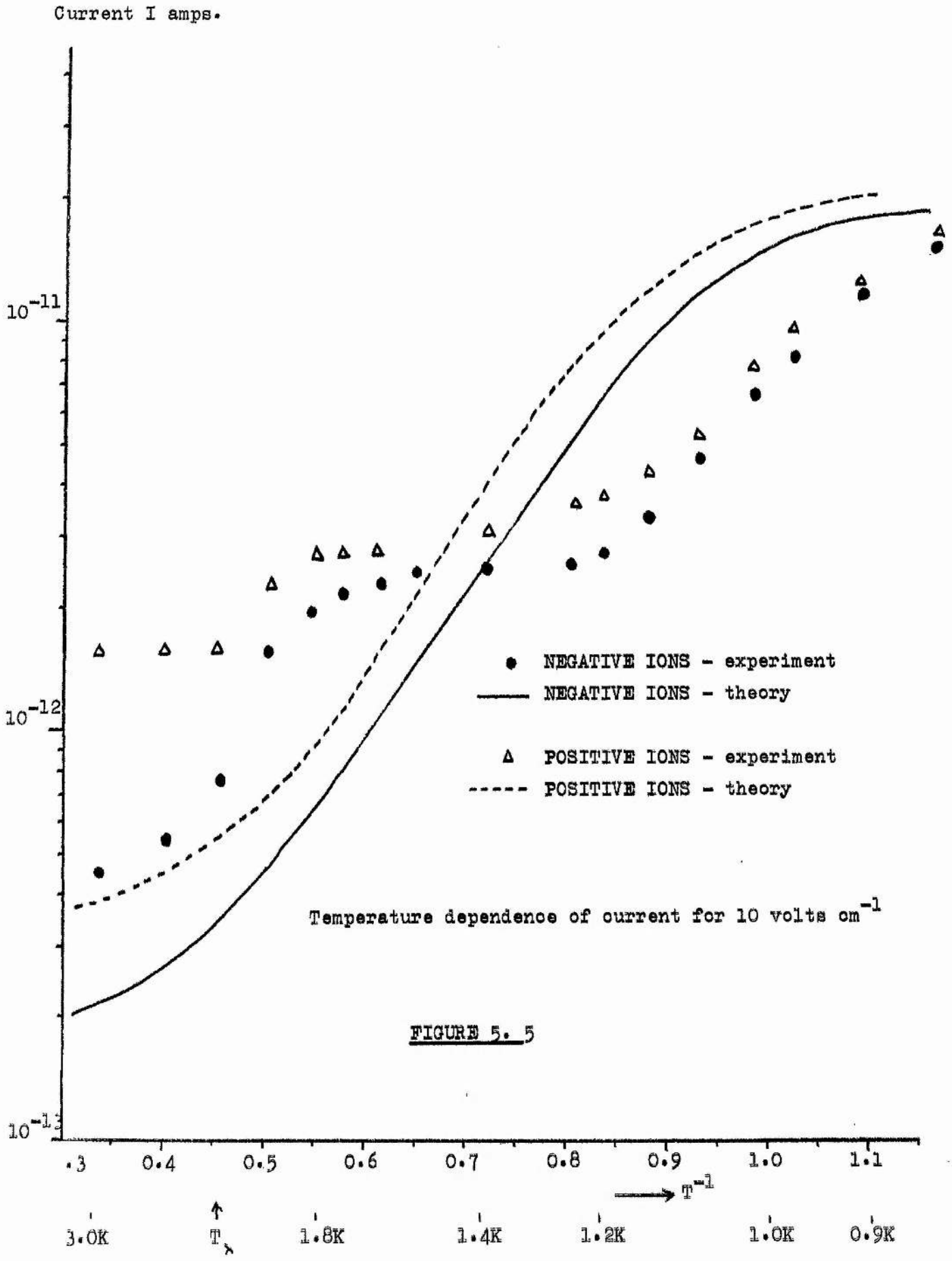
Current I amps.
$10^{-11}$
$10^{-12}$
$10^{-13}$
NEGATIVE IONS - experiment
NEGATIVE IONS - theory
POSITIVE IONS - experiment
POSITIVE IONS - theory
Temperature dependence of current for 10 volts $cm^{-1}$
.3
0.4
0.5
0.6
0.7
0.8
0.9
1.0
1.1
$T^{-1}$
3.0K
$T_\lambda$
1.8K
1.4K
1.2K
1.0K
0.9K

FIGURE 5. 5

equation and the general expression for current, two assumptions were made about the nature of ion extraction from the source. These assumptions are,

( i) that the current J extracted from the source depends upon the square root of the field at the source, and

(ii) in the limit of very low temperatures there is a maximum extractable current $J_o$ which can be obtained for a given extracting field.

The latter assumption appears to be borne out by the low temperature saturation effect becoming apparent from the data in figures 5.1, 5.3 and 5.4. The final solution relating current J and mobility $\mu$ is,

$$-\frac{16\ d^3}{\varepsilon_o\ V^2}\ \frac{J}{\mu} = (9-12\beta^2) + \sqrt{81 - 216\beta^2 + 192\beta^3 - 48\beta^4} \qquad (7)$$

where $\beta = (J/J_o)^2$, d is the source-collector distance, V is the collector potential, $\mu$ is the ionic mobility, and $\varepsilon_o$ is the dielectric constant of the liquid. The derivation of equation (7) is given in Appendix 1.

The dependence of J upon $\mu$ from equation (7) has been plotted in figure 5.5 along with the experimentally determined characteristics for a field of 10 volts $cm^{-1}$ in the Polonium 210 diode. While the agreement is far from satisfactory, the interesting point which emerges is that space charge effects are probably important for this low field at high temperatures, since equation (7) essentially illustrates the effects of space charge between the electrodes on the final collected current. In other words, between 4.2 K and 1.7 K the ionic currents extracted by very low fields are probably space charge limited. The absence of substantial temperature dependence in the same temperature range for the higher fields suggests that here

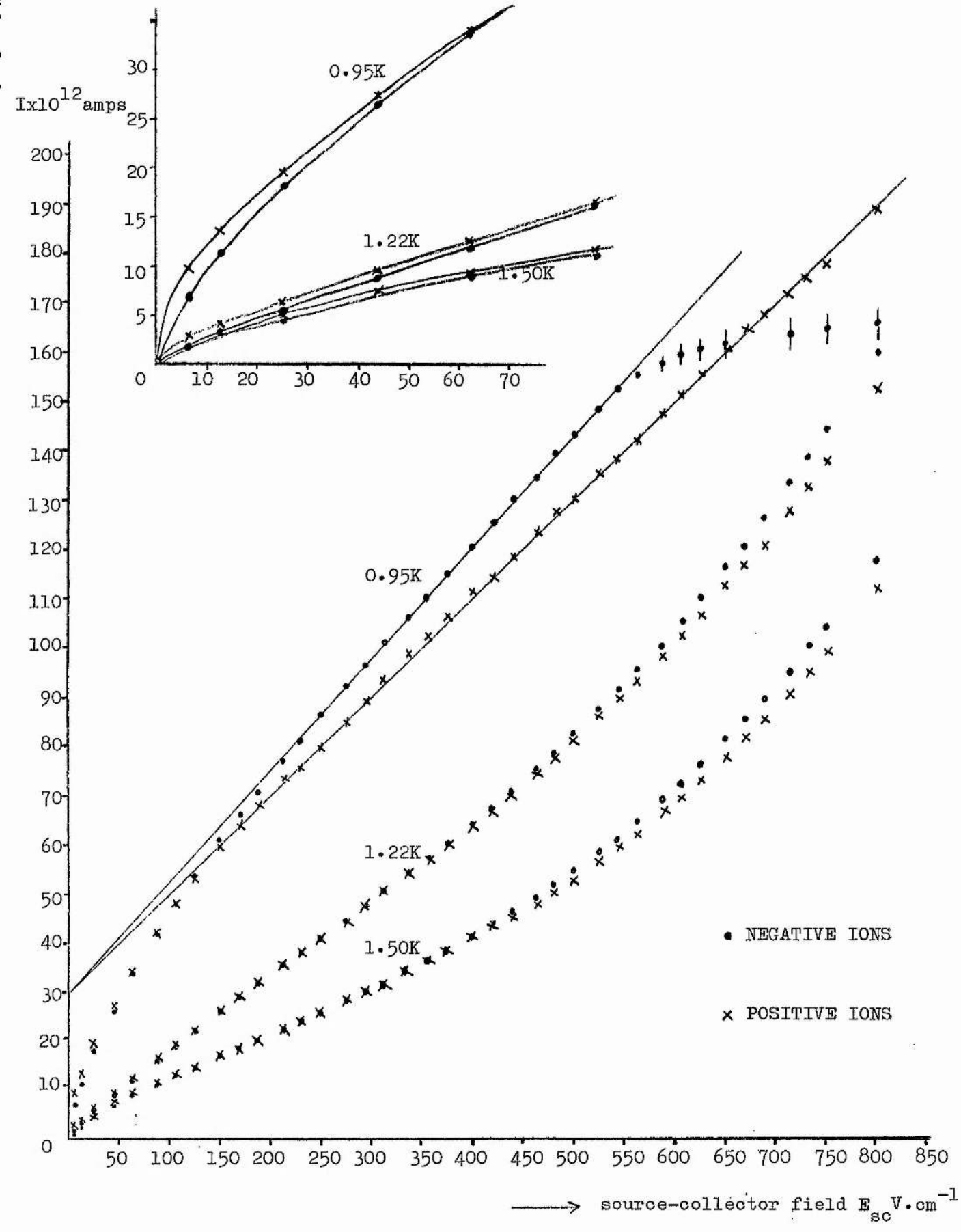


Field dependance of diode current at various temperatures

FIGURE 5.6

space charge effects are not important.

Close inspection of figures 5.3 and 5.4 reveals that at the lowest fields and highest temperatures, the extracted positive ion current was always greater than the negative one, while at the highest fields and lowest temperatures the negative ion current is greater than the positive one. In order to examine this effect in more detail, the positive and negative ion currents were measured as a function of extracting field at constant temperature. This is shown in figure 5.6 where those points in the neighbourhood of the origin have been plotted in more detail in the expanded insert. It may be seen that as the field was increased, the negative ion current gradually became equal to, and then greater than, the positive ion current. The effect was more pronounced at the lowest temperature, 0.95 K.

At 0.95 K, above about 600 volts $cm^{-1}$, the negative ion current became very unstable and deviated from its behaviour below this field. This is interpreted as being due to the negative ions becoming trapped by the vortex rings they have created, so that any further increase in field would result in an increase in vortex ring size and a corresponding decrease in ring and ion velocity.

The 0.95 K characteristic also exhibits almost linear behaviour above 150 volts $cm^{-1}$, as predicted by the Kramers theory (equation 6); this will be discussed in the next section.

## 6 Discussion

The linear portions of the 0.95 K characteristic shown in figure 5.6 may be described by the relation

$$I = 2.9 \times 10^{-12} E + 3 \times 10^{-11} \text{ for -ve ions,} \qquad (8)$$

$$\text{and} \quad I = 2.6 \times 10^{-12} E + 3 \times 10^{-11} \text{ for +ve ions,} \qquad (9)$$

where I is the current in amps, and E is the field in volts $cm^{-1}$. The low field solution of the Kramers theory, equation (6), for a temperature of 0.95 K, may be written in the form,

$$I = b.10^{-7} E + 10^{-11}, \qquad (10)$$

where b is the radius of the ionic cylinder created by the α particle. The agreement in the constant terms between experiment (equations 8 and 9) and theory (equation 10), to a factor of 3 is almost certainly fortuitous. In order to fit the experimentally determined gradients to the Kramers theory, b would have to assume a value of the order $10^{-5}$ cm, which is about ten times larger than its expected value of $10^{-6}$ cm. The fact that the negative and positive ion characteristics (equations 8 and 9) have different gradients would suggest a larger value of b for negative ion extraction than for positive.

Attention will now be focussed on the results shown in figures 5.1 to 5.4, where it was noted that below about 2 K, the data, at least for fields below about 400 volts $cm^{-1}$, describe two reasonably well-defined regions, one temperature-dependent, and the other not.

According to Gaeta, the horizontal temperature-independent region arises in the following way. The density and distribution of charges in the ionized layer in front of the source will be determined both by diffusion which tends to separate and spread the ionic columns, and by recombination which tends to destroy the ionic columns. Now since both the diffusion and recombination coefficients depend upon the first power of the mobility and are opposing factors in the determination, the final uniform ionic density will be independent of

mobility, and will therefore show no rapid variation with temperature. That is, in equation (3), once the balance between the (r) and (d) terms has been established, then $\partial n/\partial t$ can only be varied by the (e) term. In other words, the extracted current should depend only on the extracting field, as is observed above 1.4 K.

The transition to, and occurrence of, a temperature-dependent region below about 1.4 K is very difficult to understand. Careri failed to account for it, while Gaeta's explanation, which will be given for the sake of completeness, will later be shown to be unsatisfactory.

Gaeta has plotted the values of the constant field intensity against the reciprocal of the temperature at which the transition occurs at that field, (i.e. the points where the "bends" occur in figure 5.2 (a)). This is shown in figure 5.2 (b), where Gaeta has plotted his values superimposed on the Careri, Cunsolo and Mazzoldi (1961) curve relating field and reciprocal temperature for the positions of the Careri "steps" in mobility. Gaeta has suggested that the transition from the temperature independent to the temperature dependent region of his results in figure 5.2 (a) should be as abrupt a change as the change in ion velocity giving rise to a sudden change in ion mobility, and that the reason this is not observed is because of the way the effect of the transition on the current is measured. He has concluded;

"This means that the balance of recombination and drift is altered, once the ions acquire sufficient speed in the external field; the new state of the system being probably one in which the recombination coefficient is decreased, so that many more ions can be pulled out from the ionized layer before they recombine."

Gaeta's explanation cannot be considered plausible for a number

of reasons:

1) Since the mean thermal velocity of the ions at the "bend" temperatures is greater than the velocity acquired in the fields that he used, it is unlikely that the transition has anything to do with the acquisition of a speed which is less than the ion's intrinsic thermal velocity. Also, the mean drift velocity of the ion in the applied field will probably not be reached until the ion has been physically extracted, and this is an event subsequent to the process of extraction which he is trying to explain.
2) If the recombination coefficient suddenly drops as he suggests, then a discontinuity in current should result. In order to explain the temperature dependence in this way, the recombination coefficient would have to undergo a continuous change with falling temperature from the form of the Langevin expression, and this has been shown not to be the case by Careri and Gaeta (1961), who measured the recombination coefficient of ions in liquid Helium down to a temperature of about 0.80 K, and observed no unusual behaviour.
3) The suggestion of a sudden transition is not substantiated by his experimental results, which show the transition occurring over about 100 millidegrees. Furthermore, the association of the transition with ion mobility discontinuities, from figure 5.2 (b), is dubious in view of the contradictions in the current literature concerning their validity and existence.

Following the procedure of Gaeta, the transition points have been obtained from the present work by extrapolating the rectilinear portions of the temperature-independent and-dependent regions of figures 5.3 and 5.4, and noting the field and temperature of the

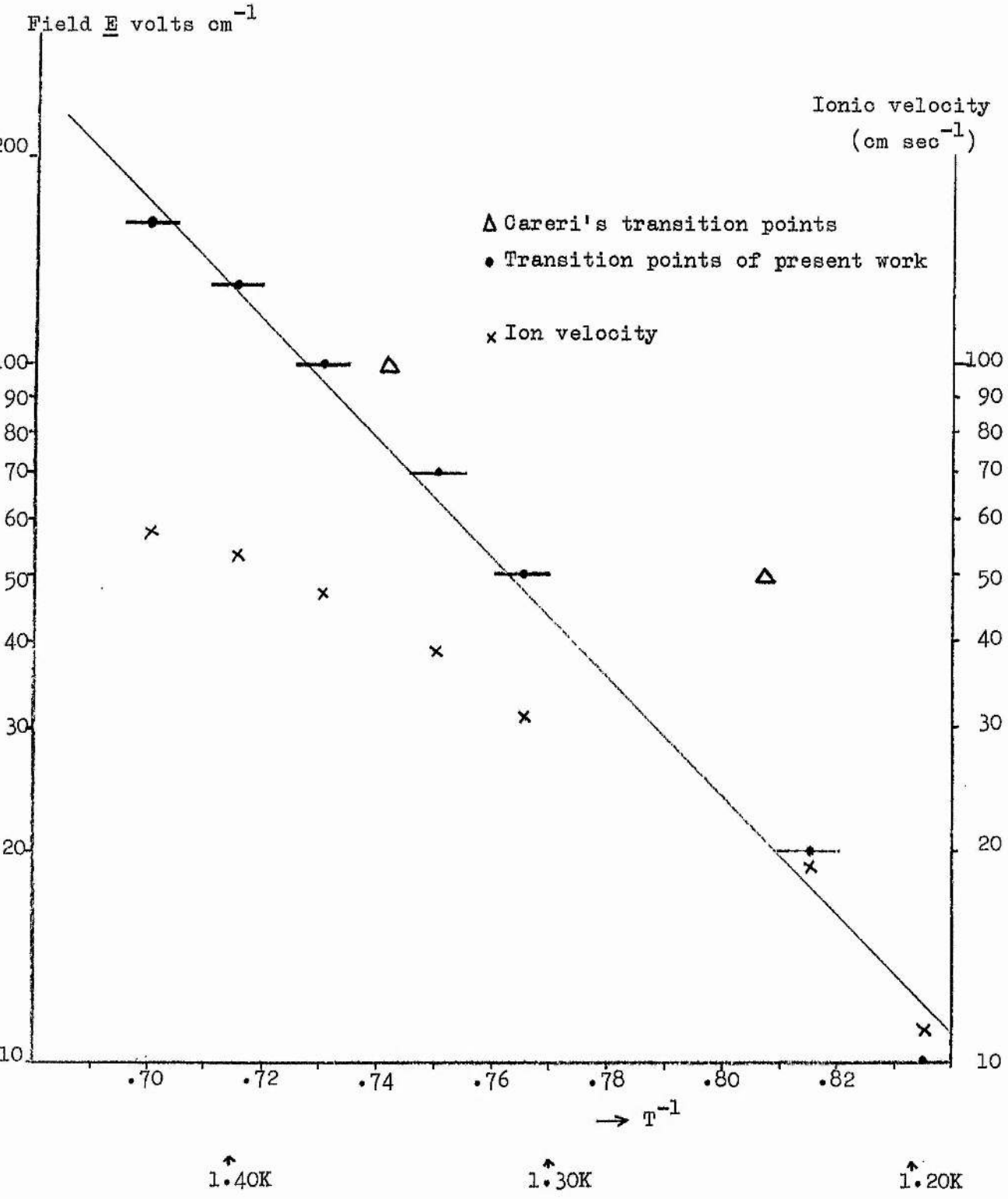


Plot of field versus temperature of bending points in figure 5.3 for NEGATIVE ions.

FIGURE 5. 7

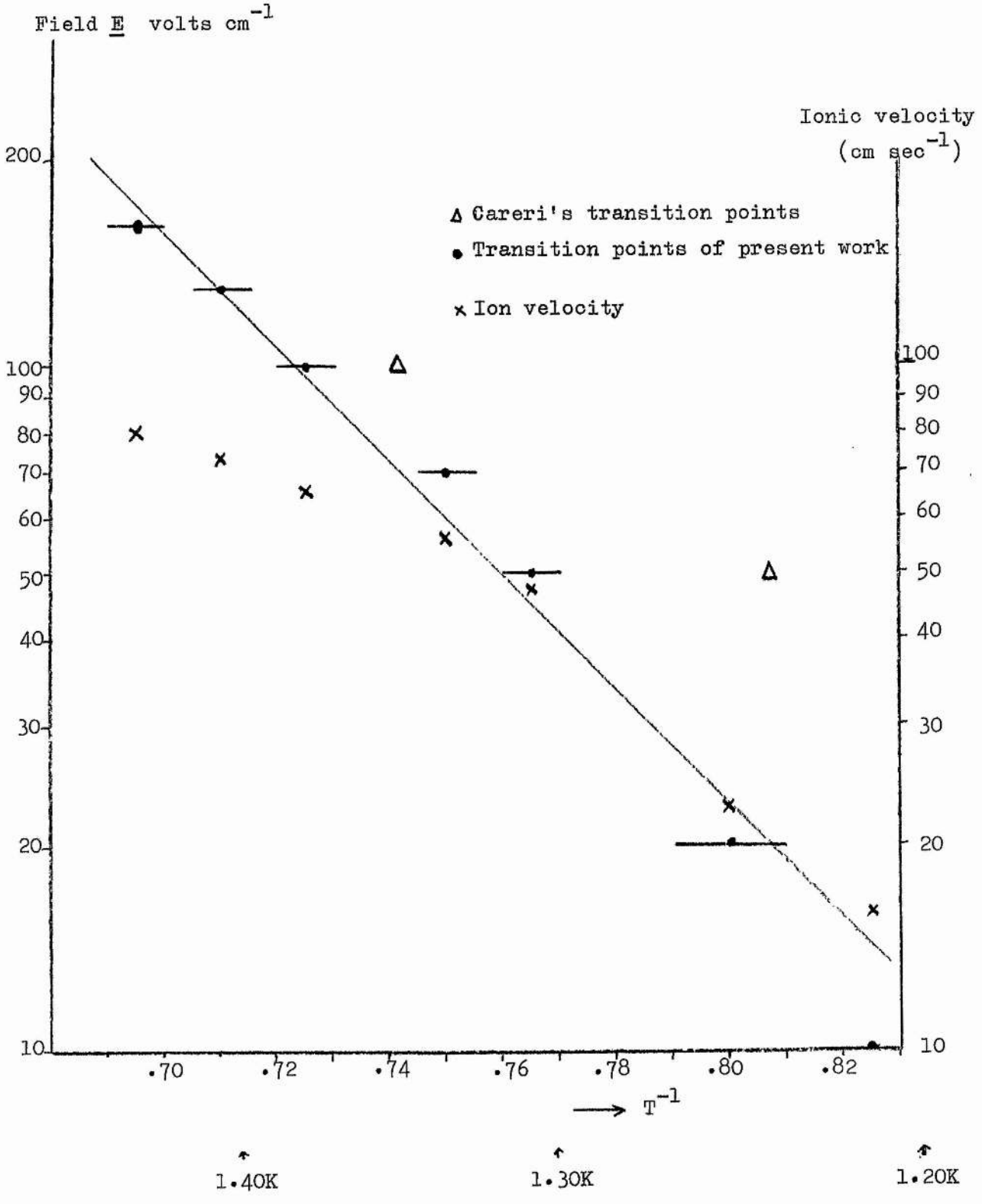


Plot of field versus temperature of bending points in figure 5.4 for POSITIVE ions.

FIGURE 5. 8

intersection point. The values of the field have been plotted against the reciprocal of temperature at the intersection point in figures 5.7 and 5.8, for negative and positive ions respectively. Some of the Careri transition points in figure 5.1 have also been plotted for comparison. It may be seen that, as observed by Gaeta in figure 5.2 (b), the present data lie, within experimental error, on a straight line, although the position of this line along the $T^{-1}$ axis is far removed from that of Gaeta in figure 5.2 (b).

In order to determine whether or not the transition was associated with an ionic velocity effect, the mobilities at various temperatures were measured. These results have already been shown in figure 4.2, and from the extrapolated data, the ionic mobility $\mu$ was determined at the various transition temperatures. The ionic velocity $v_T$ was then determined from $v_T = \mu_T E$, at the transition temperature T corresponding to the field E, and also plotted on the figures 5.7 and 5.8, using the same logarithmic scale for velocity as was used for the field. It may be seen from the two figures that there is little correlation between the variation of velocities, at the transition temperatures, and the variation of the corresponding field, so that it is unlikely that the transition is associated with the attainment of a particular velocity in the applied field.

Cope and Gribbon (1970) have advanced a possible explanation of the temperature dependent region of Gaeta's results. They have suggested that the tangled mass of vorticity, which will almost certainly exist in the immediate vicinity of the source, provides a means of ions avoiding recombination by being trapped in the vortex cores. That is, a trapped ion should find it difficult to recombine, since in order for it to do so, an oppositely charged ion must either penetrate into the vortex core, or the trapped ion must escape.

Tanner (1966) has measured the negative ion-vortex line capture cross-section as a function of temperature and field. He found that the capture cross-section increased with decreasing applied field, and that it displayed a maximum value between 0.9 K and 1.7 K. That is, below 0.9 K negative ions are not easily captured by vortex lines, while above 1.7 K the escape probability is so large that the lifetime in the vortex is very small (Donnelly 1967). Thus any effect in the source region between the ions and vortices should be negligible above about 1.7 K. As the temperature is lowered, the capture cross section increases so that the mechanism suggested by Cope and Gribbon should cause the current to rise, and also that this rise should be steeper for the smaller fields, since the capture cross section increases with decreasing field. This is as observed in figures 5.1, 5.3 and 5.4. As the temperature is lowered still further, the capture cross section falls off, so that the current should deviate from its initial slope and begin to level off. This is also observed in the figures 5.1, 5.3 and 5.4. It is interesting to speculate on the behaviour of the constant field currents which would result if the temperature were lowered still further. If the vortex-ion trapping suggestion has any foundation then the currents should fall off, if the capture cross section continues to decline. Unfortunately the present apparatus was not able to reach low enough temperatures to confirm this.

It is also possible to extend Cope and Gribbon's suggestion to account for the unusual current versus field characteristics shown in figure 5.6, where at high fields the negative ion current was greater than the positive one. The fact that, at low fields, the positive ion current was greater than the negative one for the same applied field could arise in the following way: after the $\alpha$ particles have

created their columns of ions and been brought to rest, they themselves will add to the ionized layer in front of the source. Since they have no immediate negative counterparts with which to recombine, this will have the effect that the positive ion density is greater than the negative one, and therefore any applied field should extract more positive ions than negative ones. However, this is seen to be only applicable at low fields. If it is assumed that there is some kind of vorticity flux away from the source, then this could provide an additional extracting mechanism favouring the negative ions, since the capture cross section, binding energy, and lifetime of the ion-vortex line, are greater for the negative ion. Any field-induced vorticity at the source would then magnify this effect, giving rise to a greater number of negative ions escaping recombination via the flux of vortices.

Cope and Gribbon's suggestion, therefore, would seem to provide a tentative explanation of the observed current versus temperature characteristics at constant field shown in figures 5.1 to 5.4. However, there are flaws in their suggestion, which are:-

1) Tanner observed the maximum in the capture cross section to lie between the temperatures of approximately 1.6 K and 1.3 K, whereas the present experiments reveal that the transition is not evident above 1.4 K, and that the currents are rising while the capture cross section is falling.
2) Tanner also observed the capture cross section to be greater for the lower fields, therefore the transition to the temperature-dependent region should occur at higher temperatures for the lower fields, whereas the opposite effect is observed.
3) The suggestion does not explain why the position of Gaeta's transition points for the $\beta$ source on the $T^{-1}$ axis in figure

5.2 (b), should be so far removed from the position obtained with the α sources in figures 5.7 and 5.8; nor does it explain why Gaeta observed the gradient of the temperature-dependent region to be greater for the higher fields.

## 7 Conclusion

While the qualitative features of the results in figures 5.1 to 5.4 are similar, there nevertheless appears to be certain fundamental differences in the temperature dependent nature of ion extraction from α and β sources immersed in liquid Helium II. This may be due in part to the different ways in which the respective particles establish the ionized layer; α particles create ionic pairs which are very closely spaced, while β particles create ionic pairs which are widely spaced.

The physical reasons underlying the temperature dependent behaviour shown in figures 5.1 to 5.4 are not clear. Careri remarked that no theory at the time could account for his results. Gaeta's explanation is wholly unsatisfactory, and the suggestion of Cope and Gribbon has been shown to be inadequate in accounting for all the results.

Finally, an effect which may be related to the temperature-dependent behaviour discussed above has been observed by Roberts and Hereford (private communication 1971) who measured the variation with temperature of the total luminescence produced in Helium II by the α particles from Polonium 210. They observed that below about 1.2 K the total luminescence decreased to a minimum at about 0.6 K and then rose again. Since the scintillation derives in part from recombination luminescence, it may be that there is a slight reluctance on the part of ionic pairs to recombine between 1.2 K and

0.6 K and this would certainly be consistent with present results. α-particle induced scintillation in liquid Helium will be considered again in chapter 9.

# CHAPTER 6

## NEGATIVE IONS AT THE LIQUID SURFACE

(Work performed by other authors)

### 1 Introduction

The differences in the temperature dependent behaviour of a beam of positive and of negative ions in the presence of the liquid-vapour interface in Helium are so great that separate chapters will be devoted to each species of ion. Chapters 6 and 7 will be concerned solely with the negative ion.

The effect of the liquid surface was first studied by Careri, Fasoli, and Gaeta (1960) while attempting to clarify some of the model structures which at that time had been proposed for the two ions. Their experiment consisted of measuring the variation of current with field at different temperatures in a diode cell when it was full of liquid, and comparing the results with those obtained when a liquid surface separated the source and collector. They observed that above the lambda point, the magnitude of the negative ion current which crossed the liquid surface was the same as the negative ion current obtained when the cell was full of liquid, while below the lambda point, the negative ions experienced increasing difficulty with decreasing temperature in crossing the liquid surface, from the liquid into the vapour.

Careri et al made no attempt systematically to study this effect as later workers have done. A summary of this work will be given in sections 2 to 5, to be followed in chapter 7 by the observations and conclusions of the present research.

(a)

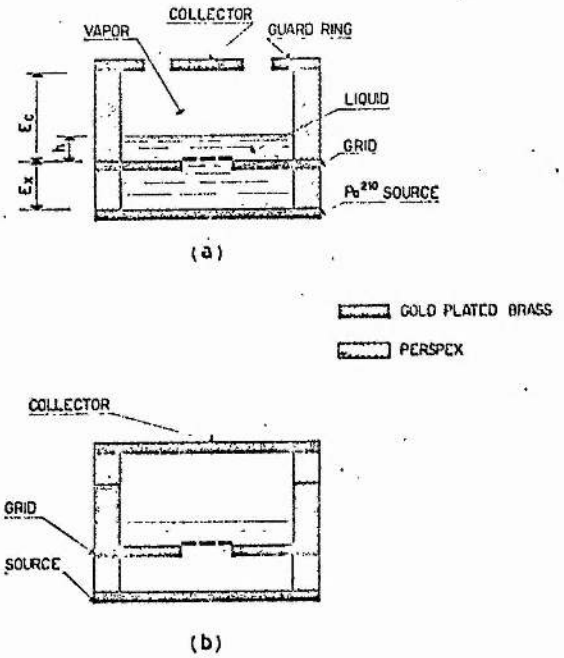


(b)

FIG. 1. Experimental cells. (a) Cell with insulating columns and guard ring, and (b) cell with conducting columns.

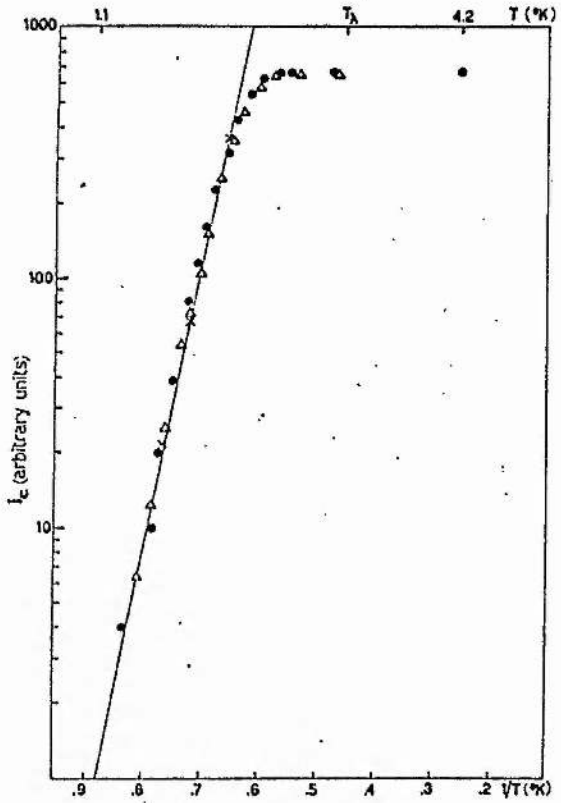


FIG. (c) Characteristic of the collected current. Circles: cell (a), $E_x = 300$ V/cm, $E_c = 200$ V/cm; triangles: cell (a), $E_x = 300$ V/cm, $E_c = 160$ V/cm; crosses: cell (b), $E_x = 400$ V/cm, $E_c = 20$ V/cm. The currents have been normalized to the same value in the TI region. The solid line is $I_c = AT^{1/2} \exp[-E_b/kT]$ with $E_b/k = 25$°K.

(c)

The results of Bruschi, Maraviglia and Moss (I966)

FIGURE 6. 1

2 Negative Ion transmission through the liquid surface

Bruschi, Maraviglia and Moss (1966) measured the temperature dependence of the negative ion current crossing the liquid surface, from the liquid into the vapour, in a constant field. The two ion cells used by them are shown in figures 6.1 (a) and 6.1 (b). Their results for two grid-collector fields of 200 and 160 volts $cm^{-1}$ with cell 6.1 (a), and a grid-collector field of 20 volts $cm^{-1}$ with cell 6.1 (b) are shown in figure 6.1 (c), where they have normalized the three characteristics to the same current value in the high temperature region. It may be seen from figure 6.1 (c) that Bruschi et al found the transmission current to lie in two reasonably well defined regions, one dependent upon temperature, and the other not. Above about 1.7 K, the current crossing the liquid surface in a constant field was independent of temperature, and was equal in magnitude to that current which was obtained in the same field if the cell was completely filled with liquid.

Below about 1.5 K, the current I was observed to fall exponentially with decreasing temperature according to

$$I = AT^{1/2} e^{-\phi/kT} ,$$

which indicated that the negative ions must surmount a potential barrier of $\phi$ in order to escape from the liquid into the vapour. Bruschi et al have estimated the energy barrier $\phi/k$ to be $25 \pm 1$ K, independent of the field applied across the surface.

Schoepe and Probst (1970) have repeated the above experiment and obtained slightly different results. They observed that the transmission current began to deviate from its horizontal, temperature-independent behaviour at higher temperatures for lower fields, and

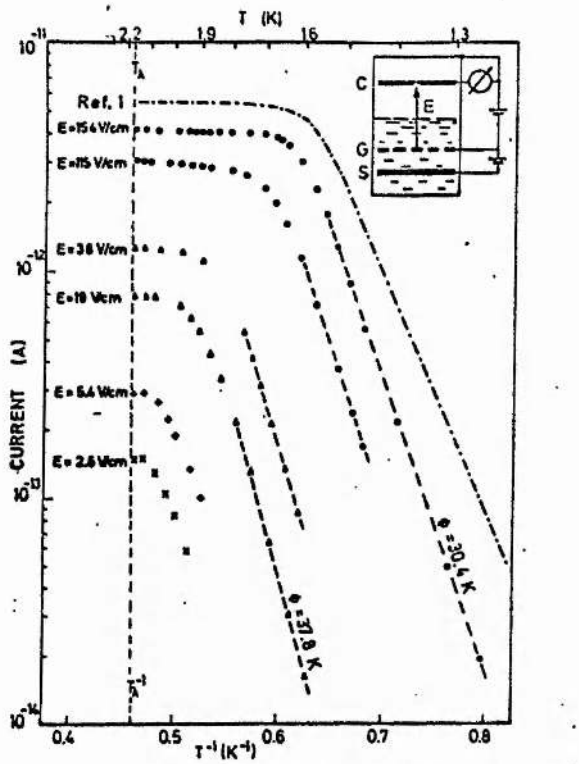


Fig. 1. Measured collector current through the surface of liquid $^4$He as a function of the temperature at different extracting fields $E$, indicated in the insert together with the electrode structure of the gold plated measuring cell (collector C, grid G, and radioactive source S). The slopes of the dashed curves yield the effective energy barrier $\phi(E)$. The relative current values of ref. [1] are indicated by the dash-dotted curve.

The results of Schoepe and Probst (I970)

FIGURE 6. 2

that the gradient of the exponential fall of current with decreasing temperature (and this determines the energy barrier) depended upon the magnitude of the field applied across the surface. That is, the energy barrier decreased with increasing applied field, varying from 30 K at 154 volts $cm^{-1}$ to 38 K at 19 volts $cm^{-1}$. Their results are shown in figure 6.2, where it may be seen that the fall in current begins closer and closer to the lambda point as the field is progressively reduced to very small values. Schoepe and Probst therefore suggested that the barrier was present only in the superfluid state, and argued that this could explain an observation of Schoepe and Dransfeld (1969) that there was no energy barrier at all when the liquid below the collector was rotating; in this latter case the negative ions escaped from the surface via the cores of the vortex lines which terminated there. That is, the absence of superfluid in the vortex core denies the existence of an energy barrier. The suggestion that the energy barrier is present only in the superfluid state will be discussed in section 7.8 (a).

Rayfield and Schoepe (1971) have measured the lifetimes of negative ions held below the free surface by the energy barrier. They observed that the trapping time was longer for the smaller applied fields across the surface, and interpreted their results as a process of thermal diffusion over a field-dependent energy barrier; the zero field barrier being 43.8 K.

Finally, Williams, Grandall and Willis (1971) performed a similar experiment to that of Rayfield and Schoepe, and obtained a value for their energy barrier of 27 K in a field of 100 volts $cm^{-1}$. This is substantially different from the 37.4 K expected for the same field from the work of Rayfield and Schoepe. A possible explanation of this difference, along with the differing results of Bruschi et al

and Schoepe and Probst will be advanced in section 7.8 (e).

3 Origins of the Energy Barrier

It is well known in electrostatics that if a charge q is located in a medium 1 of dielectric constant $\varepsilon_1$ at a distance x from a medium 2 of dielectric constant $\varepsilon_2$, then for problems concerning the charge q, the medium 2 may be replaced by an image charge q' located at an equal distance x on the opposite side of the boundary separating the two dielectrics, where

$$q' = \left( \frac{\varepsilon_1 - \varepsilon_2}{\varepsilon_1 + \varepsilon_2} \right) q \, .$$

Thus if $\varepsilon_1 > \varepsilon_2$ the image charge is of the same sign as the real charge, and the real charge will experience a repulsion from the boundary. If, however, $\varepsilon_1 < \varepsilon_2$ then the image charge will be of opposite sign and the real charge will experience an attraction to the opposite dielectric.

Thus, an ion which finds itself in liquid Helium near the liquid-vapour interface will experience a repulsive potential preventing it from crossing into the vapour. Conversely, an ion which finds itself in the vapour above the liquid will experience an attractive potential towards the liquid.

The repulsive image potential $\phi_a (x)$ presented to an ion, of charge e, in the liquid by the liquid surface is

$$\phi_a (x) = \frac{e}{8\pi} \frac{(\varepsilon - \varepsilon_o)}{\varepsilon (\varepsilon + \varepsilon_o} \frac{1}{x} \, , \qquad (1)$$

where $\varepsilon$ and $\varepsilon_o$ are the dielectric constants of the liquid and vapour respectively, and x is the distance from the ion to the liquid surface

which is assumed to be flat. The macroscopic expression (1) will break down when the distance x is of the order of the interatomic spacing, since otherwise an infinite potential barrier would result.

Bruschi et al noted that the magnitude of $\phi_a(x)$ for values of x approaching the ion radius was about an order of magnitude greater than their observed value of 25 K. They suggested than an ion located very close to the liquid surface might be able to reduce its electrostatic energy by creating a bulge in the liquid surface. The energy needed to create such a bulge would then be equal to the decrease in electrostatic energy which would result from the addition of liquid to the unperturbed surface above the ion.

The energy required to create a bulge of thickness d and of radius r (where r is assumed to be greater than x), against the liquid surface tension $\gamma$ can be shown to be,

$$\gamma \pi d^2 .$$

We ignore the gravitational energy of such a bulge which is about $10^{10}$ times smaller than the surface energy. Thus,

$$A \cdot \frac{1}{x} - A \cdot \frac{1}{x + d} = \gamma \pi d^2 , \qquad (2)$$

where A is given by,

$$A = \frac{e^2}{8\pi} \frac{(\varepsilon - \varepsilon_o)}{\varepsilon (\varepsilon + \varepsilon_o)} . \qquad (3)$$

Assuming x to be of the order of the negative ion bubble radius, equations (2) and (3) yield $d \sim 10$ Å, so that a relatively large bulge in the surface may be created. Inserting (x + d) in place of

x in equation (1) and taking x to be of the order of the bubble radius, of 12.4 Å as estimated by Hiroike, Kestner, Rice and Jortner (1965), gives a value of the image potential energy barrier $\phi_a'$ of about 100 K which is closer to, but still much greater than the observed energy barrier.

Bruschi et al have considered a further influence on the magnitude of the energy barrier. This is the repulsive interaction between the negative ion (electron) and the atoms of the liquid. As the ion approaches the liquid surface it should experience an attractive potential into the vapour due to the short range repulsion between the electron and the liquid. This attractive potential $\phi_b(x)$ may be written as,

$$\phi_b = \int \psi_\xi^* \phi_e \psi_\xi \, d^3r$$

$$= \int |\psi_\xi|^2 \phi_e \, d^3r \, . \qquad (4)$$

This follows from the results of Jortner, Kestner, Rice and Cohen (1965) and of Hiroike et al, where

$$\psi_\xi = (\xi^3/\pi)^{1/2} \, e^{-\xi r} \qquad (5)$$

is the electron wave function, and $\xi$ is a variational parameter used in the minimization of the energy, and where

$$\phi_e = \int V_\xi(r) \, \rho(r) \, d^3r \qquad (6)$$

is the potential seen by the excess electron. $V_\xi$ is the electron-Helium atom pseudopotential and $\rho(r)$ is the density distribution,

such that $\rho = 0$ inside the negative ion bubble which has radius R, and $\rho = \rho_o$, the liquid density, outside the bubble. Bruschi et al have taken the pseudo potential to be

$$V_\xi = C.e^{-2\xi r} . \tag{7}$$

Equations (6) and (7) lead to

$$\phi_e = \frac{2\pi C}{\xi^3} \rho_o e^{-2\xi R} \left[(\xi R)^2 + (\xi R) + \frac{1}{2}\right] . \tag{8}$$

Equations (4), (5) and (8) then yield the final result for the attractive potential,

$$\phi_b (x) = \frac{C\pi\rho_o}{4\xi^3} \left[(\xi R)^2 + (\xi R) + \frac{1}{2}\right] e^{-2\xi(x - R)} .$$

Using the relevant values of $\xi$, C, and R, from the results of Hiroike et al, and for values of x approaching R, $\phi_b$ is of order 10 K.

The final energy barrier $\phi$ presented by the liquid surface to a beam of negative ions is then given by,

$$\phi = \phi_a' \text{ (image + bulge)} - \phi_b \text{ (interaction)} ,$$

and for values of x approaching the ionic radius,

$$\phi \sim 90 \text{ K} ,$$

which is still about a factor of three greater than the observed energy barrier.

The inability of the image potential (1) to account for an

observed energy barrier of 25 K has also been noted by Kuchnir, Roach and Ketterson (1970) who found an energy barrier of about 4.5 K to the transmission of negative ions through the $He^4$ - $He^3$ phase boundary from the $He^4$ rich side. The observed energy barrier was less than half the value predicted by the image potential and they could only explain this by assuming that the $He^4$ - $He^3$ phase boundary has a finite width of about 5 Å.

4 Field dependence of the energy barrier.

The energy barrier at the liquid-vapour surface in Helium manifests itself in the exponential decay of current crossing that surface with decreasing temperature. This process has been described by

$$I \propto e^{-\phi/kT},$$

and is analagous to the process of thermionic emission of electrons from a metal, where an electron must gain an energy of at least the work function in order to escape. That is, a negative ion which finds itself below the liquid surface can only cross into the vapour if it acquires a velocity normal to the surface greater than some critical value.

The height of the energy barrier which the negative ion must actually surmount in order to escape will depend upon the field which exists inside the liquid. This is because the potential of an ion inside the liquid is the sum of the image potential (1) and the potential due to the electric field gradient. If the ionic potential in the liquid is V (x), where x is the distance from the ion to the liquid surface, then,

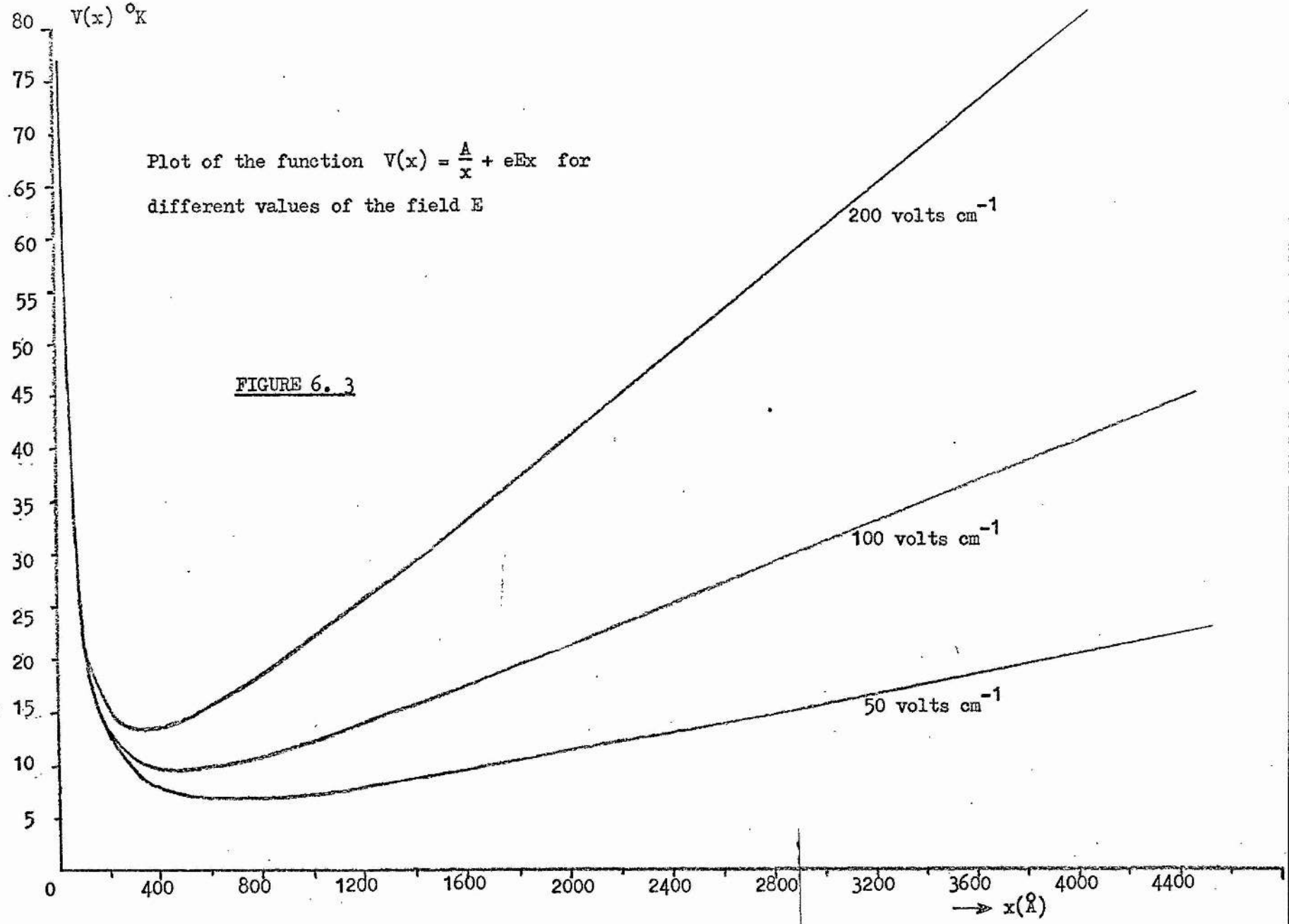


Plot of the function $V(x) = \frac{A}{x} + eEx$ for different values of the field E

FIGURE 6. 3

$$V(x) = \frac{A}{x} + e E x \quad , \tag{9}$$

where A is given by (3) and E is the field inside the liquid. The form of equation (9) has been plotted in figure 6.3 for three different values of the field strength. The minimum in the curve occurs at $V = 2\sqrt{AeE}$ and therefore the barrier which the negative ion must surmount is equal to $\phi_E$ where

$$\phi_E = \phi_o - 2\sqrt{AeE} \quad , \tag{10}$$

and $\phi_o$ is the zero field barrier. From the field dependence of their results Rayfield and Schoepe estimated $\phi_o$ to be 43.8 K, while Bruschi et al obtained a value for $\phi$ of 25 K, which was independent of the applied field.

5 Work on Film currents

By measuring the current collected on the guard ring of the cell 6.1 (a), Bruschi et al observed that when the negative ion current crossing the liquid surface was falling rapidly with decreasing temperature the current collected on the guard ring was rising in such a way that the sum of the transmission and guard ring currents was equal to the current which was collected when the cell was full of liquid. They therefore concluded that no space charge was built up in the region below the surface, and that the negative ion current collected on the guard ring was due to negative ions travelling in the Helium film covering the cell walls.

Maraviglia (1967) extended this work, finding that whenever the collecting electrode of an ion cell was connected to the liquid surface by the Helium film on an insulating support, an ionic current

would always be collected, even when the current crossing the liquid surface was negligible. The current was therefore assumed to travel via the Helium film. He further found that the current was equal in magnitude to that which was obtained when the cell was full of liquid. On this assumption, he measured the mobility of the ions in the film and obtained a result for the negative ion which was about twenty times smaller than the mobility in the bulk liquid at the same temperature.

Using a diode cell in a glass beaker, Bianconi and Maraviglia (1969) found the positive ion current in the film to be sensitive to film flow, and in fact observed oscillations in the positive ion film current at twice the frequency with which the level of liquid in the beaker was oscillating due to inertial film oscillations. They did not experiment with negative ions, "because of their tendency to evaporate at $T > 1.2$ K". However, they were able to work in a temperature range down to about 0.9 K which makes the statement difficult to understand.

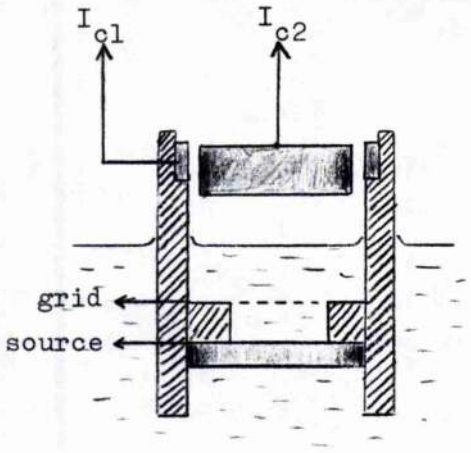


(a) PERSPEX TRIODE

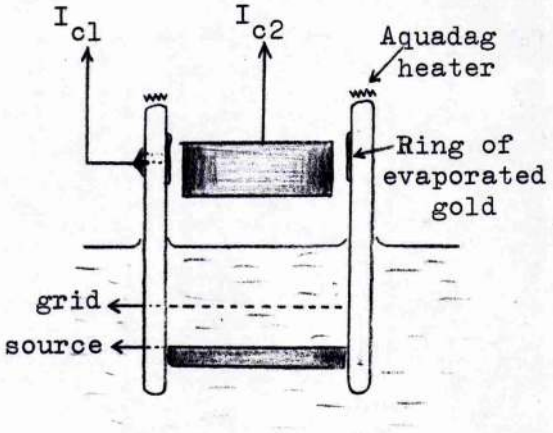


(b) GLASS TRIODE

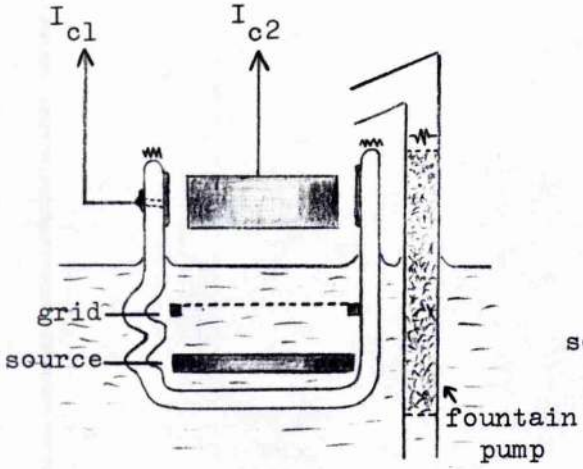


(c) TRIODE IN GLASS BEAKER

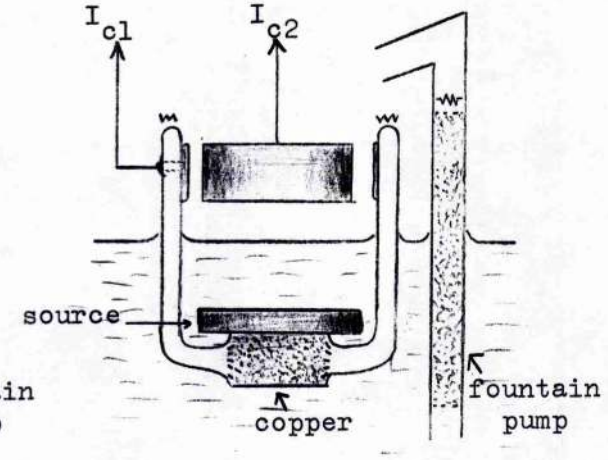


(d) DIODE IN GLASS BEAKER

Ion cells used in the present work

FIGURE 7. 1

# CHAPTER 7

## NEGATIVE IONS AT THE LIQUID SURFACE

(Work performed during the present research)

### Experimental Procedure and Observations

#### 1 Design of Ion Cells

Typical ion cells which were used in the present work are shown in figure 7.1. Each cell is characterized by having two collectors, C1 which is a gold ring around the rim of the cell and C2 which is a gold plated brass disc suspended above the liquid surface. The current $I_{c2}$ was that crossing the liquid surface to C2. The current $I_{c1}$ was that which was collected by C1, and travelled either through the Helium film which covered the cell walls or by some other path from the source. In perspex cells, C1 was a gold plated brass ring inserted into the cell rim, while in glass cells it consisted of a ring of evaporated gold. Both perspex and glass were used to study any effect the nature of the substrate might have on the currents $I_{c1}$.

The inside surfaces of the glass cells were flame polished to reduce surface irregularities.

Electrical contact was made to the evaporated gold rings by pressing Indium through a hole which had previously been bored through the glass and smearing it out on the inside and outside surfaces around the hole. Contact was improved on the inside by silver painting round the smear, while contact to the collector lead on the outside was achieved by carefully welding a fine wire to the outside smear.

Electrical contact with the grid and source of the triode in the glass beaker 7.1(c) was made via two Tungsten wires sealed into the

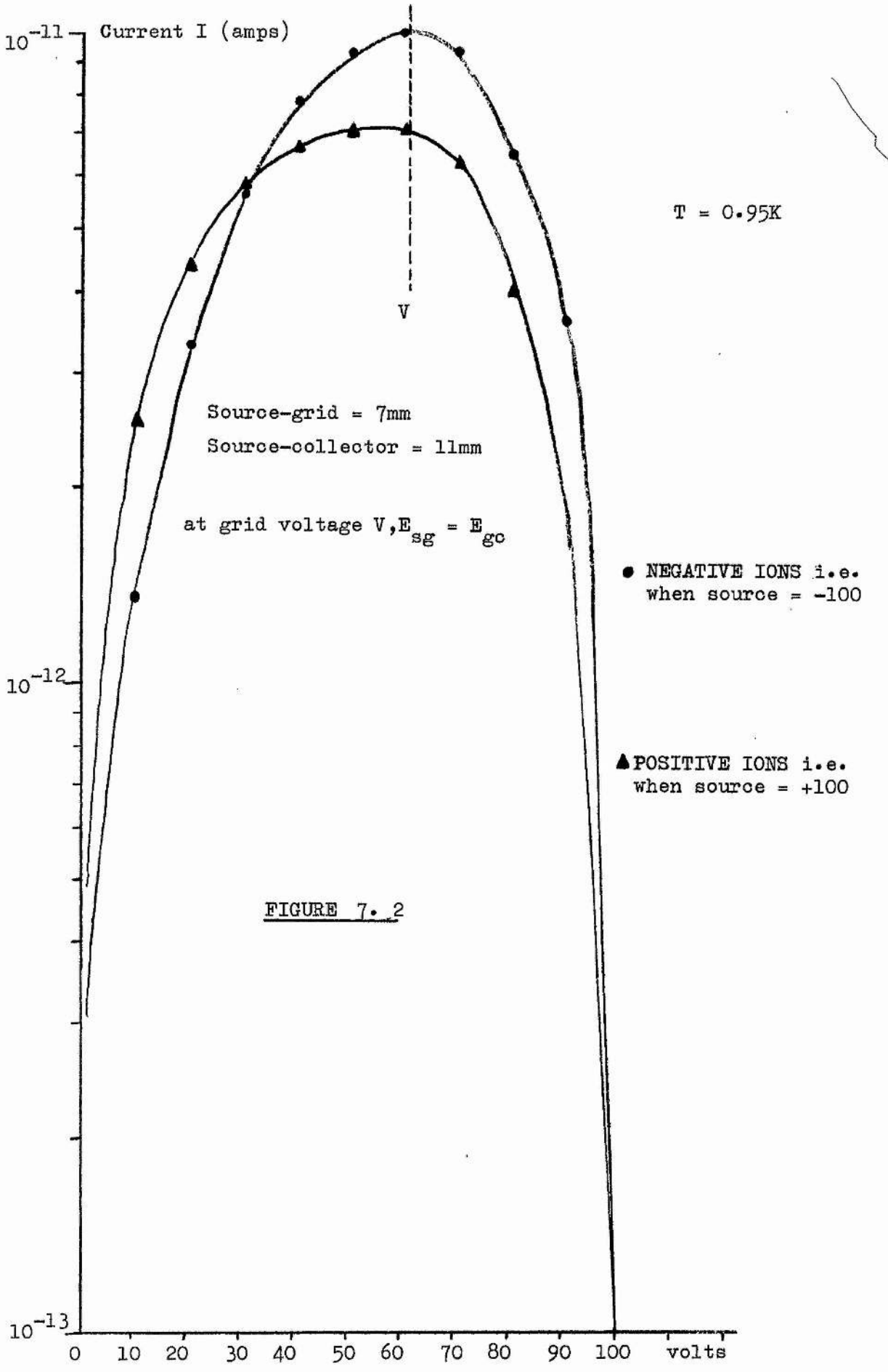
Current I (amps)
$10^{-11}$
$10^{-12}$
$10^{-13}$
V
T = 0.95K
Source-grid = 7mm
Source-collector = 11mm
at grid voltage V, $E_{sg} = E_{gc}$
● NEGATIVE IONS i.e. when source = -100
▲ POSITIVE IONS i.e. when source = +100
0 10 20 30 40 50 60 70 80 90 100 volts
Voltage applied to grid when source voltage kept constant at ± 100 volts

FIGURE 7. 2

pyrex glass. Contact with the source of the diode in the glass beaker 7.1(d) was made via the copper post sealed into the glass bottom. The beakers shown in figures 7.1(c) and (d) could be filled, or have their liquid level increased by using a small fountain pump located beside each beaker.

A film of Aquadag was painted around the lip of each glass cell and electrical contact made to it by silver paint and two fine wires. By passing a current through the Aquadag it was possible to "drive" the film thermally in order to study any effect the film's motion might have on the current.

In the design of each cell it was essential that no current be collected on the film collector C1 when the cell was full of liquid, so that any current $I_{c1}$ subsequently detected when a liquid surface separated the grid and collector, or source and collector, might be attributed to its passage through the film.

## 2 Experimental Procedure

When examining the temperature dependence and D.C. characteristics of a triode cell, such as figure 7.1(a), (b) or (c), the extracting field $E_{sg}$ between the source and grid was always kept at the same value as the field $E_{gc}$ between the grid and collector. The reason for this is demonstrated in figure 7.2. If a constant voltage is applied to the source of a triode which is fully immersed in the liquid, and the grid voltage is varied between zero and the voltage on the source, then the collected current exhibits the behaviour shown in the figure. This is because the conditions vary from maximum extracting field but zero collecting field to maximum collecting field but zero extracting field. The maximum in the collected current occurs at the voltage V, at which point $E_{sg} = E_{gc}$.

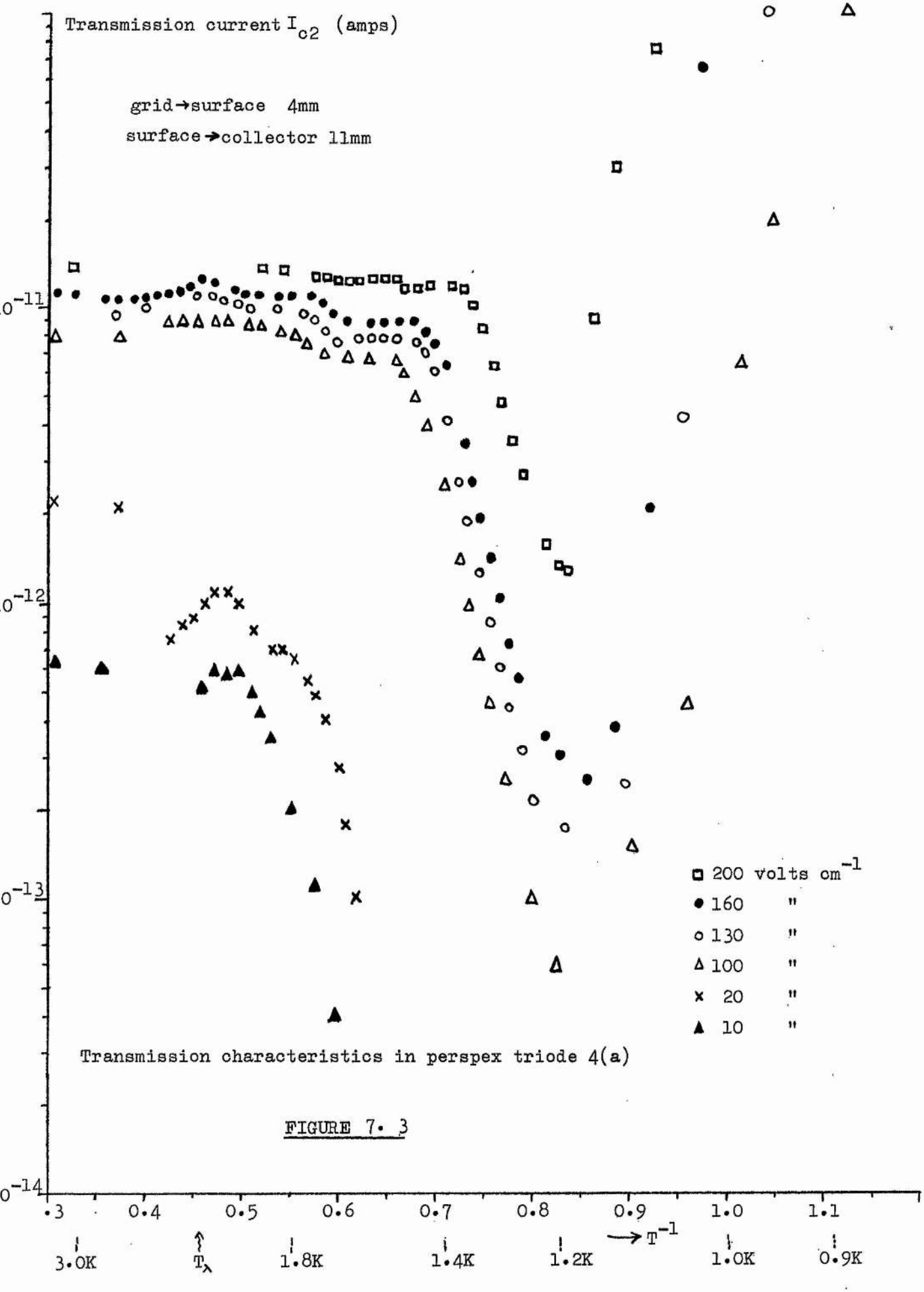
Transmission current $I_{c2}$ (amps)
grid→surface 4mm
surface→collector 11mm
$10^{-11}$
$10^{-12}$
$10^{-13}$
$10^{-14}$
200 volts $cm^{-1}$
160 "
130 "
100 "
20 "
10 "
Transmission characteristics in perspex triode 4(a)
FIGURE 7. 3
·3
0·4
0·5
0·6
0·7
0·8
0·9
1·0
1·1
$\rightarrow T^{-1}$
3·0K
$T_\lambda$
1·8K
1·4K
1·2K
1·0K
0·9K

It may therefore be deduced that the effect of a grid on an ion beam is minimal when the fields on both sides of it are equal.

Before observing the variation of currents with field and temperature in the presence of the liquid surface, the cell being used would normally be completely filled with liquid and the constant field current versus temperature characteristics would be noted. For both triode and diode cells the results display the features already shown in figure 5.3.

In order to record the variation of current with temperature in a constant field, for different constant values of the field, either the temperature could be held constant and the field varied, or the field could be held constant and the temperature varied. The latter method was found to be preferable since changing the field to take a new reading often involved a long wait before a stable reading could be observed.

## 3 The Transmission Current $I_{c2}$ for Negative Ions

The variation of current crossing the liquid surface with temperature in a constant applied field in the perspex triode cell 7.1(a) is shown in figure 7.3, for some fields between 200 and 10 volts $cm^{-1}$, when the liquid surface was 4 mm above the grid and 11 mm below the collector C2. The striking effect of the liquid surface is clearly seen by comparing the features of figure 5.3 with figure 7.3.

It may be seen from figure 7.3 that above about 1.2 K, the results are very similar to those of Schoepe and Probst shown in figure 6.2, in that the fall in current due to the effect of the surface barrier occurs at higher temperatures for lower fields.

A comparison of the figure 7.3 with the results obtained when

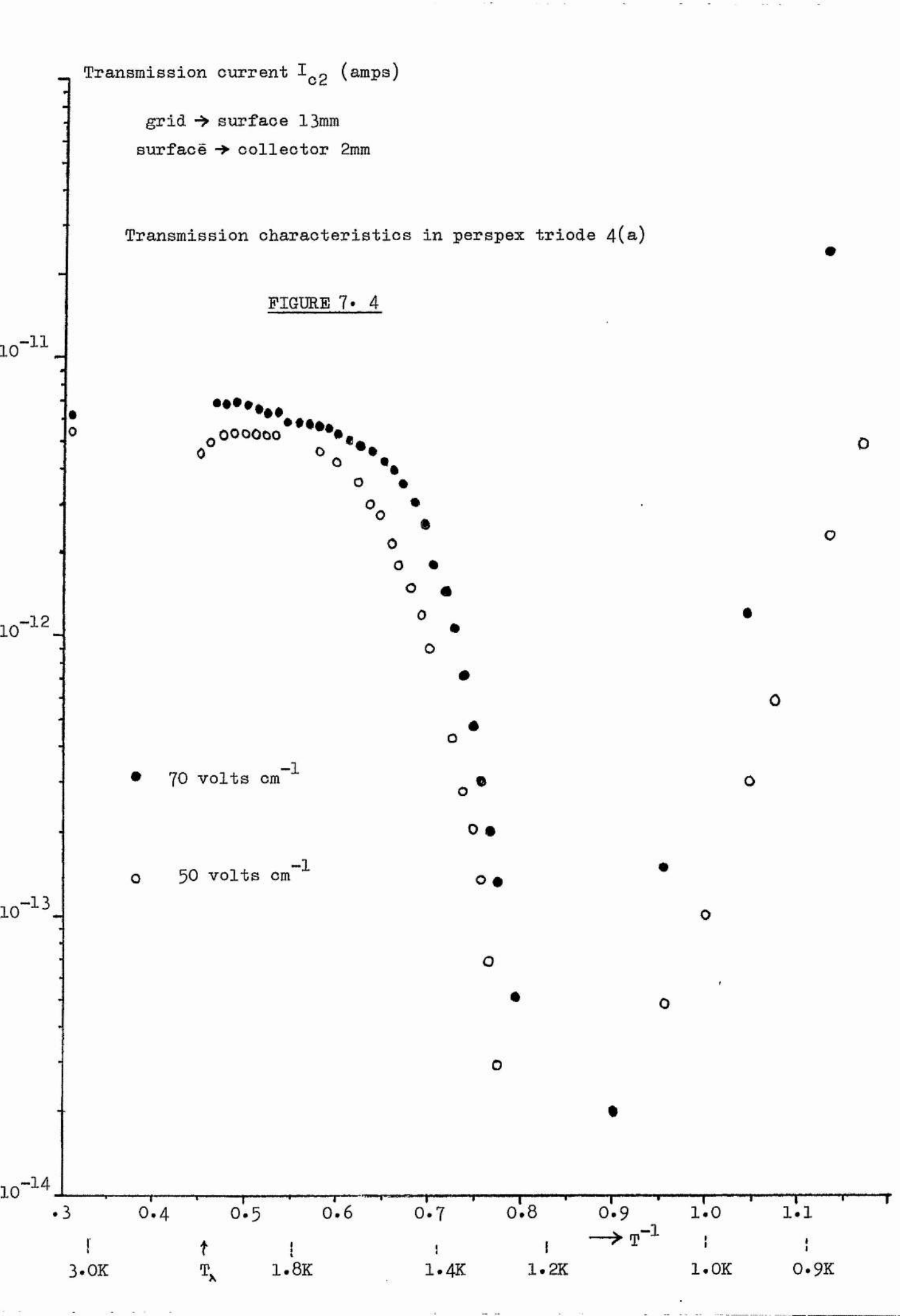
Transmission current $I_{c2}$ (amps)
grid → surface 13mm
surface → collector 2mm
Transmission characteristics in perspex triode 4(a)
FIGURE 7. 4
$10^{-11}$
$10^{-12}$
$10^{-13}$
$10^{-14}$
70 volts $cm^{-1}$
50 volts $cm^{-1}$
.3
0.4
0.5
0.6
0.7
0.8
0.9
1.0
1.1
$\rightarrow T^{-1}$
3.0K
$T_\lambda$
1.8K
1.4K
1.2K
1.0K
0.9K

TABLE 1

| Grid-Collector field $\underline{E}$ | Energy Barrier $\phi_E$ | Zero field barrier $\phi_o$ $\phi_o = \phi_E + 2\sqrt{AeE}$ |
|---|---|---|
| 200 volts $cm^{-1}$ | 26 $\pm$ 2 K | 47 $\pm$ 2 K |
| 160 volts $cm^{-1}$ | 30 $\pm$ 2 K | 48 $\pm$ 2 K |
| 130 volts $cm^{-1}$ | 32 $\pm$ 2 K | 48 $\pm$ 2 K |
| 100 volts $cm^{-1}$ | 34 $\pm$ 2 K | 48 $\pm$ 2 K |

The energy barrier $\phi_E$ measured from the results of Fig. 7·3 when,

grid → surface = 4 mm

surface → collector = 11 mm,

and the calculated value of the zero field barrier $\phi_o$.

the cell 7.1(a) was full of liquid reveals that for the two low field characteristics (i.e. 10 and 20 volts $cm^{-1}$), above about 2.5 K, the current crossing the liquid surface is greater than the current which was obtained when the cell was full of liquid. This is consistent with the suggestion in chapter 5 that the low field currents in a cell are limited by space charge in the liquid.

For fields greater than about 100 volts $cm^{-1}$, in all the ion cells used, it was always possible to draw a reasonable straight line through the data points in the region where the current $I_{c2}$ was falling with decreasing temperature, and therefore it was possible to measure the energy barrier since this corresponded to an exponential fall in current.

For fields below about 100 volts $cm^{-1}$ the behaviour of the transmission current was generally less well defined, and the transition from the temperature-independent region to the temperature-dependent fall was often very gradual indeed, as can be seen from figure 7.4, where the results of the 50 and 70 volts $cm^{-1}$ characteristic for the perspex triode have been shown.

The measured energy barriers for fields between 200 and 100 volts $cm^{-1}$ display a field dependence. The results from the perspex triode shown in figure 7.3 are shown in table 1, where the zero field barrier $\phi_o$ given by equation 6.(10) has been calculated. The value of $\phi_o$ in table 1 is only meaningful for the particular ion cell used and with the liquid surface in the stated position. This is because the values of the measured energy varrier $\phi_E$ varied from cell to cell, with the applied field, and, as will be discussed later, with the liquid level in the cell.

It can be seen in figures 7.3 and 7.4 that below about 1.15 K the transmission current stops falling and begins to rise with falling

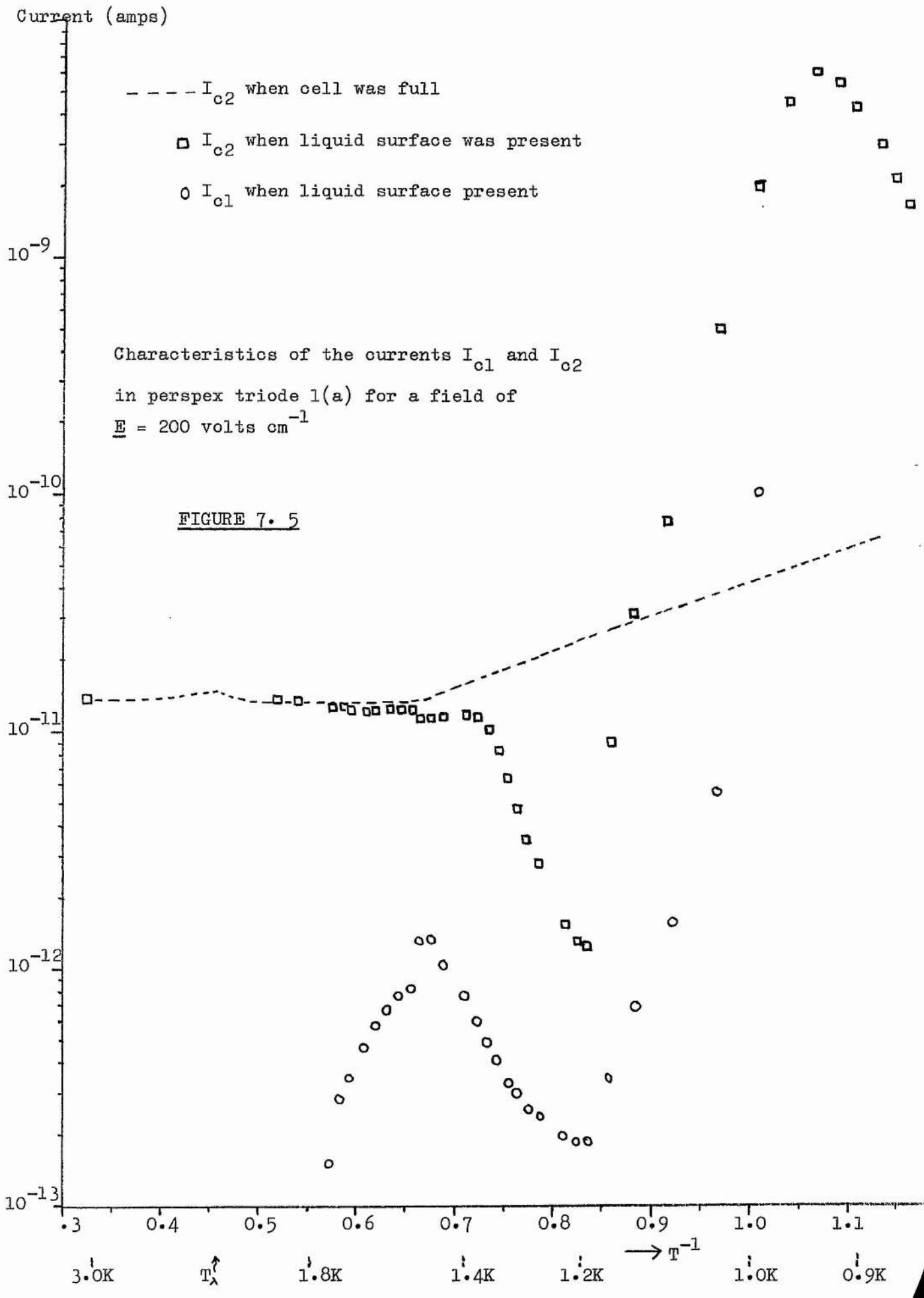
Current (amps)
- - - - $I_{c2}$ when cell was full
$I_{c2}$ when liquid surface was present
$I_{c1}$ when liquid surface present
$10^{-9}$
$10^{-10}$
$10^{-11}$
$10^{-12}$
$10^{-13}$
Characteristics of the currents $I_{c1}$ and $I_{c2}$
in perspex triode 1(a) for a field of
$\underline{E}$ = 200 volts $cm^{-1}$
FIGURE 7. 5
·3
0·4
0·5
0·6
0·7
0·8
0·9
1·0
1·1
$\rightarrow T^{-1}$
3·0K
$T_\lambda$
1·8K
1·4K
1·2K
1·0K
0·9K

temperature, with the exception of the 10 and 20 volts $cm^{-1}$ characteristics which showed no low temperature rise for the liquid level quoted, although for higher liquid levels these characteristics also showed a low temperature rise, (see figures 7.9 and 7.10). For the higher fields, the rise was very steep, and reached a high peak as the temperature was reduced. This is shown in figure 7.5 for the 200 volts $cm^{-1}$ characteristic. The dotted line in figure 7.5 shows for comparison, the current collected on C2 when the perspex triode cell of 7.1(a) was completely full of liquid. The current collected on the film collector C1 when a liquid surface separated the grid and collector C2 is also shown. This current $I_{c1}$ will be discussed in section 7.6 when the current carried by the film is considered.

The current peak shown in figure 7.5 was only observed for fields greater than about 160 volts $cm^{-1}$ and occurred at lower temperatures for lower fields. This is because as the temperature is reduced, (i.e. at lower vapour pressures), smaller voltages are required to breakdown the vapour (as will be shown in section 7.4), and it will be argued in section 7.8(d) that the low temperature rise in the transmission current is directly associated with dielectric breakdown in the vapour.

4 Dielectric Breakdown of the Vapour

The rapid rise in the transmission current $I_{c2}$ for the high fields at temperatures below about 1.15 K, in figures 7.3, 7.4 and 7.5, suggested that it could be due to electrical breakdown in the vapour above the liquid surface. Fallou, Galland and Bouvier (1970) extended their measurements on the dielectric strength of gaseous Helium at atmospheric pressure down to 4.2 K, but there have been no published results on the breakdown potential of the vapour at

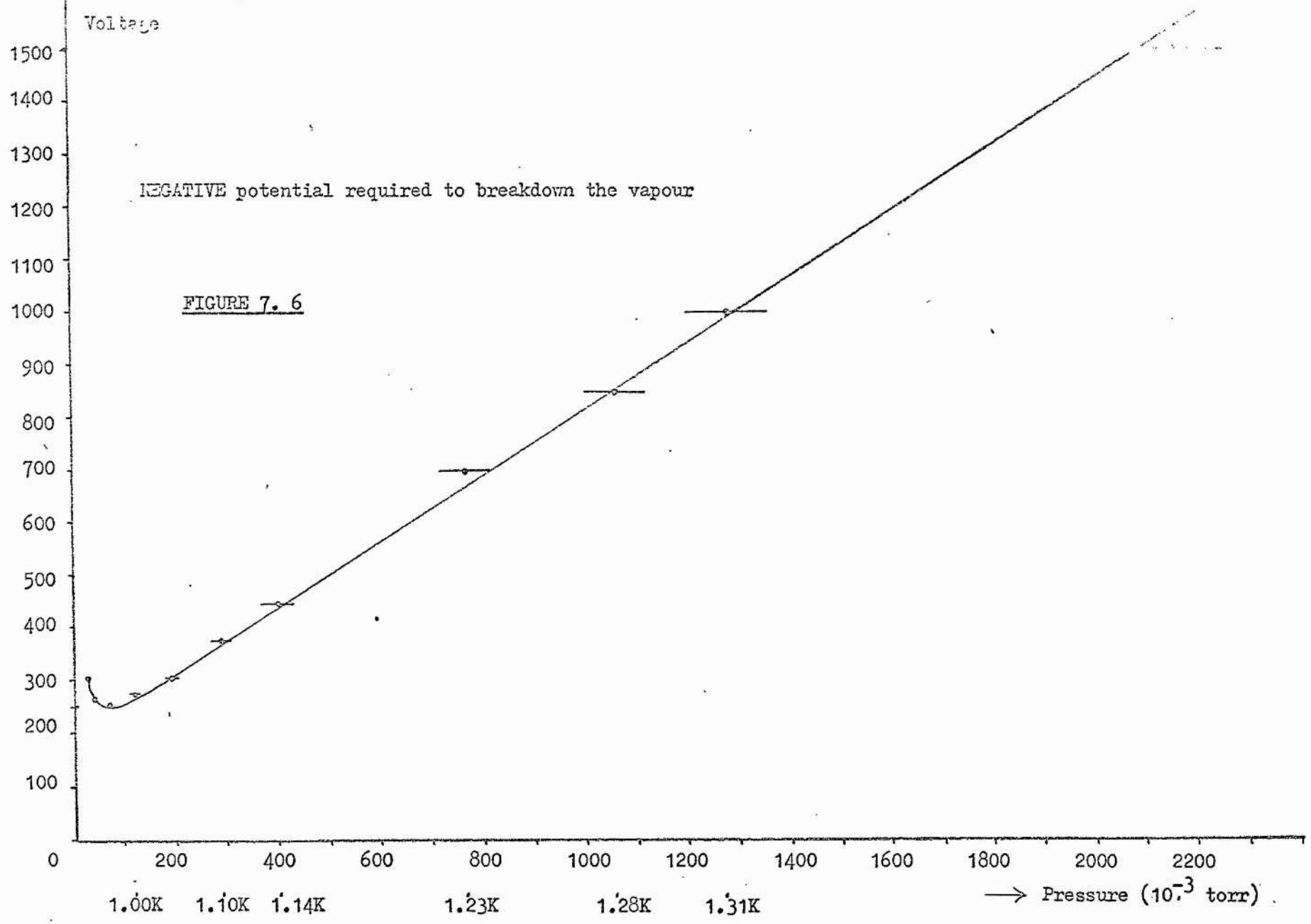


NEGATIVE potential required to breakdown the vapour

FIGURE 7. 6

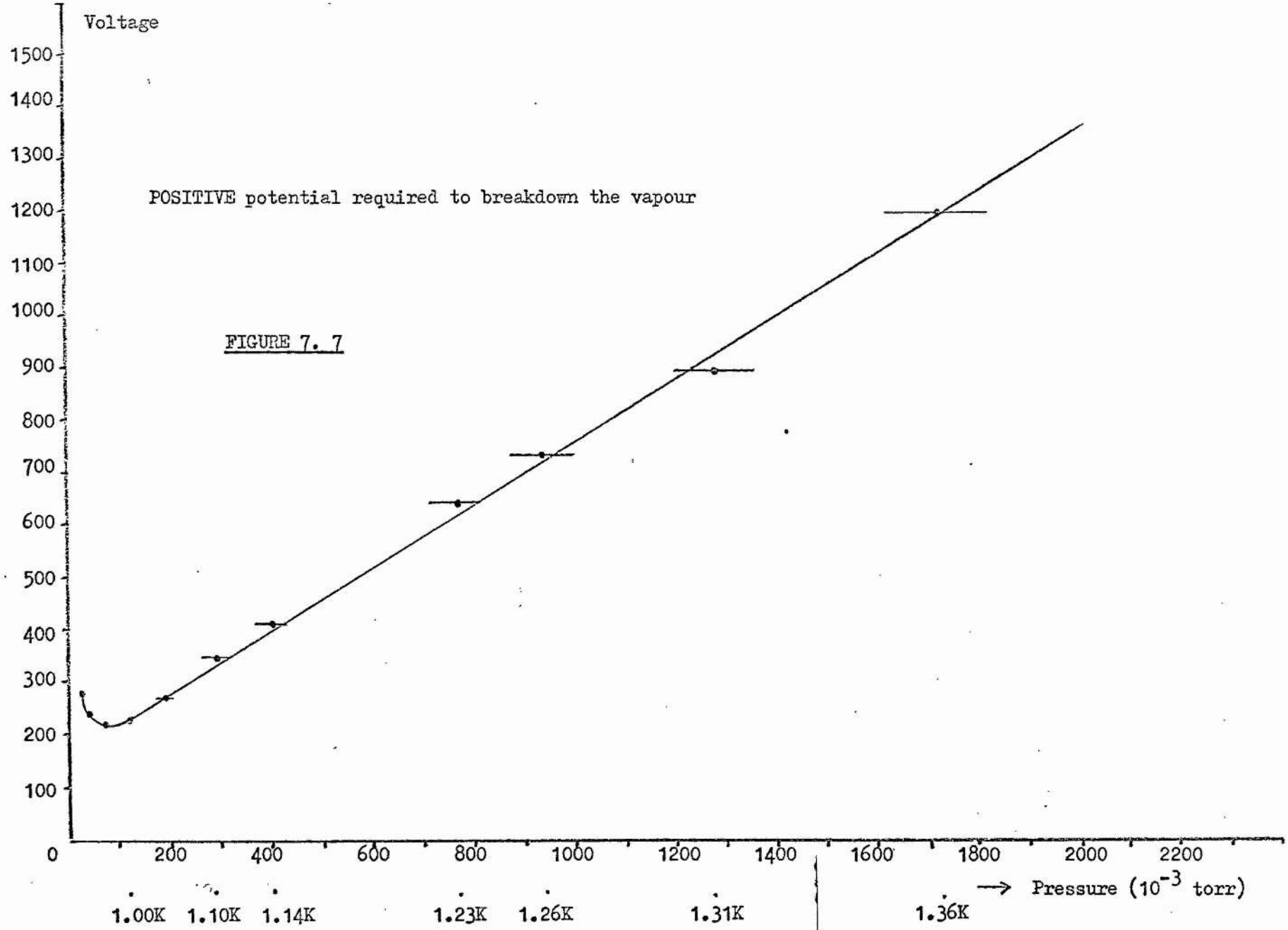


POSITIVE potential required to breakdown the vapour

FIGURE 7. 7

temperatures below 4.2 K.

In an effort to obtain an estimate of the voltage at which the vapour above the liquid will breakdown, the following procedure was adopted. During the experiments with the perspex triode 7.1(a), with the source directly earthed and a liquid surface between the grid and collector, the potential on the grid was very carefully increased until a large current suddenly appeared sending the electrometer on the collector C2 off scale, at which point the grid potential was quickly reduced to zero. This was repeated at various temperatures and for both positive and negative potentials of the grid.

The values of the grid voltage thus obtained have been plotted against the vapour pressure above the liquid, for negative ions in figure 7.6 and for positive ions in figure 7.7. For vapour pressures corresponding to temperatures above 1 K, Paschen's law is obeyed. (Paschen's law essentially states that the breakdown potential of a gas depends only on the product of the gas pressure and distance between the electrodes).

The minimum in the breakdown potential occurs where the electron mean free path is of the order of the distance between the surface and the collector C2.

With a grid-collector distance of 1.5 cm, the minimum field to cause breakdown was in the neighbourhood of 170 volts $cm^{-1}$ for negative ions and 150 volts $cm^{-1}$ for positive ions.

5 The Dependence of the Transmission Current on Liquid Level

Bruschi et al reported that the current transmission across the free liquid surface was independent of the position of the liquid level between the grid and the collector. No other authors appear to have conducted an investigation of this phenomenon.

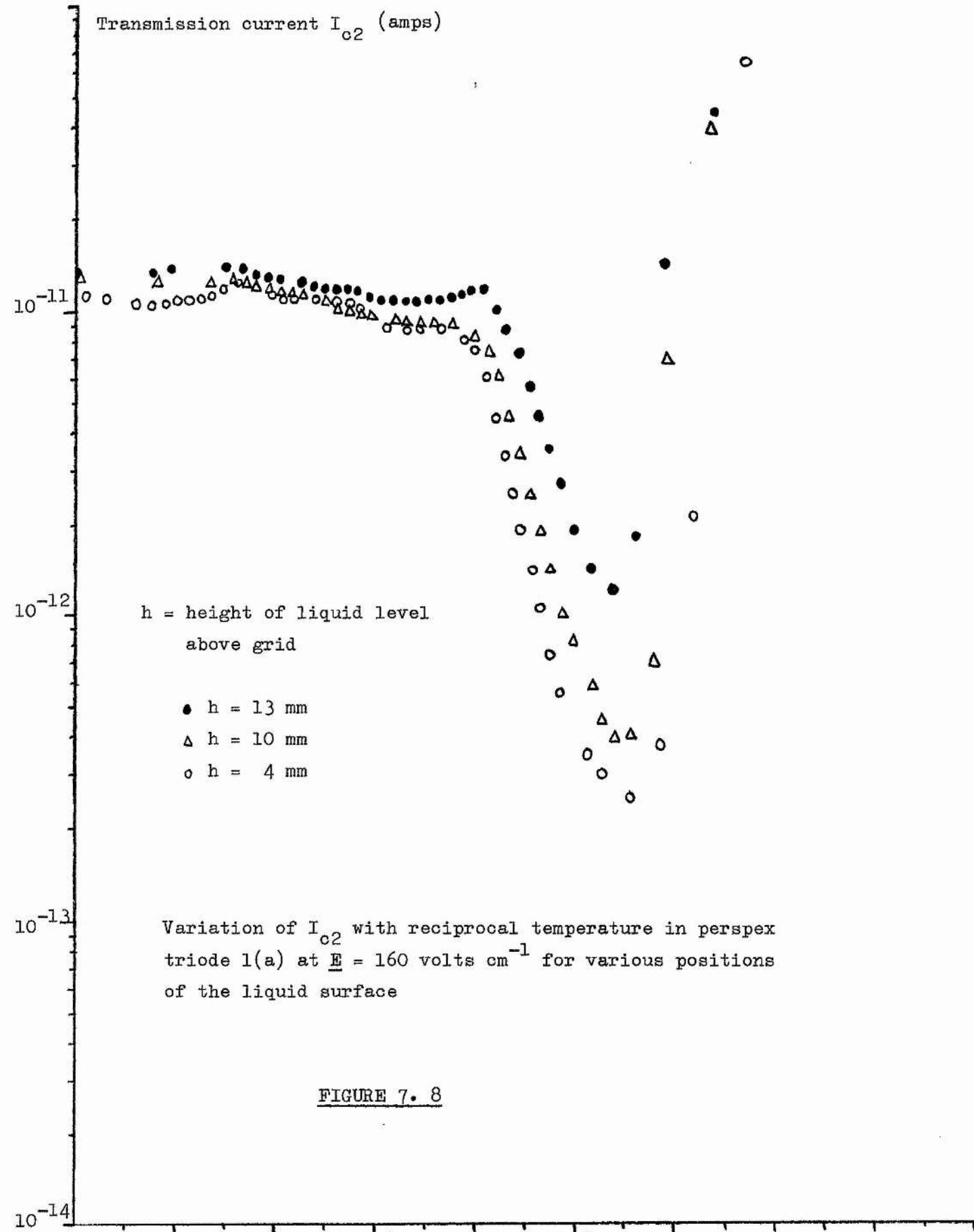


Variation of $I_{c2}$ with reciprocal temperature in perspex triode 1(a) at $\underline{E}$ = 160 volts $cm^{-1}$ for various positions of the liquid surface

FIGURE 7. 8

TABLE 2

| Height of liquid level above the grid | Measured energy barrier $\phi_E$ |
|---|---|
| 13 mm | 24 ± 2 K |
| 10 mm | 28 ± 2 K |
| 4 mm | 30 ± 2 K |

The variation of the energy barrier with the position of the liquid surface between the grid and collector of the perspex triode 1(a); applied field $\underline{E}$ = 160 v.cm$^{-1}$

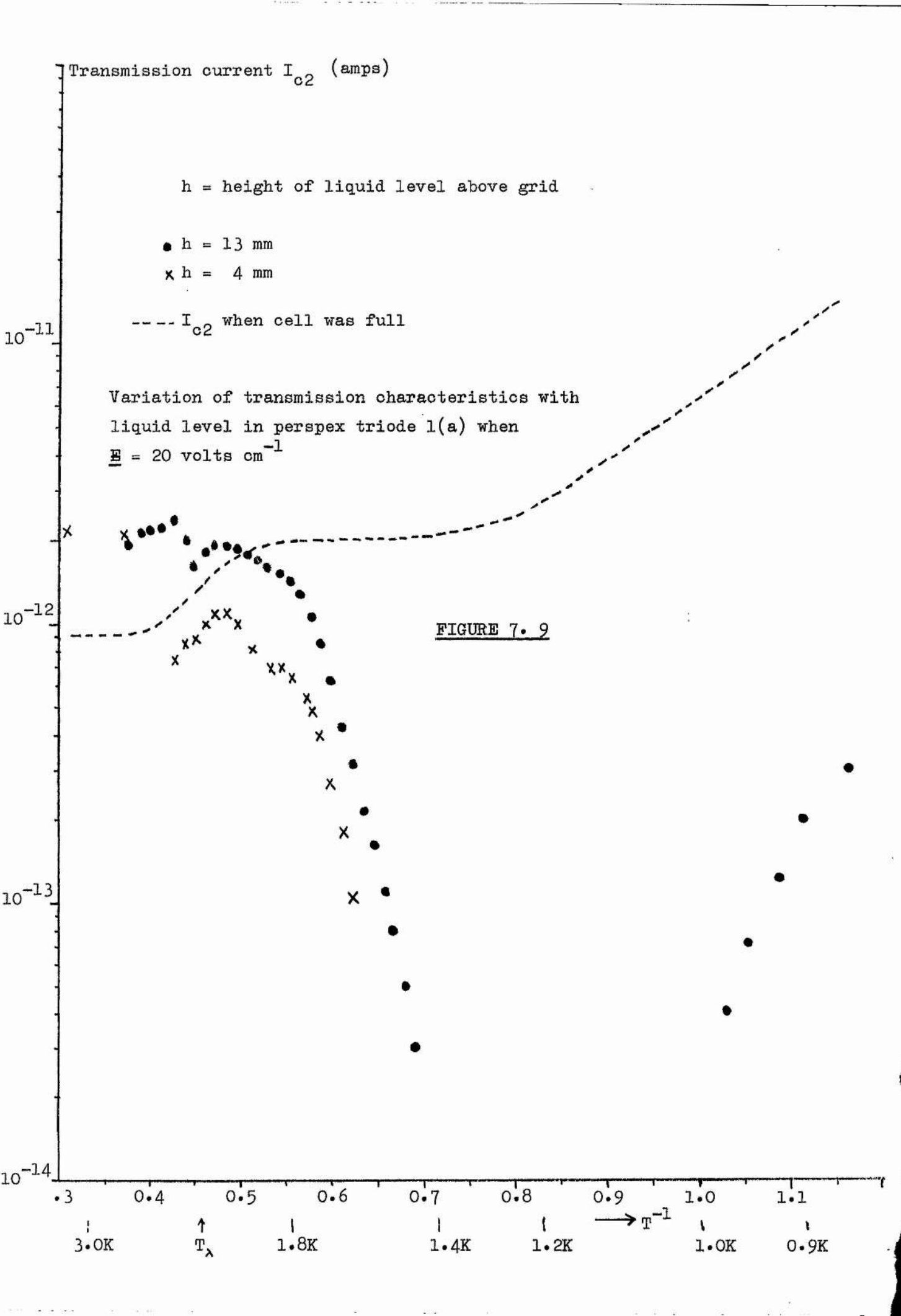
Transmission current $I_{c2}$ (amps)
h = height of liquid level above grid
● h = 13 mm
× h = 4 mm
---- $I_{c2}$ when cell was full
Variation of transmission characteristics with liquid level in perspex triode 1(a) when $\underline{E}$ = 20 volts cm$^{-1}$
$10^{-11}$
$10^{-12}$
$10^{-13}$
$10^{-14}$
.3
0.4
0.5
0.6
0.7
0.8
0.9
1.0
1.1
$T^{-1}$
3.0K
$T_\lambda$
1.8K
1.4K
1.2K
1.0K
0.9K

FIGURE 7. 9

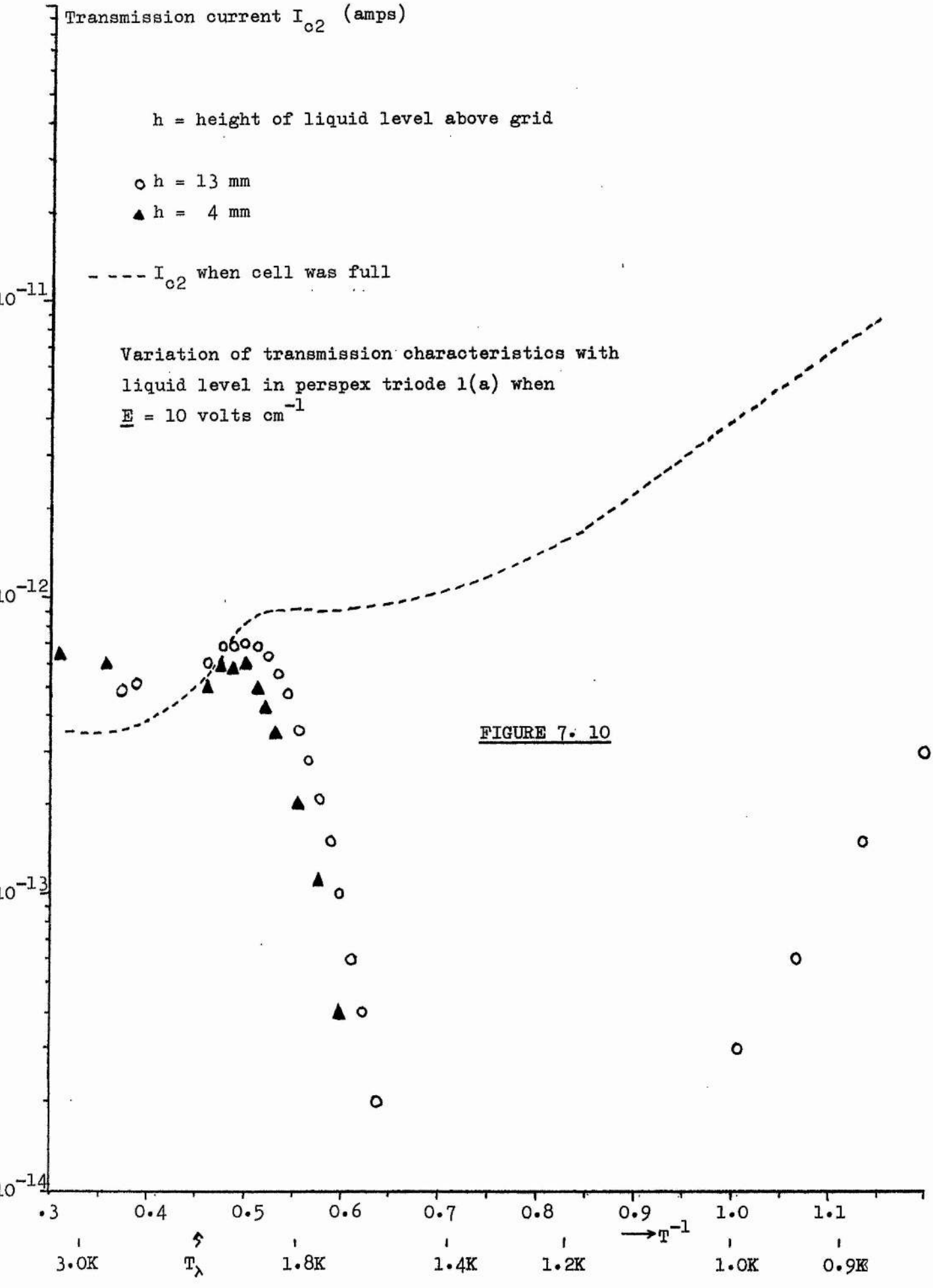
Transmission current $I_{c2}$ (amps)
h = height of liquid level above grid
h = 13 mm
h = 4 mm
$I_{c2}$ when cell was full
Variation of transmission characteristics with liquid level in perspex triode 1(a) when $\underline{E}$ = 10 volts $cm^{-1}$
$10^{-11}$
$10^{-12}$
$10^{-13}$
$10^{-14}$
·3
0.4
0.5
0.6
0.7
0.8
0.9
1.0
1.1
$\rightarrow T^{-1}$
3.0K
$T_\lambda$
1.8K
1.4K
1.2K
1.0K
0.9K

FIGURE 7. 10

The present work has revealed, on the contrary, that the position of the liquid level has a pronounced effect on the characteristics of the transmission current. Figure 7.8 shows the results of three runs for the same applied field of 160 volts $cm^{-1}$ in the perspex triode 7.1(a), with the liquid level at 4 mm, 10 mm and 13 mm above the grid, which was itself 15 mm below the collector C2. Three distinct effects can be seen, as the depth of liquid above the grid increased,

(a) the magnitude of the observed energy barrier (i.e. the slope of the temperature dependent fall in current) decreased,

(b) the minimum in the curve occurred at higher current values and higher temperatures, and

(c) the transition from the roughly temperature-independent behaviour to the exponential fall occurred at slightly lower temperatures, although this may not be significant.

The variation of the measured energy barrier with liquid level above the grid for the perspex triode 7.1(a) is shown in table 2. The effects of the liquid depth on the characteristics for the two lowest fields of 20 and 10 volts $cm^{-1}$ are shown in figures 7.9 and 7.10 respectively. Also shown in these figures is the temperature variation of the current collected on C2 when the cell was full of liquid. The important observation in this case is that when the liquid surface was close to the collector C2 a low temperature rise in current was seen, whereas when the liquid surface was far from the collector C2 no rise was seen.

These effects will be discussed more fully in section 7.8(d).

6 The Current Detected on the Collector C1

Whenever a reading was taken of the transmission current through

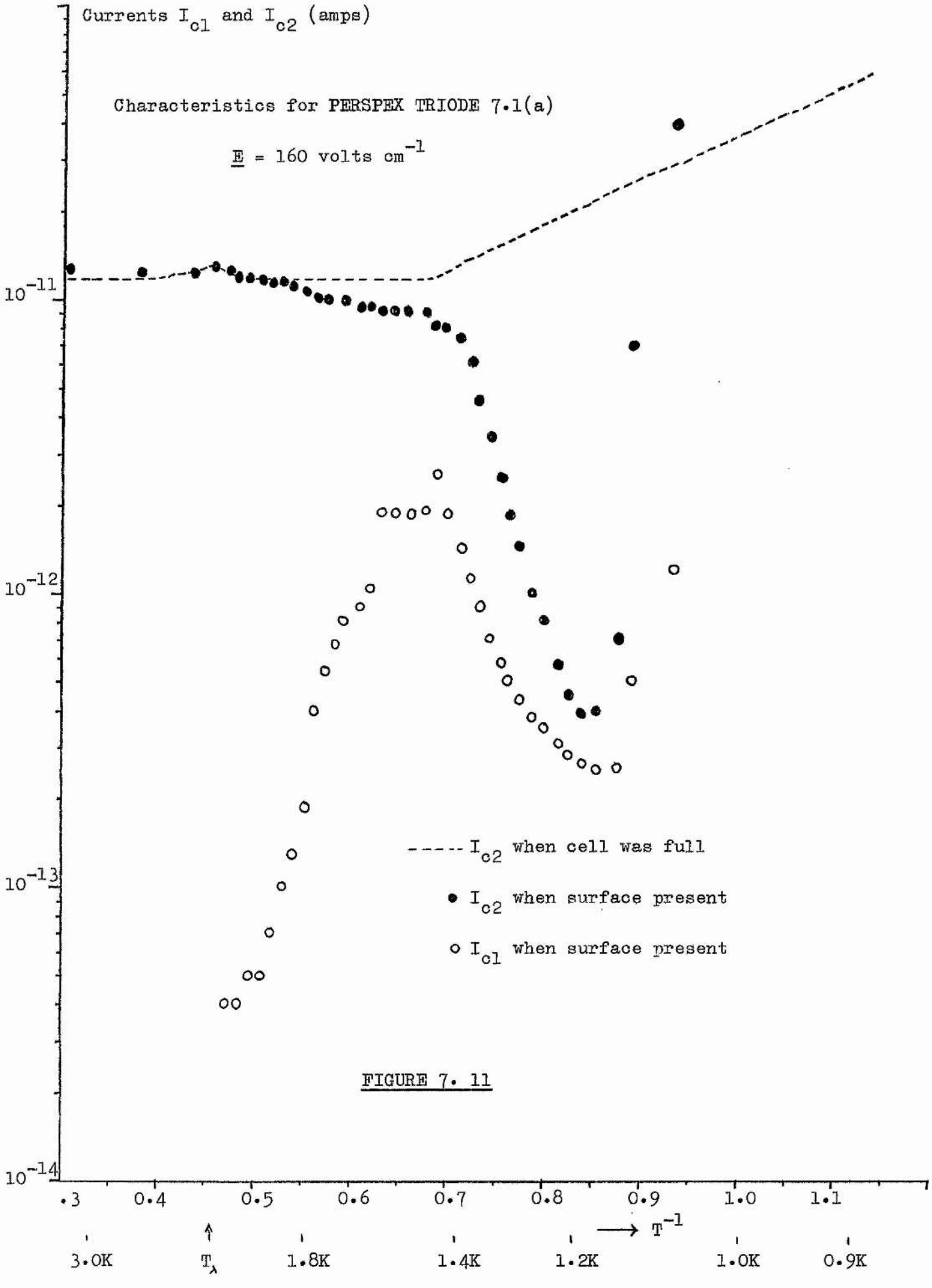
Currents $I_{c1}$ and $I_{c2}$ (amps)
Characteristics for PERSPEX TRIODE 7.1(a)
$\underline{E}$ = 160 volts cm$^{-1}$
$10^{-11}$
$10^{-12}$
$10^{-13}$
$10^{-14}$
----- $I_{c2}$ when cell was full
• $I_{c2}$ when surface present
o $I_{c1}$ when surface present
.3
0.4
0.5
0.6
0.7
0.8
0.9
1.0
1.1
$T^{-1}$
3.0K
$T_\lambda$
1.8K
1.4K
1.2K
1.0K
0.9K

FIGURE 7. 11

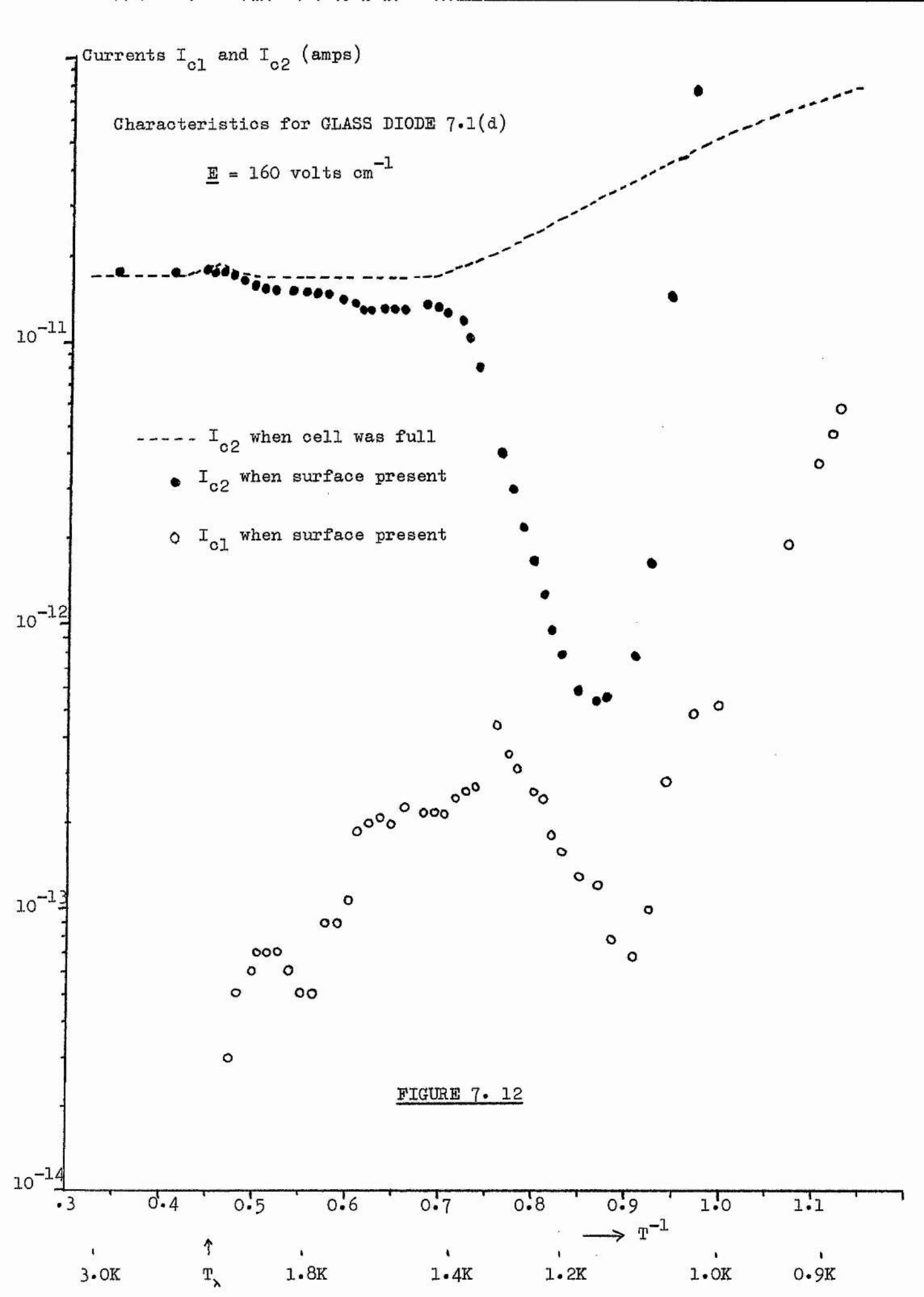
Currents $I_{c1}$ and $I_{c2}$ (amps)
Characteristics for GLASS DIODE 7.1(d)
$\underline{E}$ = 160 volts $cm^{-1}$
$10^{-11}$
$10^{-12}$
$10^{-13}$
$10^{-14}$
----- $I_{c2}$ when cell was full
$I_{c2}$ when surface present
$I_{c1}$ when surface present
.3
0.4
0.5
0.6
0.7
0.8
0.9
1.0
1.1
$\rightarrow T^{-1}$
3.0K
$T_\lambda$
1.8K
1.4K
1.2K
1.0K
0.9K

FIGURE 7. 12

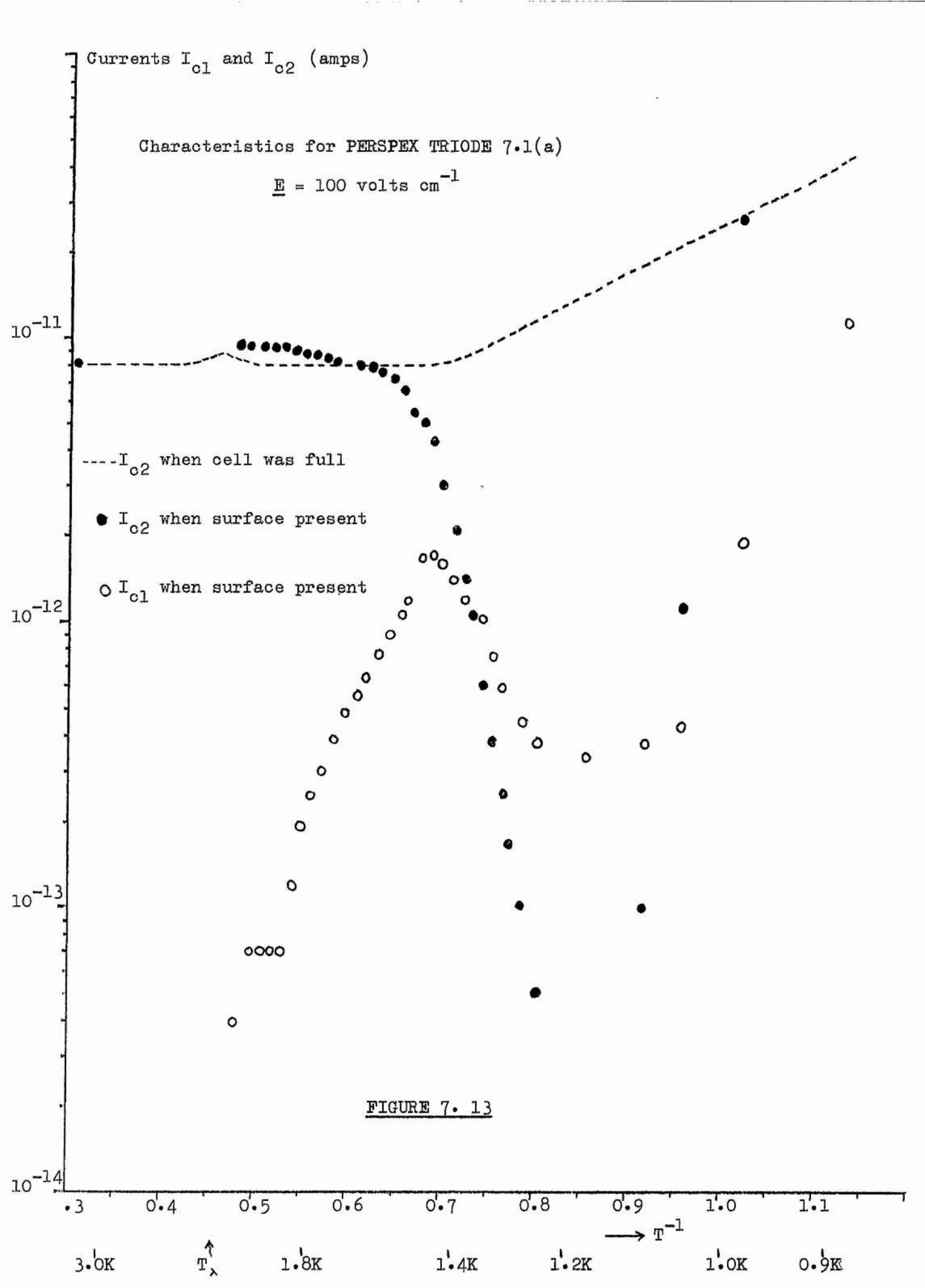
Currents $I_{c1}$ and $I_{c2}$ (amps)
Characteristics for PERSPEX TRIODE 7.1(a)
$\underline{E}$ = 100 volts $cm^{-1}$
$10^{-11}$
$10^{-12}$
$10^{-13}$
$10^{-14}$
----$I_{c2}$ when cell was full
● $I_{c2}$ when surface present
○ $I_{c1}$ when surface present
.3
0.4
0.5
0.6
0.7
0.8
0.9
1.0
1.1
$\rightarrow T^{-1}$
3.0K
$T_\lambda$
1.8K
1.4K
1.2K
1.0K
0.9K

FIGURE 7. 13

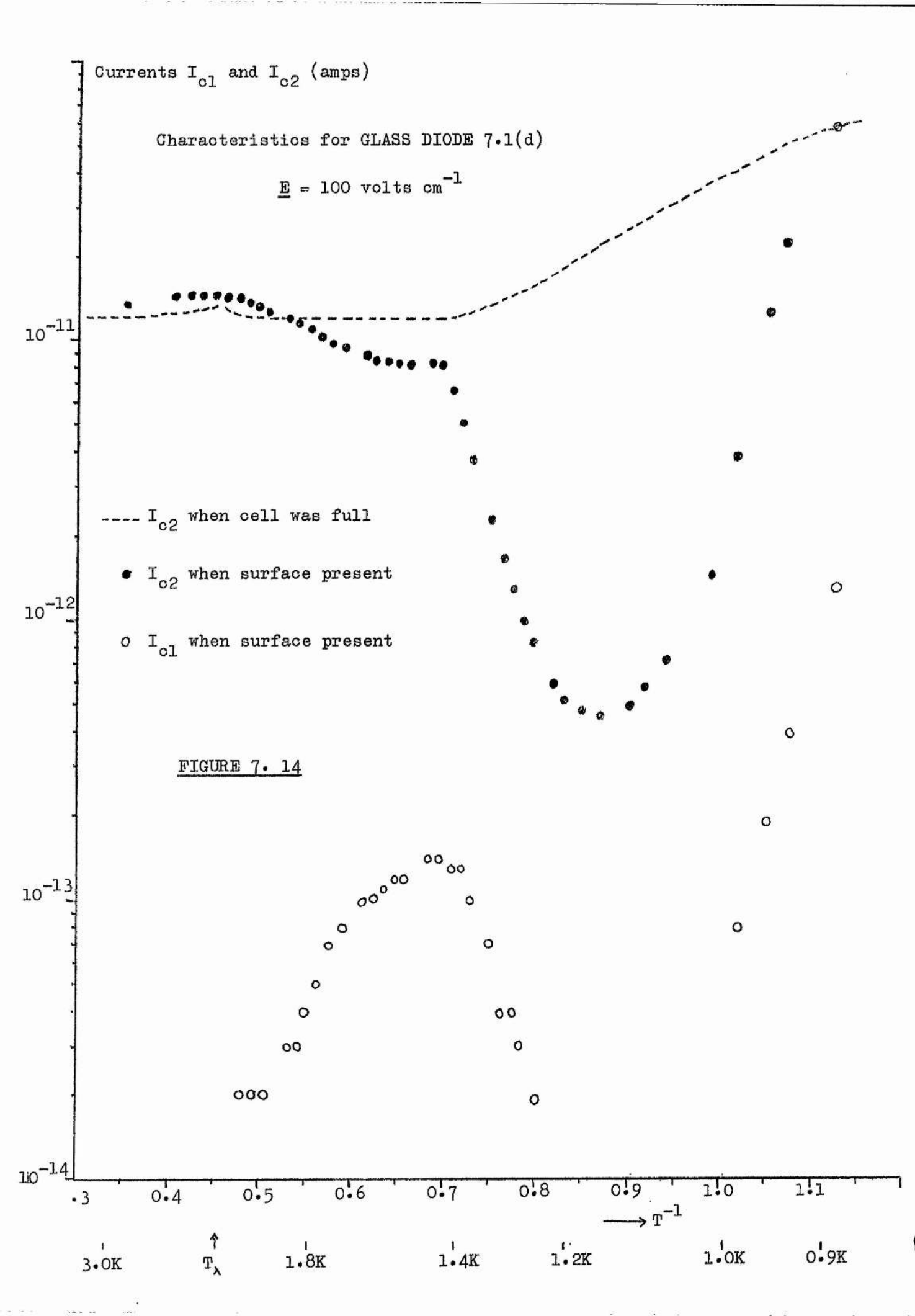
Currents $I_{c1}$ and $I_{c2}$ (amps)
Characteristics for GLASS DIODE 7.1(d)
$\underline{E}$ = 100 volts $cm^{-1}$
$10^{-11}$
$10^{-12}$
$10^{-13}$
$10^{-14}$
---- $I_{c2}$ when cell was full
• $I_{c2}$ when surface present
o $I_{c1}$ when surface present
.3
0.4
0.5
0.6
0.7
0.8
0.9
1.0
1.1
$\longrightarrow T^{-1}$
3.0K
$T_\lambda$
1.8K
1.4K
1.2K
1.0K
0.9K

FIGURE 7. 14

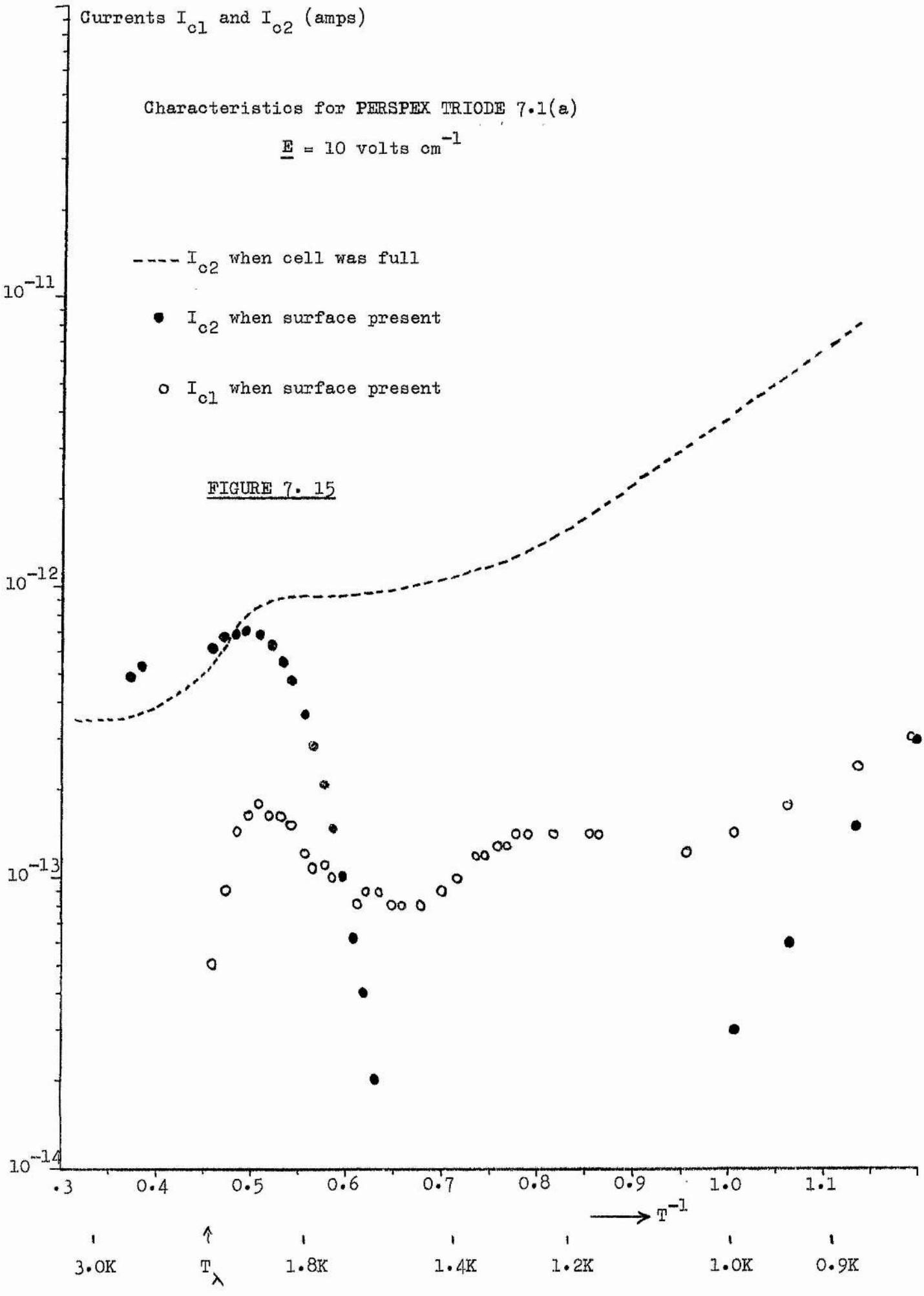
Currents $I_{c1}$ and $I_{c2}$ (amps)
Characteristics for PERSPEX TRIODE 7.1(a)
$\underline{E}$ = 10 volts cm$^{-1}$
---- $I_{c2}$ when cell was full
• $I_{c2}$ when surface present
o $I_{c1}$ when surface present
$10^{-11}$
$10^{-12}$
$10^{-13}$
$10^{-14}$
.3
0.4
0.5
0.6
0.7
0.8
0.9
1.0
1.1
$T^{-1}$
3.0K
$T_\lambda$
1.8K
1.4K
1.2K
1.0K
0.9K

FIGURE 7. 15

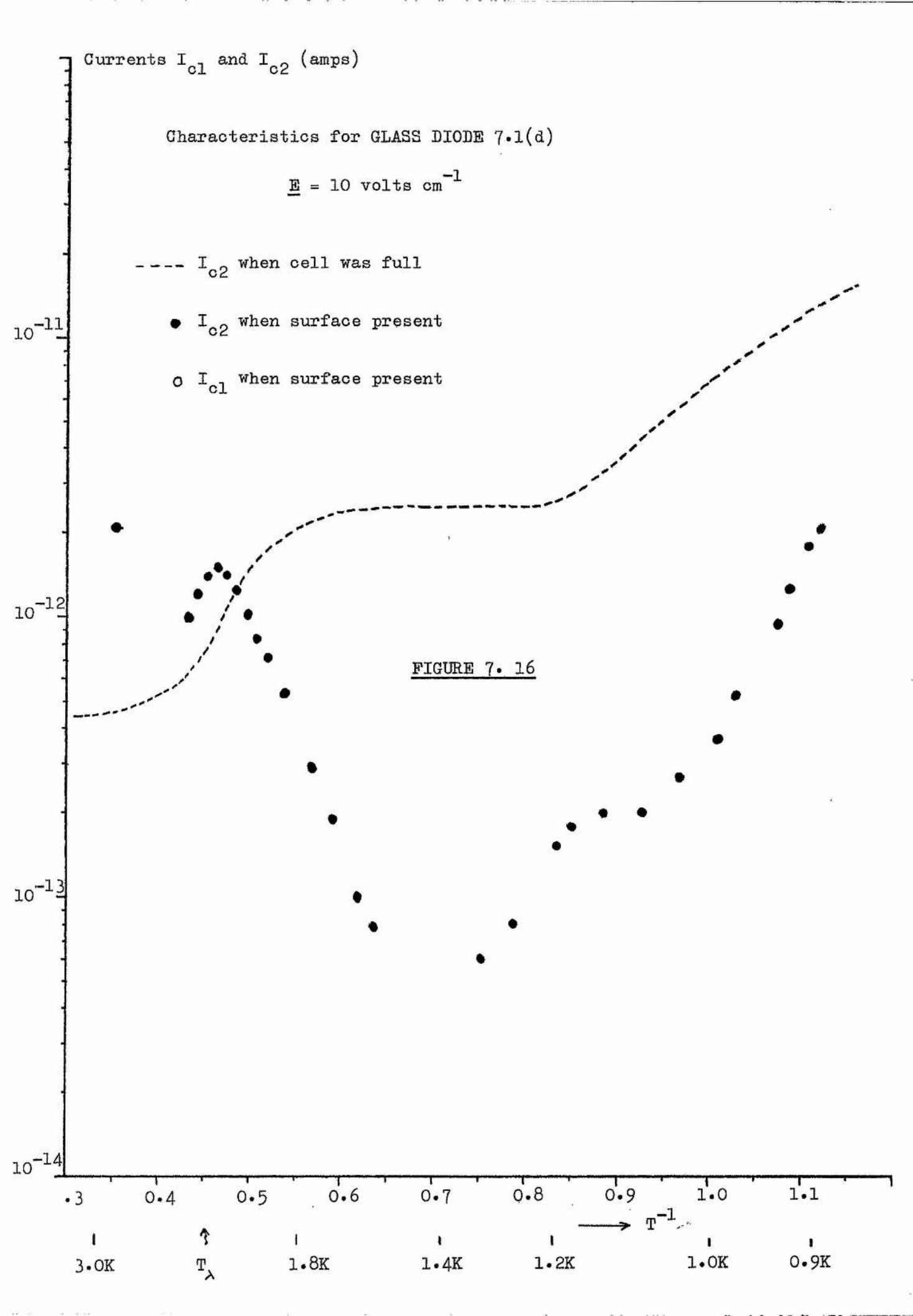
Currents $I_{c1}$ and $I_{c2}$ (amps)
Characteristics for GLASS DIODE 7.1(d)
$\underline{E}$ = 10 volts $cm^{-1}$
---- $I_{c2}$ when cell was full
● $I_{c2}$ when surface present
o $I_{c1}$ when surface present
$10^{-11}$
$10^{-12}$
$10^{-13}$
$10^{-14}$
.3
0.4
0.5
0.6
0.7
0.8
0.9
1.0
1.1
$T^{-1}$
3.0K
$T_\lambda$
1.8K
1.4K
1.2K
1.0K
0.9K

FIGURE 7. 16

the liquid surface, the current $I_{c1}$ arriving at the film collector C1 was also recorded. Typical corresponding curves of $I_{c2}$ and $I_{c1}$ are shown in figures 7.11 to 7.16, some for the perspex triode 7.1(a) and some for the glass diode 7.1(d). Each figure illustrates the variation of $I_{c1}$ and $I_{c2}$ in a constant field with temperature. For comparison, each figure shows the variation of the current $I_{c2}$ which was collected when the cell was full of liquid. When the cell was full, no $I_{c1}$ currents were detected.

We can see that the values of $I_{c1}$ were greater for the perspex substrate than for the glass one. More significantly, for the 10 and 20 volts $cm^{-1}$ fields in the glass diode, no currents at all were detected on the film collector C1.

With the glass diode, the results for $I_{c1}$ in the constant fields varying between 50 and 130 volts $cm^{-1}$ were all very similar and are typified by figure 7.14. Above the lambda point, no film currents were ever detectable, while below the lambda point, the film current first rose to a maximum value with decreasing temperature and then fell to zero again at about 1.2 K. As the temperature was lowered still further, a film current reappeared, increasing with falling temperature. In no case in the glass diode did $I_{c2}$ ever fall to zero at any temperature; this result, together with the behaviour of the film current in the glass diode, will be discussed further in Section 7.8(c).

The runs with the glass triode 7.1(b) yielded similar results to those already described for the perspex triode and glass diode. In an effort to understand why the film current did not rise in sympathy with the fall in the transmission current $I_{c2}$ as observed by Bruschi et al, and what happened to that fraction of the current which did not cross the liquid surface, it was decided to measure at the same time

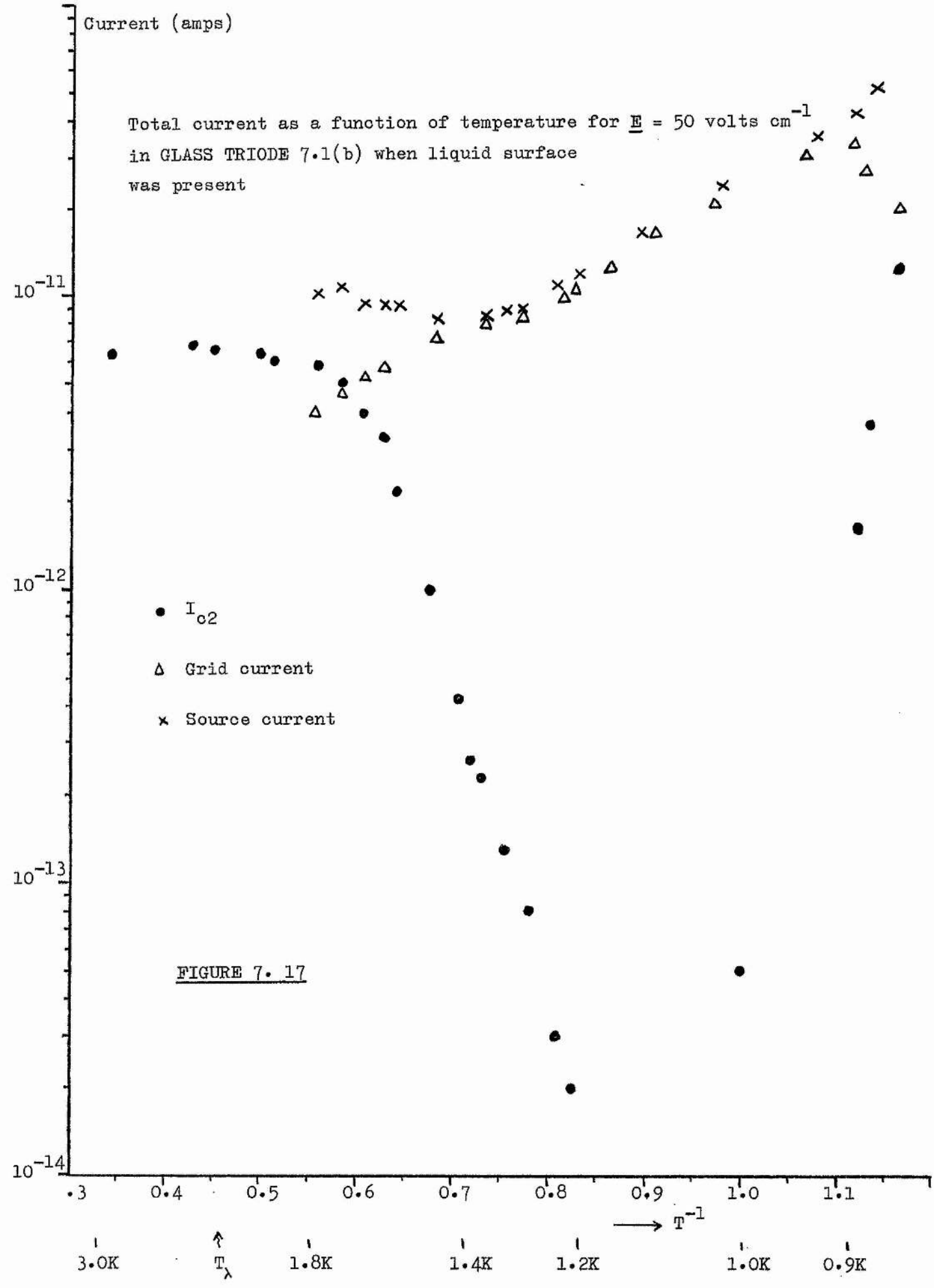
Current (amps)
Total current as a function of temperature for E = 50 volts cm$^{-1}$ in GLASS TRIODE 7.1(b) when liquid surface was present
$10^{-11}$
$10^{-12}$
$10^{-13}$
$10^{-14}$
$I_{c2}$
Grid current
Source current
.3
0.4
0.5
0.6
0.7
0.8
0.9
1.0
1.1
$T^{-1}$
3.0K
$T_\lambda$
1.8K
1.4K
1.2K
1.0K
0.9K

FIGURE 7. 17

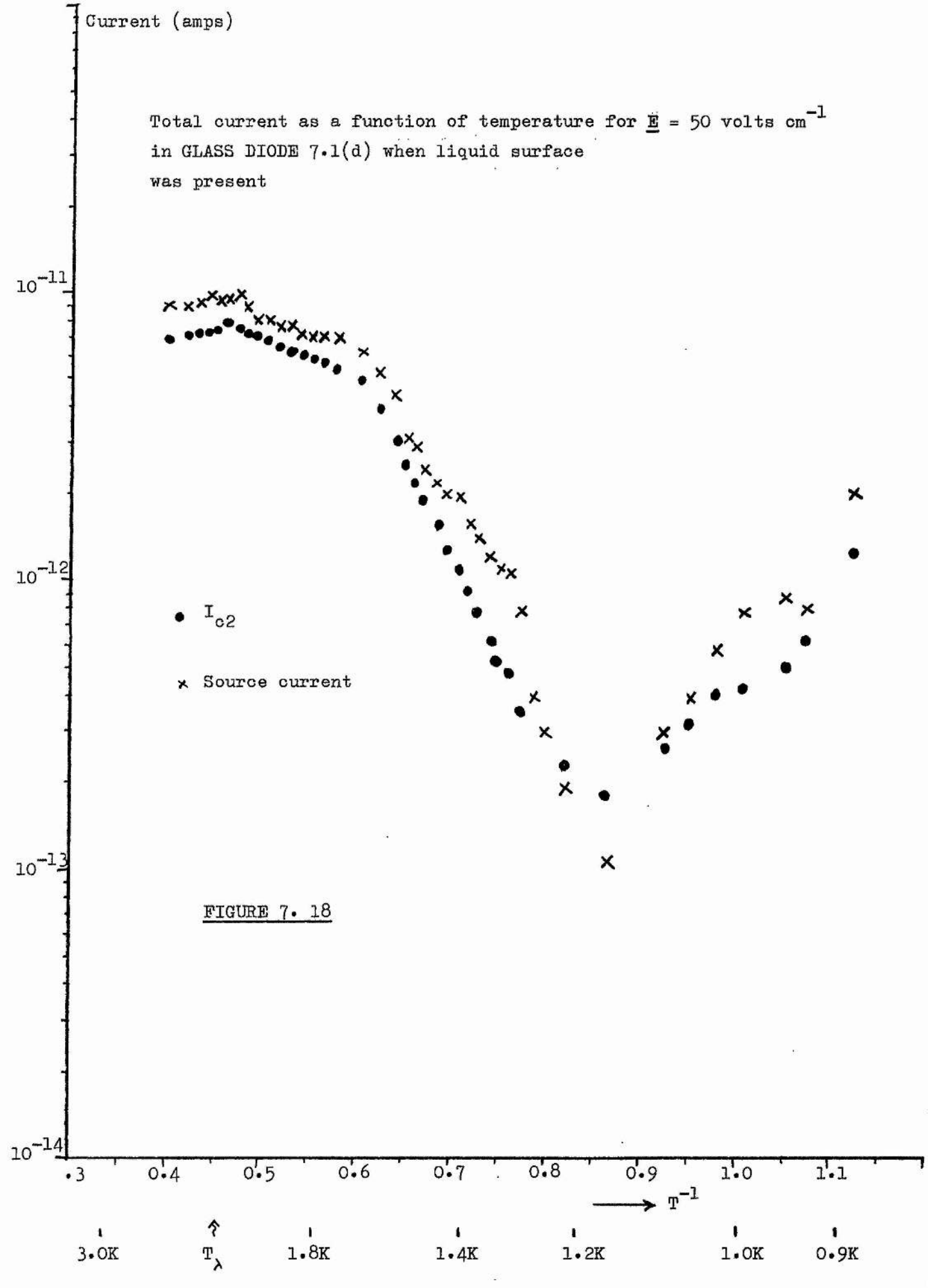
Current (amps)
Total current as a function of temperature for E = 50 volts cm$^{-1}$ in GLASS DIODE 7.1(d) when liquid surface was present
$10^{-11}$
$10^{-12}$
$10^{-13}$
$10^{-14}$
$I_{c2}$
Source current
.3
0.4
0.5
0.6
0.7
0.8
0.9
1.0
1.1
$T^{-1}$
3.0K
$T_\lambda$
1.8K
1.4K
1.2K
1.0K
0.9K

FIGURE 7. 18

the current leaving the source and the current drawn by the grid. This was done by employing a very useful feature of the Keithley 602 electrometer; that is, its ability to measure current at a floating potential. This meant that the Keithley 602 could be alternately inserted into the source and grid bias circuits to measure the current from each electrode, while the Wayne Kerr electrometer continuously monitored the transmission current $I_{c2}$. The result in the glass triode 7.1(b) for an applied field of 50 volts $cm^{-1}$ is shown in figure 7.17. Here, the source current displayed the characteristics already discussed in chapter 5. As $I_{c2}$ fell with decreasing temperature, the grid current rose until it reached approximately the value of the current leaving the source. As the temperature was further reduced, almost all the current leaving the source was collected by the grid, until $I_{c2}$ experienced its low temperature rise and the grid current reached a maximum and then declined.

The same procedure of floating the Keithley 602 on the source bias circuit was employed during the runs with the glass diode 7.1(d). The result is shown in figure 7.18, where it may be seen that as the transmission current decreased with falling temperature below the lambda point, so the negative ion emission from the source decreased in sympathy, until at about 1.14 K, when $I_{c2}$ stopped falling and began to rise, the current leaving the source began to rise also.

The interpretation of the results shown in figures 7.17 and 7.18 will be discussed in section 7.8(b).

7 Level Oscillations

Oscillations can be produced in a beaker which is filling or emptying by film flow due to the periodic interchange of energy between the kinetic energy of the film and the potential energy of the liquid

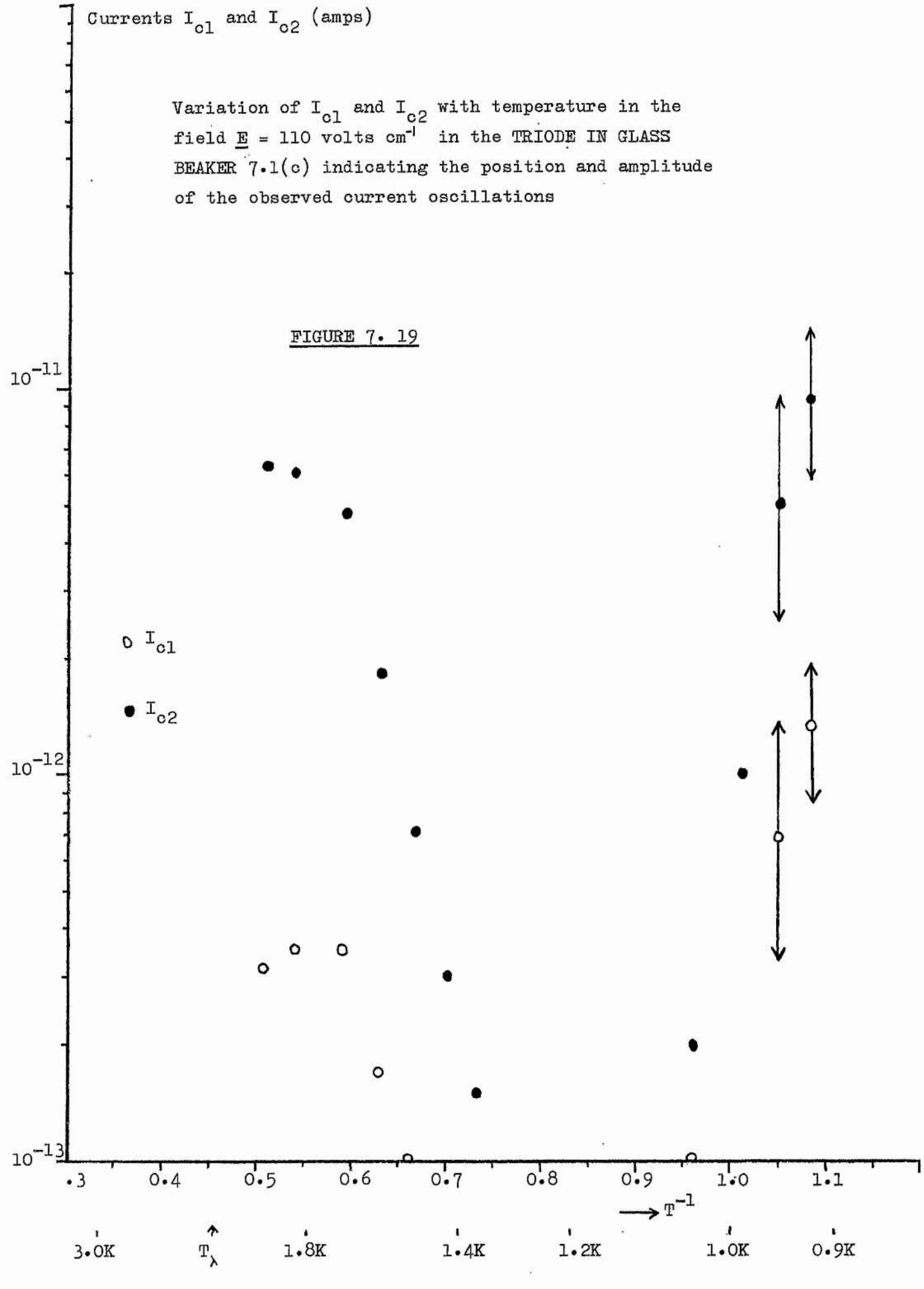


Variation of $I_{c1}$ and $I_{c2}$ with temperature in the field $\underline{E}$ = 110 volts $cm^{-1}$ in the TRIODE IN GLASS BEAKER 7.1(c) indicating the position and amplitude of the observed current oscillations

FIGURE 7. 19

inside the beaker.

It was briefly mentioned in section 6.5 that Bianconi and Maraviglia observed oscillations in the positive ion film current at twice the frequency with which the level of liquid inside the beaker, which contained the ion cell, was oscillating. They did not experiment with negative ions.

During the runs with the triode in the glass beaker shown in figure 7.1(c) oscillations were sometimes observed in the currents $I_{c1}$ and $I_{c2}$, both current oscillations being at the same frequency. The appearance of these oscillations was completely unpredictable; any attempt artificially to produce them by the creation of a level difference via the small fountain pump shown in figure 7.1(c) was always unsuccessful. For example, the beaker was often completely filled using the fountain pump and the grid and source biases adjusted to provide a desired field. With the temperature held constant, the output from the electrometers on the collectors C1 and C2 were left running on chart recorders for periods of greater than 10 hours while the level in the beaker fell to that of the bath via film flow. Examination of the recorder tracings revealed the point where the liquid surface overcame the collector C2 but no current oscillations.

The oscillations which were observed were invariably produced by rapid temperature fluctuations in the ion chamber, for example when cooling down quickly with the fridge. The most well defined oscillations were produced at the lowest temperatures where the current was rapidly increasing function of temperature. This meant that the oscillations were in fact superimposed on the steady state current which was obtained at the particular temperature and field. Figure 7.19 shows the position and amplitude of two sets of

oscillations obtained during a typical run.

It was difficult to obtain a true measure of the damping of the oscillations since the particular current which was being modulated was often itself slowly drifting. Whenever an estimate of the damping could be made it was always found to be heavier than that observed by Hammel, Keller and Sherman (1970) in mechanical film oscillations at similar temperatures.

The period of the observed current oscillations was of the order of 100 seconds which was close to the estimated value for film oscillations into and out of the cell.

After the first few periods, the frequency of the oscillations was found to increase, as observed by Hammel et al. There can therefore be little doubt that the oscillations observed in the currents $I_{c1}$ and $I_{c2}$ were due to oscillations of the liquid level in the beaker coupled to the ion chamber bath via the Helium film, but it is not clear why oscillations of the liquid level of very small amplitude should produce oscillations in the currents of such large amplitude.

When the triode glass beaker 7.1(c) was replaced by the diode glass beaker 7.1(d) with a copper bottom, no current oscillations were ever observed, although exactly the same procedure was followed. To check that this was not due to a leak having been developed in the glass-metal seal on the bottom, the beaker 7.1 (d) was inserted into a glass dewar system and found to be completely tight to the superfluid.

The oscillations would appear to be intimately related to temperature differences inside and outside the beaker. When the beaker is all glass it might be possible to produce relatively large temperature differences, while a copper bottom in the beaker prevents this. The actual mechanism of sustaining the oscillations at the frequency with which the beaker level is oscillating is not understood.

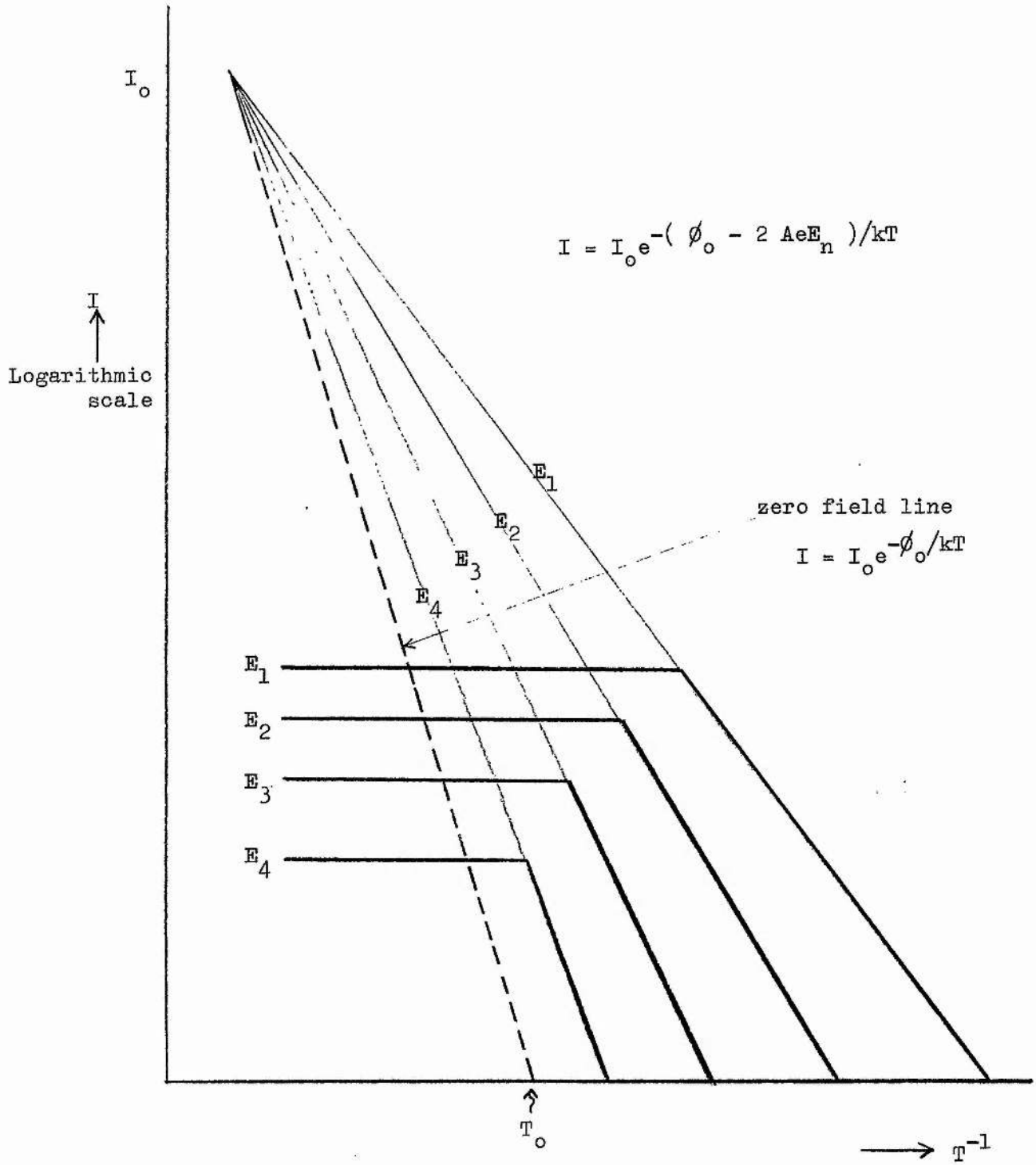


Possible explanation of the origin of the temperature dependent behaviour of the transmission current $I_{c2}$

FIGURE 7. 20

Finally, when the film was driven thermally by the Aquadag heaters, no oscillations in $I_{c1}$ were observed, nor was any effect of the motion of the film on $I_{c1}$ observed.

## 8 Discussion of Results

### (a) The Transmission Current $I_{c2}$

We recall that above 1.2 K the negative ion transmission current $I_{c2}$ first rises exponentially with temperature and then becomes roughly temperature independent. A possible explanation of this behaviour is illustrated in figure 7.20. Suppose that at high temperatures the source is capable of supplying a large current $I_o$. When this current meets the liquid surface it will be attenuated according to the relation

$$I = I_o e^{-(\phi_o - 2\sqrt{AeE})/kT} \qquad (1)$$

where $(\phi_o - 2\sqrt{AeE})$ is the energy barrier in the field E as explained in equation 6.(10). As the field E is reduced, the I versus $T^{-1}$ lines will approach closer and closer to the broken zero field line shown. The source, however, is incapable of delivering very large currents, and for any given field E the current drawn will be very small. When the negative ions of this current meet the surface barrier they may be supposed to make repeated attempts to cross into the vapour by surmounting the barrier. Let this attempt frequency be $\nu$. If, on average, an ion makes n attempts before it surmounts the barrier, then the ion will on average remain below the free surface for a time of order $n\nu^{-1}$. If this time is less than the average time separation of ions arriving at the liquid surface then the

transmission current will not be affected by the liquid surface. If one assumes the attempt frequency to decrease with falling temperature, at some point the time $n\nu^{-1}$ will become greater than the time separation of ions arriving at the surface. This point will be where the constant field, temperature-independent current meets the line I(E) corresponding to the field E. If the temperature is then further reduced, the transmission current will fall according to equation (1). Thus the shape of the temperature dependence of the transmission current will be given by the heavy black lines of figure 7.20.

This could explain why the transition from the temperature-independent region to the exponential fall occurred at higher temperatures for lower fields, and tended to an upper limit of temperature $T_o$ in the limit of zero field. It may be fortuitous that $T_o$ was very close to the lambda point. If this is so, the suggestion of Schoepe and Probst that the surface energy barrier is present only in the superfluid state, may be incorrect.

(b) Surface Charge

The results of floating the Keithley electrometer in the source and grid bias circuits of the glass triode 7.1(b) and in the source bias circuit of the glass diode 7.1(d) were shown in figures 7.17 and 7.18 respectively. These experiments provide clear evidence that the fraction of the total current which can travel in the Helium film covering the walls of the ion cell must be very small. If we examine the region between $T_\lambda$ and 1.2K, since the transmission current $I_{c2}$ across the liquid surface was observed to decrease, the current arriving at the liquid surface from below must also have decreased. That is, the field which exists between the grid and the liquid surface, $E_{g1}$, or the field between the source and the liquid surface

$E_{s1}$, must decrease as $I_{c2}$ decreases. This can only mean that a layer of charge was built up below the liquid surface, such that if $\sigma$ is the surface charge density then,

$$\sigma = D_v - D_l \ , \qquad (2)$$

where $D_v$ and $D_l$ are the electric displacements in the vapour and liquid respectively. If $I_{c2}$ falls to a very low value it means that $E_{gl}$ or $E_{sl}$ will be almost zero, so that the liquid surface will have adopted the potential V of the grid or source. The surface charge density which gives rise to this potential on the liquid surface will then be

$$\sigma = D_v = \varepsilon_o \frac{V}{d_{lc}} \ , \qquad (3)$$

where $d_{lc}$ is the distance from the liquid surface to the collector C2. Thus the position of the liquid surface is critical in determining the amount of surface charge which will reside below the free surface, and therefore in determining the field $E_{lc}$ which will exist between the surface and the collector C2.

The build up of surface charge is thus a direct consequence of the difficulty experienced by the negative ions in trying to leak away via the Helium film. This means that the field applied across the surface is not constant with falling temperature, since as $I_{c2}$ falls, charge will deposit itself below the free surface causing the potential of the surface to rise with falling $I_{c2}$. Therefore the field between the liquid surface and the collector rises as $I_{c2}$ falls.

(c) The "Film" Current $I_{c1}$

The temperature dependence of the currents $I_{c1}$, collected C1 when a liquid surface separated the grid or source and collector C2, below 1.4 K where a temperature-dependent fall similar to the fall in current $I_{c2}$, was observed, would suggest that these currents $I_{c1}$ were not wholly due to negative ions travelling in the Helium film. A large proportion of this "film" current probably originates at the meniscus around the inside surface of the ion cell. The initial appearance of a current on the collector C1 could be due to the initial stages of surface charge build-up, which could sufficiently distort the field in the vapour so that some of the ions crossing the liquid surface find their way to C1. It may be that some of these ions could travel to C1 along the outside surface of the film, trapped in the image-potential-induced surface states predicted by Cole and Cohen (1969). In any event, the fact that at least part of $I_{c1}$ showed a temperature-dependent change similar to that observed for the current $I_{c2}$ can only be due to that part having originated from transmission across the surface.

It is then necessary to explain why a substantial current did not flow in the film, as was observed by Bruschi et al and by Maraviglia. Since the dielectric constant of the substrate (i.e. glass or perspex) will be greater than that of the liquid, an ion which finds itself in the Helium film will experience a large attractive image potential to the substrate. This image potential will be

$$V(x) = \frac{e}{8\pi} \frac{(\varepsilon_s - \varepsilon_L)}{\varepsilon_L (\varepsilon_s + \varepsilon_L)} \frac{1}{x} \text{ ev} , \qquad (4)$$

where $\varepsilon_s$ and $\varepsilon_L$ are the dielectric constants of the substrate and liquid respectively, and x is the distance of the ion from the substrate.

Taking for x the value of the ionic bubble radius of 12.4 Å, the binding potential of the ion to the substrate may be written

$$V(\varepsilon_s) = 0.63 \frac{(\varepsilon_s - 1)}{(\varepsilon_s + 1)} \text{ electron volts .} \qquad (5)$$

The values of the dielectric constants of glass and perspex at the temperatures of liquid Helium could not be found from the literature. However from Sutton (1960), an extrapolated value for glass of between 3 and 4 would be reasonable. This means that the negative ion will bind to a glass substrate with a potential of about 0.35 ev. Since the substrate will inevitably be rough on an atomic scale, the combination of the image potential and the roughness will act like a glue, causing the ionic mobility and hence the current to be very small.

If the dielectric constant of perspex around 1 K is slightly less than the dielectric constant of glass at this temperature, then this would account for the film currents being slightly greater on the perspex substrate, since the binding of the ion to the substrate by equation (5) would be less.

Any currents which do exist in the Helium film must be two dimensional. This is because it is energetically very unfavourable for there to be more than one layer of charge, since two similar ions separated by a distance of the order of the thickness of the film, experience a repulsive potential of the order of 600 K which is about twenty times greater than the potential barrier preventing them from boiling out of the film through the liquid surface.

(d) The Rise in the Transmission Current $I_{c2}$ below 1.15 K

The emergence of negative ions from the liquid surface into the vapour at temperatures below 1 K has previously been observed by

Cunsolo, Dall'Oglio, Maraviglia and Ricci (1968), and also by Surko and Reif (1968). Cunsolo et al performed their experiment at 0.4 K where they observed that a negatively charged vortex ring annihilated at the liquid surface and transferred all of its energy into the ejected electron. On the otherhand, Surko and Reif observed that below about 0.7 K negatively charged vortex rings could annihilate at the free surface but that the ejected electron had negligible energy.

The appearance of a rise in the transmission current at temperatures above 1 K in the present work could not be due to charged vortex rings annihilating at the free surface, since the energy loss of a charged vortex ring at this relatively high temperature would prevent it from travelling a significant distance in the liquid.

It was discussed in section 7.8(b) that the build-up of charge just below the liquid surface causes the field in the vapour $V/d_{lc}$ to be much larger than it would be in the absence of surface charge. For example, if the applied field were required to be, say, 50 volts $cm^{-1}$, when the grid-collector distance $d_{gc}$ was 1.5 cm, then -75 volts should be applied to the grid. If the liquid surface were then, say, 0.5 cm from the collector, and $I_{c2}$ had substantially fallen so that the liquid surface had adopted the grid potential, then the field in the vapour between the surface and the collector C2 would no longer be 50 volts $cm^{-1}$ but 150 volts $cm^{-1}$.

It was shown in section 7.4 and figure 7.6 that a field of 170 volts $cm^{-1}$ can break down the vapour above the liquid at 1 K. It seems plausible therefore to associate the low temperature rise in the transmission current with some form of breakdown process in the vapour. Where the rise in current was very steep, for the higher fields, there was probably complete dielectric breakdown in the vapour. The appearance of a peak in this current as the temperature was reduced,

as shown in figure 7.5, is undoubtedly associated with an electron mean free path effect, as discussed in section 7.4 for the minimum in the breakdown potential (figure 7.6).

The more gradual rise in current for the lower fields could have been due to a pre-breakdown process, where those ions which do manage to cross the liquid surface will ionize the atoms of the vapour with which they collide so that a multiplication process can result.

It is not surprising that an electron which escapes from a region of surface charge at low temperatures is capable of causing ionization in the vapour. The average potential of a negative ion, located below the free surface in a region of surface charge $\sigma$, due to the presence of all the other ions can be shown to be $\overline{U}$, where

$$\overline{U} = \frac{R\sigma}{6\varepsilon_o} = \frac{RV}{6d_{lc}} \quad , \qquad (6)$$

where R is the radius of the surface which has potential V and $d_{lc}$ is the distance from the collector C2. Equation (6) is derived in Appendix 2.

Taking typical values of R (1.5 cm), V (100 volts), and $d_{lc}$ (0.5 cm), equation (6) yields a potential of 50 ev to the escaping electron, which is much greater than the ionization potential of the Helium atom.

It was observed in figures 7.9 and 7.10 with the triode 7.1(a), that when the liquid surface was not close to the collector C2 no low temperature rise in current was observed for the two fields of 10 and 20 volts $cm^{-1}$, while a rise was observed when the surface was close to the collector C2.

This can be explained by noting that when the surface is far from the collector the field which will exist in the vapour, when the liquid

surface has adopted the grid potential, will be small, as also will be the average potential, from equation (6). Therefore little or no ionization in the vapour will result. When the liquid surface is close to the collector, however, both the field in the vapour and the average potential will be large so that a rise in current due to ionization in the vapour can result.

The rise in the transmission current at low temperatures due to ionization in the vapour is therefore seen to be a direct consequence of the build up of charge below the free surface.

(e) Parameters Involved in the Determination of the Energy Barrier

It was shown in section 6.4 that the energy barrier which the negative ion must surmount in order to pass from the liquid into the vapour, will depend upon the field which exists inside the liquid. The present work, however, has revealed that this field is not constant during the course of a measurement of the variation of the transmission current with temperature, due to the build up of charge below the liquid surface. As the charge deposits itself below the surface the field in the liquid decreases and so the energy barrier presented to the ion in the liquid should increase. However, it has been observed in section 7.5 that the energy barrier depends upon the liquid level; this is equivalent to a dependence on the field between the liquid surface and collector, such that as this field increases so the energy barrier decreases.

Thus the build up of surface charge gives rise to two opposing forces determining the energy barrier. That is, the decrease of the field in the liquid causes an increase in the energy barrier, and an increase in the field between the liquid surface and collector causes a decrease in the energy barrier. The value of the energy barrier which is measured will be the result of this competition.

Finally the measured energy barrier will be a function of the ion cell design. If the ions which reach the surface, and immediately experience difficulty in surmounting the potential barrier, are offered an alternative route to earth, either by the cell having conducting walls at zero potential, or by the walls being so smooth that the ions can easily run up the Helium film, then the transmission current should fall quickly with falling temperature, since very little space charge will be built up below the free surface. If the impedance to earth is greater, for example by the substrate being so rough that the film current is very small, then surface charge will establish itself. The rate of build up of this surface charge will depend upon the rate at which ions, reaching the surface, can be removed through the film to earth. Since the presence of surface charge has already been shown to affect the measured energy barrier, so the ion cell design will affect it. The energy barrier, which is measured from the exponential fall in the transmission current with falling temperature, will thus be a function not only of the applied field, but also of the liquid level in the ion cell, and of the ion cell itself. The energy barriers measured during the present work, some of which are shown in tables 1 and 2 are therefore only meaningful in the particular circumstances in which they were measured.

The dependence of the value of the energy barrier on the three parameters mentioned could thus account for the inconsistency between the various values quoted in the literature, which were touched upon in section 6.2.

Appendix 3 contains a re-analysis of the data of the present chapter. A new current I, defined as the sum of $I_{c1}$ and $I_{c2}$, was used as a fresh source of energy barriers $\phi_E$. The field and level dependence, and general scatter of these new measurements gave rise to the same conclusions already discussed in the present section.

# CHAPTER 8

## POSITIVE IONS AT THE LIQUID SURFACE

(Work performed by other authors)

### 1 Introduction

There is little information in the literature concerning the behaviour of positive ions in the presence of the liquid surface. Those workers who have examined this behaviour have each observed slightly different phenomena, which will be summarised in section 2. The most consistent piece of information resulting from this work is that positive ions experience great difficulty in crossing from the liquid into the vapour, and this is not surprising, since by the nature of its structure, the positive ion is likely to bind strongly to the dense liquid. Also if the ion approaches the liquid surface to a distance of the order of its radius, the image repulsive potential, given by equation 6.(1), which it will experience is of the order of 400 K.

### 2 The Transmission Current $I_{c2}$

It was mentioned in section 6.1 that Careri, Fasoli and Gaeta (1960) were the first to examine the effect of the liquid surface on an ion current. They observed that, above the lambda point, the positive ion current was unattenuated by the liquid surface, while below the lambda point it quickly fell to zero with falling temperature. Bruschi, Maraviglia and Moss (1966), however, were unable to detect a current of positive ions across the liquid surface at any temperature.

Cunsolo, Dall'Oglio, Maraviglia and Ricci (1968) reported that at 0.4 K positively charged vortex rings were annihilated at the

liquid surface, giving rise to a current of positive ions across the surface. Surko and Reif (1968), however, working in a similar temperature range, found no such effect.

The observation of Bruschi et al was partly confirmed by Bianconi and Maraviglia (1969), who found a large positive ion current across the liquid surface, but only when that surface was at a critical height above the source. They employed a diode cell with a Polonium 210 source. At all other liquid depths between the source and collector, no positive ion current was detected, although a very small current was obtained when there was no liquid at all between the electrodes. At the critical depth of liquid, when the surface was about 2 mm above the source, they detected a large current, of order $10^{-11}$ amps, but this was very sensitive to the liquid depth. They made no mention of what fields were used, or of the temperature dependence of the phenomenon, although from their data it is clear that they were able to detect it at temperatures up to 1.8 K. This effect will be considered along with the observations of the present work in section 9.4.

3 Positive Ion Currents in the Film

It has already been mentioned in section 6.5 that other workers found that a negative ion current was collected through the Helium film on an insulating support. Maraviglia (1967) repeated his work using positive ions, and observed that positive ions could also be collected on an electrode as a result of having travelled through the Helium film. He also found that, like the negative ion, the positive ion's mobility in the film was significantly lower than in the bulk liquid at the same temperature. Bianconi and Maraviglia extended this work using a diode cell in a glass beaker, and found that the

positive ion current in the film was sensitive to the motion of the film. They in fact observed oscillations in this current at twice the frequency with which the level of liquid in the beaker was oscillating due to inertial film oscillations.

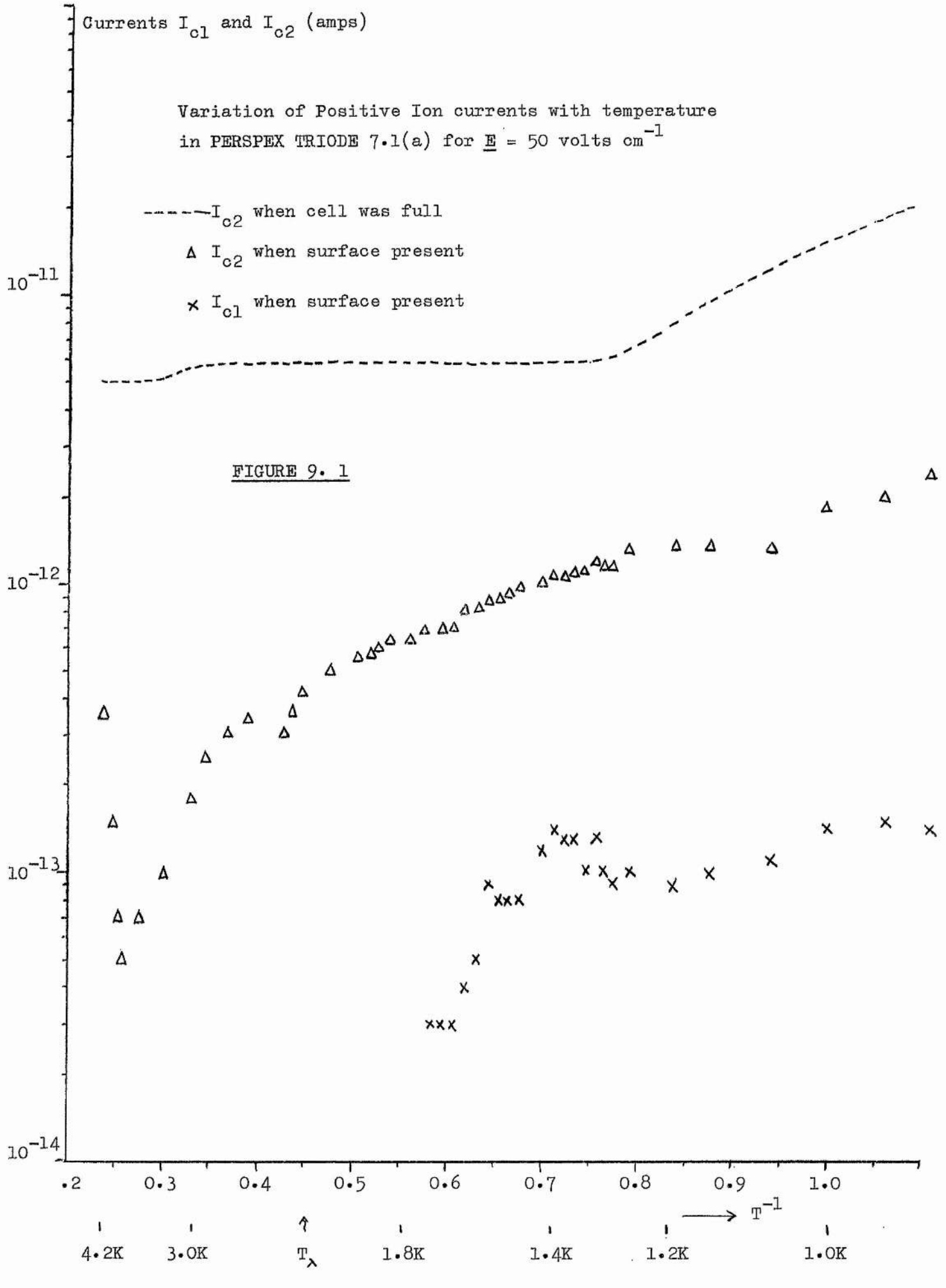
Currents $I_{c1}$ and $I_{c2}$ (amps)
Variation of Positive Ion currents with temperature
in PERSPEX TRIODE 7.1(a) for $\underline{E}$ = 50 volts $cm^{-1}$
$I_{c2}$ when cell was full
$I_{c2}$ when surface present
$I_{c1}$ when surface present
$10^{-11}$
$10^{-12}$
$10^{-13}$
$10^{-14}$
.2
0.3
0.4
0.5
0.6
0.7
0.8
0.9
1.0
$T^{-1}$
4.2K
3.0K
$T_\lambda$
1.8K
1.4K
1.2K
1.0K

FIGURE 9. 1

# CHAPTER 9

## POSITIVE IONS AT THE LIQUID SURFACE

(Work performed during the present research)

### 1 Experimental Procedures and Observations

The experimental procedures described in chapter 7 for negative ions also applied to the present work with positive ions. The ion cells used to study the negative ion behaviour shown in figure 7.1(a) to (d) were also used to study the positive ion behaviour.

### 2 The Transmission Current $I_{c2}$

During the course of the present work it was always found to be possible to detect a positive ion current of some kind across the liquid surface. At any particular temperature and applied field, this current was not very reproducible, nor was it particularly sensitive to the applied field. A typical temperature variation of the positive ion current collected across the liquid surface for an applied field of 50 volts $cm^{-1}$ in the perspex triode cell 7.1(a) is shown in figure 9.1. It may be seen from the figure that between 4.2 K and about 3.8 K, $I_{c2}$ fell very sharply, then between 3.8 K and 1.3 K it rose again, and remained constant down to 1 K when it began to rise again. The rise in the transmission current for positive ions at temperatures below about 1 K was similar to that for negative ions discussed in section 7.3; that is, the rise was steeper for the higher applied fields, and for very high fields ( $>$ 160 volts $cm^{-1}$) it displayed a peak in current with falling temperature. Figure 9.1 also shows the variation of the current $I_{c2}$ collected on C2 when the cell was full of liquid, as well as the current $I_{c1}$ collected on the

Variation of current collected on C2 with grid-collector field $E_{gc}$ in GLASS TRIODE 7.1(b) when Source was held at zero potential

FIGURE 9. 2

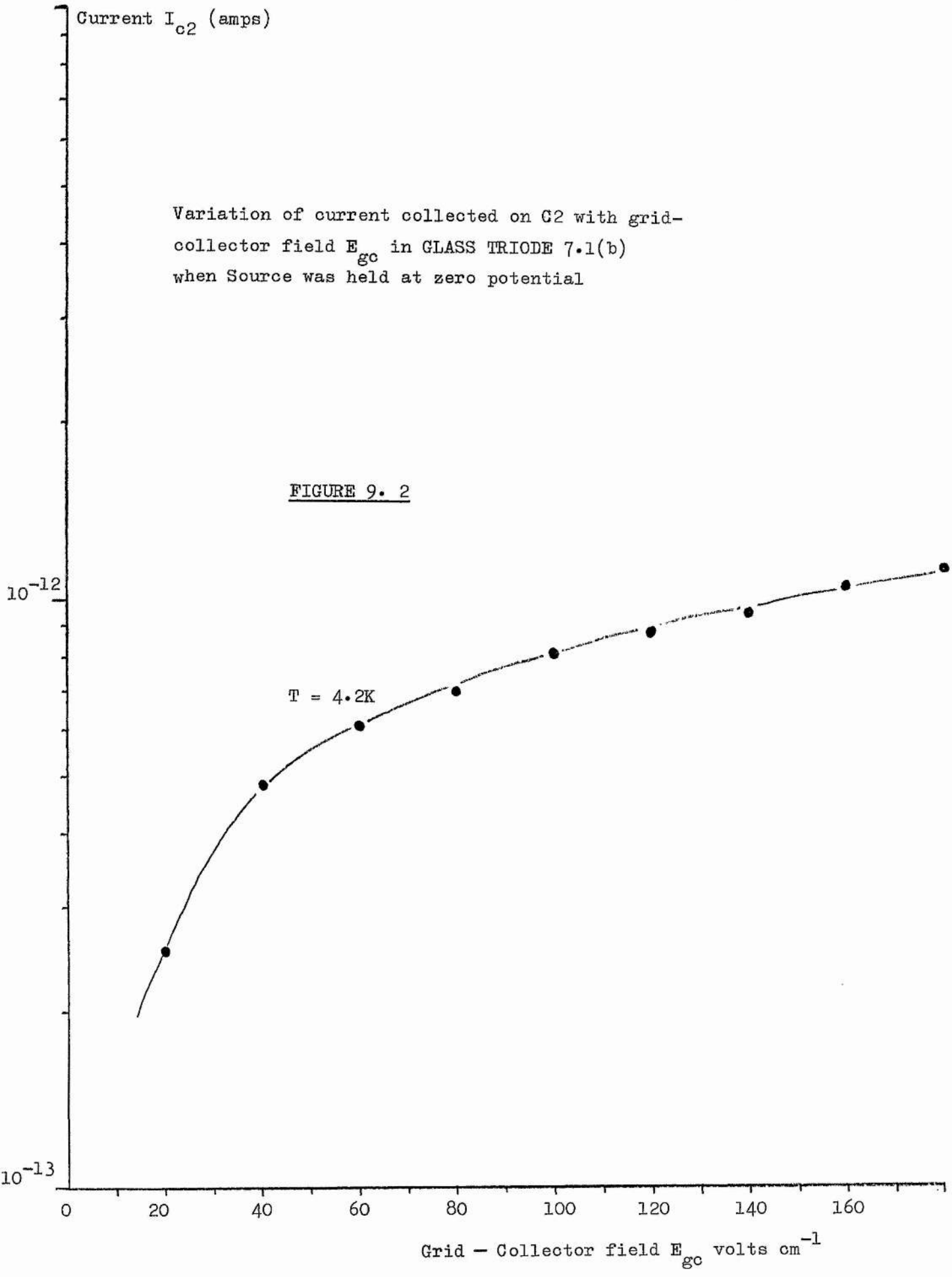

film collector C1 when the liquid surface was present between the grid and collector C2.

It was initially observed that the current $I_{c2}$ collected across the liquid surface in a triode cell, depended only upon the grid-collector field and was independent of any voltage applied to the source. This meant that even with the source earthed, currents could still be observed on C2 by applying a positive potential to the grid. A typical result of the variation of the transmission current $I_{c2}$ with grid-collector field for the source at zero potential is shown in figure 9.2. Further investigation of this somewhat remarkable effect revealed that it was possible to detect zero current on the grid while at the same time collecting a positive ion current on C1 and C2, as well as a negative ion current leaving the source. This was done by floating the Keithley 602 in the grid bias circuit and suitably adjusting the source potential. For example, in the glass triode 7.1(c) with the grid voltage $V_g$ = + 100 volts and the source voltage $V_s$ = + 107 volts, the current collected on the grid was zero while $I_{c1} = 2 \times 10^{-13}$ amp, $I_{c2} = 8 \times 10^{-13}$ amp, and the source current $= 1.2 \times 10^{-12}$ amp. This could only be explained if electrons were somehow reaching the grid from the collectors above, while positive ions were reaching the grid from the source below, so that the two ionic currents exactly cancelled each other at the grid. That this effect of obtaining an apparent positive ion current across the liquid surface simply by making the grid positive was in fact a transient one , was demonstrated by the following procedure. With the source-grid field and grid-collector field, (which are normally equal), suitably biased to provide a flow of positive ions towards the liquid surface, a steady current was collected on C2. The source potential was then switched to zero and the transmission current $I_{c2}$

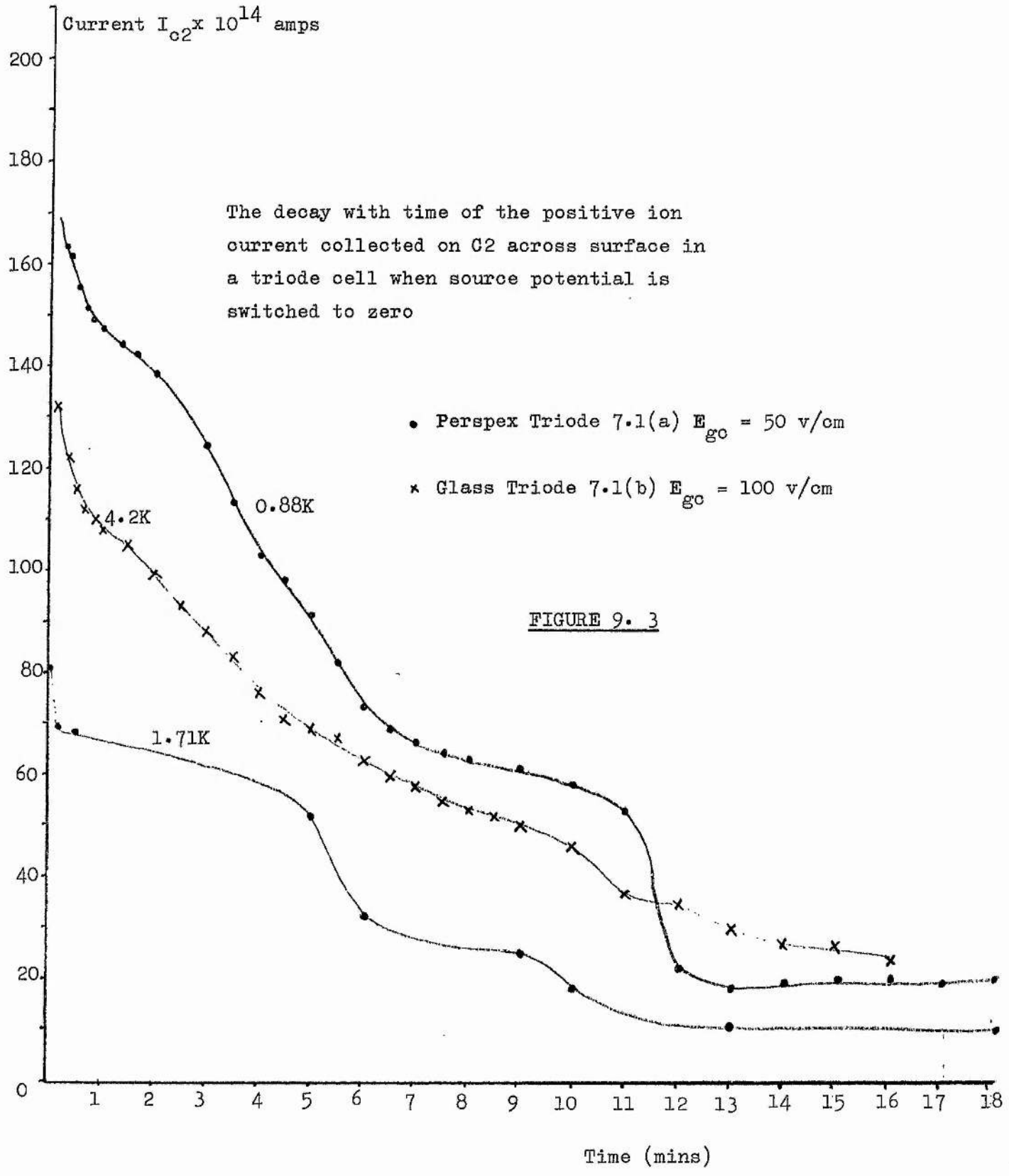
Current $I_{c2}$ x $10^{14}$ amps
200
180
160
140
120
100
80
60
40
20
0
1
2
3
4
5
6
7
8
9
10
11
12
13
14
15
16
17
18
Time (mins)
The decay with time of the positive ion current collected on C2 across surface in a triode cell when source potential is switched to zero
• Perspex Triode 7.1(a) $E_{gc}$ = 50 v/cm
× Glass Triode 7.1(b) $E_{gc}$ = 100 v/cm
0.88K
4.2K
1.71K

FIGURE 9. 3

was observed to decay with time. This is shown in figure 9.3, both at 1.71 K and 0.88 K for a grid-collector field of 50 volts $cm^{-1}$ in the perspex triode 7.1 (a), and at 4.2 K for a grid-collector field of 100 volts $cm^{-1}$ in the glass triode 7.1(b).

It must be stressed that the above effect was only seen when a liquid surface separated the grid and collector C2. Varying the grid voltage when the triode cell was full of liquid gave rise only to pick-up on C2, which decayed in a few seconds.

The appearance of a temperature-dependent positive ion current crossing the liquid surface, shown in figure 9.1, was very unusual indeed. No other reports of such behaviour have been found in the literature.

Since there is no observational difference at an electrode between the arrival of positive ions or the emission of electrons, then electron emission from the collector C2 surface could account for the observation. These electrons could combine with the positive ions below the liquid surface, so giving rise to a steady current. It would appear that emission from the collector surface could only be due to the photoelectric effect caused by photons originating at the source. Since all the early ion experiments were carried out using Americium 241 as the source, it was initially felt that these photons must be the gamma rays from the Am 241, where almost every event in the complicated decay scheme has a gamma ray associated with it. A survey of the literature revealed that every previous experimenter working with a source in the presence of the liquid surface had used Polonium 210. Since Po 210 has a gamma emission about $10^5$ times smaller than Am 241, this might explain why the effect had not been reported.

In order to test this hypothesis, a run was made with a thin

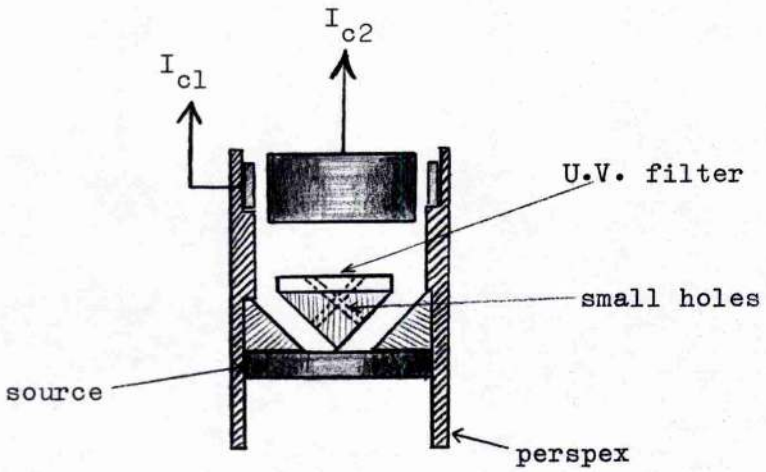


Diode cell with shielded source

FIGURE 9. 4

metal foil covering the Americium source. This would have the effect of stopping all of the α particles, but not the gammas. The experiment, however, yielded no currents whatsoever, either transient or otherwise, showing that it was very unlikely that photoemission by gamma rays was the cause. In any case, when a Polonium 210 source was obtained, and exhibited similar phenomena to those illustrated in figures 9.1 to 9.3, a search had to be made for some other source of photons of sufficiently high energy to cause photoemission.

The passage of high energy α particles through liquid Helium is known to cause scintillations in the liquid. Simmons and Perkins (1961) showed that liquid Helium scintillates in the extreme ultraviolet, below 1200 Å. It was subsequently shown by Hereford and Moss (1966) that a substantial fraction of the scintillation intensity (photons per α particle) derives from recombination luminescence. That is, a considerable amount of uv light is emitted in the region of an α source immersed in the liquid due to de-excitation and recombination processes. The energy associated with photons in the far uv is of order 10 e.v. which is much greater than the work function of the gold plating (5 e.v.) of the collector surface.

It was therefore plausible to assume that what appeared to be a positive ion current crossing the liquid surface, was in fact photoelectric emission of electrons from the surface of the collector C2 caused by the uv originating at the α source.

In order to test this hypothesis, the source was shielded from the collector C2 by the insertion of a uv filter. This proved to be a very difficult operation, since the first three cells which were designed and built with the source shielded from C2 yielded no currents at all, even when the cell was completely full of liquid. The diode cell shown in figure 9.4, however, did yield results. In this ion

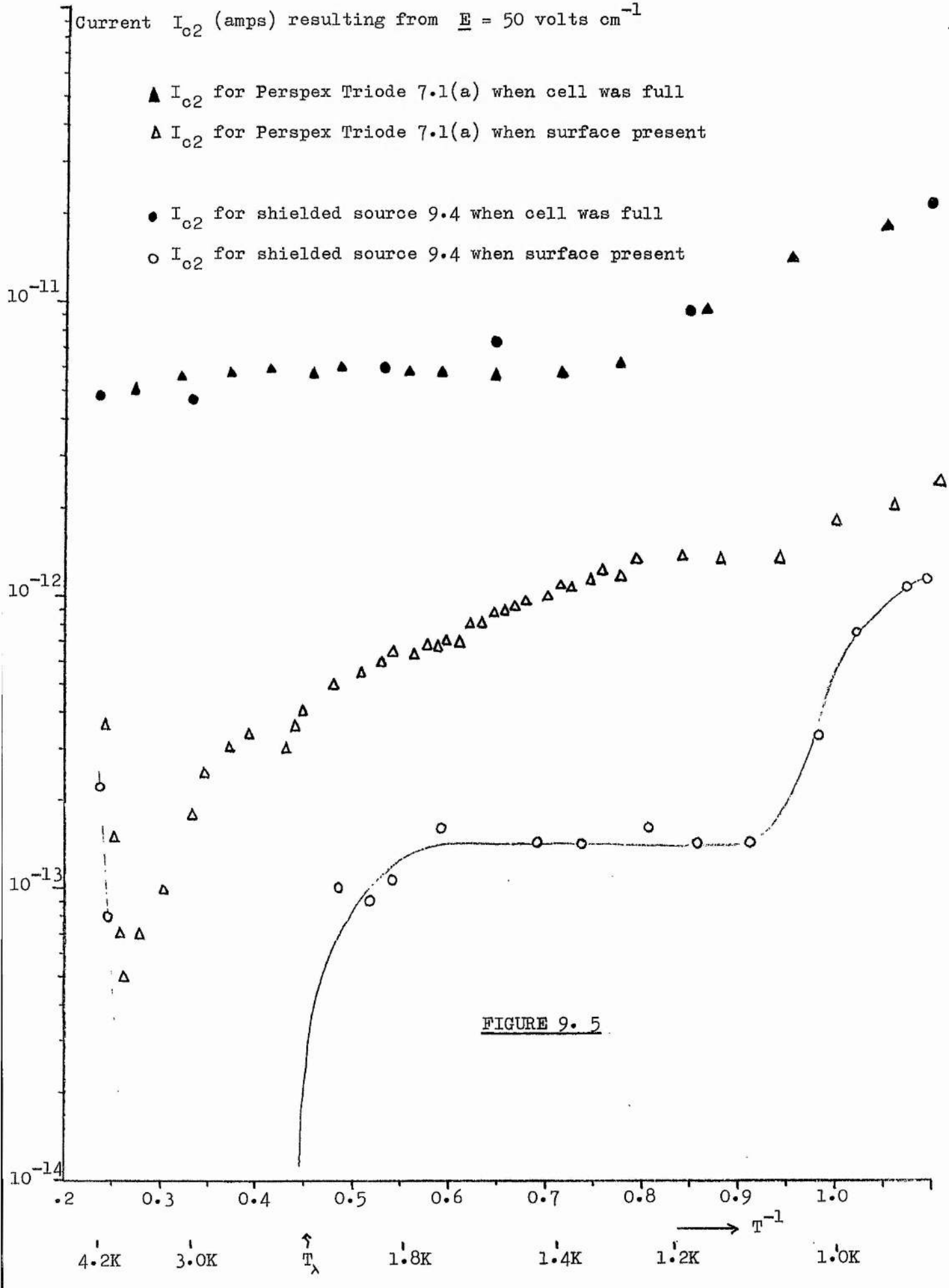
Current $I_{c2}$ (amps) resulting from $\underline{E}$ = 50 volts cm$^{-1}$
▲ $I_{c2}$ for Perspex Triode 7.1(a) when cell was full
△ $I_{c2}$ for Perspex Triode 7.1(a) when surface present
● $I_{c2}$ for shielded source 9.4 when cell was full
○ $I_{c2}$ for shielded source 9.4 when surface present
$10^{-11}$
$10^{-12}$
$10^{-13}$
$10^{-14}$
.2
0.3
0.4
0.5
0.6
0.7
0.8
0.9
1.0
$T^{-1}$
4.2K
3.0K
$T_\lambda$
1.8K
1.4K
1.2K
1.0K

FIGURE 9. 5

cell, the source was shielded from the collectors by a perspex cone, on top of which rested a disc made from a uv filter material. This filter absorbs all photons below 4000 Å (3 e.v.). Four small bore holes were drilled through the cone to increase the number of paths available to the positive ions in their excursion from the source either to the collector or to the liquid surface. The source used in this experiment was the same as that used in the perspex triode 7.1(a), the results from which were shown in figure 9.1. These results have been re-plotted in figure 9.5 for comparison with those obtained when the source was shielded.

When the cell of figure 9.4 was completely full of liquid, the current collected at C2 was almost the same as that collected in the perspex triode. This is shown in figure 9.5 for the same applied field of 50 volts $cm^{-1}$. It may therefore be deduced that the shield did not substantially inhibit the flow of positive ions from the source to the collector through the bulk liquid.

When a liquid surface separated the collector C2 from the source and shield of the diode in figure 9.4, the current $I_{c2}$ displayed the temperature dependence shown in figure 9.5. These results were obtained for the same applied field of 50 volts $cm^{-1}$ as the other results quoted in the figure. It should be pointed out that the currents collected on C2 when a liquid surface was present in the shielded diode were not transient, since each point plotted in figure 9.5 was the result of at least half an hour's wait at the particular field and temperature of measurement.

It may be seen from figure 9.5 that the current $I_{c2}$ collected across the surface for the shielded source fell very quickly to zero between 4.2 K and about 3.8 K. Between 3.8 K and the lambda point it was zero, while below the lambda point it rose quickly to an almost

temperature independent value of about $1.5 \times 10^{-13}$ amp. The value of $I_{c2}$ was found to be very insensitive to applied fields between 10 and 100 volts $cm^{-1}$, although making the field zero, by earthing the source, caused $I_{c2}$ to fall to zero. The sharp rise in the current below 1.0 K was probably due to a breakdown process in the vapour, similar to that discussed for negative ions in section 7.8(d).

The effect of the uv shield will be further discussed in section 9.6.

3 The Positive Ion Current Collected on C1.

The currents $I_{c1}$ which were sometimes observed were always very small. They exhibited no particular field or temperature dependence and were not very reproducible. The temperature dependence of the positive ion current collected during one run on C1 of the perspex triode 7.1(a) when a liquid surface separated the grid and collector C2 is shown in figure 9.1.

During the runs with the shielded source in figure 9.4, no currents were ever observed on the collector C1 at any temperature or field, and for any position of the liquid level. This evidence would suggest that all previously recorded positive ion film currents were not in fact due to positive ions travelling in the film but due to photoemission from the surface of the collector C1.

Indeed it is not at all surprising that if the negative ion current experiences great difficulty in travelling in the Helium film, as discussed in section 7.8(c), then the positive ion should experience even greater difficulty in doing so. This is because the smaller radius of the positive ion should cause it to approach closer to the substrate than the negative ion, and therefore to experience a greater binding image potential to the substrate. From equation 7.(4) this

potential should be about 0.7 e.v.

4 The Peak in the $I_{c2}$ Current observed by Bianconi and Maraviglia

It was mentioned in section 8.2 that Bianconi and Maraviglia had observed a large positive ion current across the liquid surface when the liquid surface was about 2 mm above their Po 210 α source. They interpreted this current as being due to positively charged vortex rings annihilating at the liquid surface and emitting the trapped positive ion.

Several attempts were made during the present work to observe this peak in current but all proved unsuccessful. For example, the diode in the glass beaker 7.1(d) was allowed to fill by film flow while the source was earthed, and the currents $I_{c1}$ and $I_{c2}$ were allowed to run on chart recorders to record any current variation as the liquid overcame the source. Examination of the recorder tracings revealed that as the liquid covered the source the current, which was being collected through the vapour, fell to zero. It is surprising that Bianconi and Maraviglia observed only a very small current when nothing but vapour separated their source and collector, since in the present work a large current was always collected on C2 through the vapour, even when the source was earthed. Any applied field between the source and collector in the vapour gave rise to very large currents. The current which was collected on C2 when the source was at zero potential, and when only vapour separated the electrodes, was a positive ion current and was sensitive to vapour pressure. This is shown in figure 9.6 where the vapour pressure was varied by varying the temperature of the liquid below the source. The reason a current can be collected on C2 when the source is grounded is that because of the high input impedance of the electrometer on C2, the collector

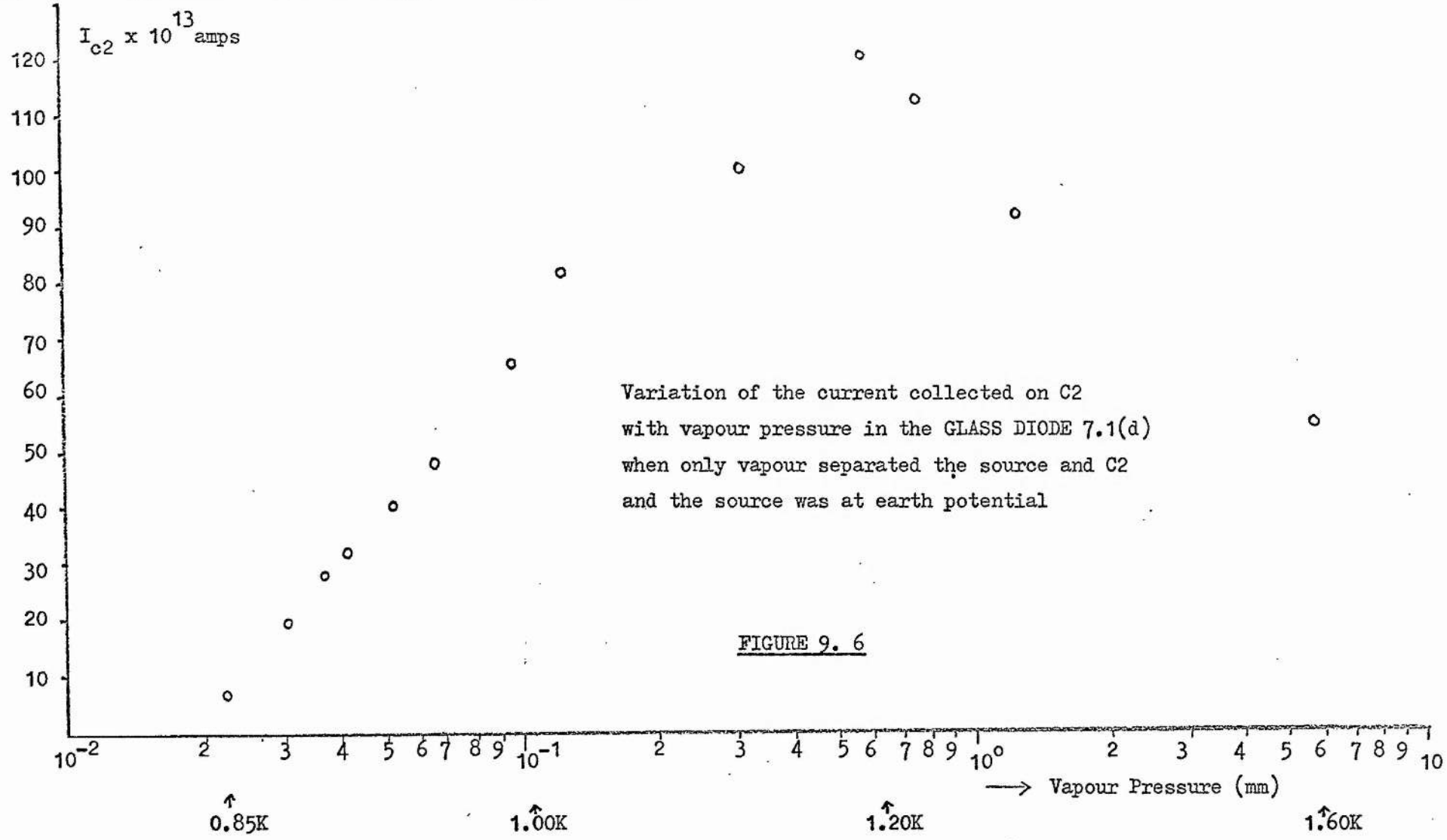


Variation of the current collected on C2 with vapour pressure in the GLASS DIODE 7.1(d) when only vapour separated the source and C2 and the source was at earth potential

FIGURE 9. 6

itself will not be at zero potential but at a small fraction of a volt below this, and this small potential difference between source and collector is sufficient to cause a large current through the vapour. It may be seen from figure 9.6 that as the vapour pressure was reduced the current $I_{c2}$ at first rose until it reached about $1.3 \times 10^{-11}$ amps at around 1 torr pressure, and then fell to a value of order $10^{-12}$ amps at about $2 \times 10^{-2}$ torr. If the vapour pressure were to be reduced further one would not expect a current of much less than $10^{-12}$ amp since the $\alpha$ particles from the 200 $\mu$ curie source constitute a current of this order. The appearance of a current larger than the $\alpha$ particle current must be due to ionization in the vapour by the $\alpha$ particles and the subsequent diffusion of these ions to their respective electrodes. If the vapour density is not too large then diffusion will be a more important process than recombination. As the vapour density increases so the current will increase due to the greater number of ion pairs created by the $\alpha$ particle and the corresponding greater number diffusing to their electrodes. However, there will come a point when recombination takes over as the dominant process and further increases in vapour density should cause a reduction in collected current.

## 5 The Determination of the Liquid Level by Negative Ion Velocity

At the beginning of the present work, what seemed at the time to be a very accurate method was tried, of determining the position of the liquid surface between the grid and the collector C2. The method was to measure the velocity of negative ions between the grid and the collector C2 across the liquid surface, when their mobility in the bulk liquid was already known at the temperature of measurement. Since the mobility in the vapour is orders of magnitude greater than

the mobility in the liquid, the time of flight of the negative ion between the grid and collector will be governed almost entirely by the distance which the ion travels in the liquid. If this time of flight was measured, the position of the liquid surface could then be computed from the known mobility in the liquid.

The method failed, however, for the following reason. The square wave technique of measuring ionic velocity, discussed in chapter 4, relies for its operation on there being a collected current during one half of the cycle, and zero current during the reverse half. For the reasons discussed in section 9.2, a current was collected on C2 during both cycles of the square wave. That is, when the grid was negative, the negative ions were driven towards the collector, and when the grid was positive the photoejected electrons from the collector surface gave rise to a current in the opposite direction. Thus the current-frequency technique was useless in exploiting this idea.

6 Discussion of the Results in Figures 9.1 to 9.5

The experiment with the uv shield provides clear evidence that what appears at first sight to be a positive ion current crossing the liquid surface, is in fact photoelectric emission from the collector surface, due to the ultraviolet emission from the source region caused by $\alpha$-particle induced scintillation. That is, the presence of the uv shield has cut down this current by an order of magnitude. The fact that the current was not reduced to zero was probably due to incomplete shielding of the source from the collector surface. This could be due either to some of the uv passing through the small holes of the shield, or the uv being radiated at relatively large distances from the source.

Attention will now be focussed on the figures 9.2 and 9.3, which were a result of the observation that by applying a positive potential to the grid of a triode when a liquid surface separated the grid and collector C2, it was possible to detect a current which took several minutes to decay, although the effect was not observed when the cell was full of liquid. It would appear that when a liquid surface is present the photoelectrons can penetrate the 300 Å of film (which will inevitably cover the collector surface) and escape into the vapour, yet they cannot escape through bulk liquid. In order to explain this effect it will first of all be necessary to examine the behaviour of an electron in the vicinity of a conducting surface:-

An electron which finds itself at a distance x from a metal surface will experience two opposing forces. One will be the field E, pulling it away from the surface, and the other will be the image potential drawing it back to the surface. The potential of the electron in front of the metal surface will be the sum of the image and field potentials. If this potential is V(x) then,

$$V(x) = -\frac{e^2}{8\pi\varepsilon_o} \cdot \frac{1}{x} - E e x \qquad (1)$$

where e is the electronic charge and $\varepsilon_o$ is the dielectric constant of the vapour in front of the surface. Equation (1) will have its maximum value $x_m$ where

$$x_m = \sqrt{\frac{e}{8\pi\varepsilon_o E}} \cdot \qquad (2)$$

The significance of this distance $x_m$ is that if the electron is located at a distance $x > x_m$, then it can escape from the metal surface, while if $x < x_m$ it will be drawn back to the collector.

In their work on tunnel junctions, Onn and Silver (1971) found that the hot electrons which were ejected from a cold cathode surface into Helium vapour were initially quasifree, and remained so until they became thermalized. This thermalization process was characterized by a certain range $x_o$, which depended on the magnitude of the applied field and also on the Helium density in front of the cathode. If this distance $x_o$ was greater than $x_m$ then the electrons could escape into the liquid; and conversely if $x_o$ was less than $x_m$ then the electron could not escape.

In the present work, if we take a typical value for the applied field E = 100 volts $cm^{-1}$, equation (2) gives for $x_m$ the value 2700 Å, which is an order of magnitude greater than the film thickness, so that the presence of the Helium film on the collector surface is probably of no great importance.

When the ion cell is full of liquid, the thermalization range $x_o$ will be small, due to the high density of liquid in front of the collector surface, and will be less than $x_m$. Thus the photoelectrons will be unable to escape from the metal surface; this accounts for the absence of the transient current when the cell was full of liquid.

When the collector is located in the vapour, and there is only the Helium film covering its surface, the effective density in front of the collector will be small, and the photoelectron will not have thermalized in the film, therefore it will still be quasifree in the vapour. The distance $x_o$ will now be much larger, and will become of the order of $x_m$ as the vapour density (i.e. temperature) is reduced. This will have the effect that some of the photoelectrons will be able to escape the influence of the collector C2. If the vapour density is very low, (at low temperatures), then $x_o$ will be much greater than $x_m$ so that almost all of the photoelectrons should be

able to escape.

It was shown in figure 9.3 that unless there is a flow of positive ions to the liquid surface from below then the currents observed by applying a positive potential to the grid were transient. This can be explained as follows. It was first shown by Sommer (1964) that electrons experience great difficulty in penetrating into the liquid from the vapour above. Williams, Crandall and Willis (1971) later showed that electrons could be deposited on the liquid surface from above and held there by a suitable field applied from below. The transient nature of the currents under discussion must be due to the slow build up of charge on the liquid surface since this charge has great difficulty in penetrating the liquid. The charge will build up until the surface has adopted the potential of the collector, so that the field drawing the photoelectrons away from the collector surface will gradually fall to zero. Thus no more electrons emitted from the collector surface will be able to escape, and therefore no more current will be recorded.

It has previously been remarked that in order to record a steady current across the liquid surface, not only is it necessary to have a flow of photoelectrons from the collector to the liquid surface, but it is also necessary to have a flow of positive ions up to the surface from below. The two currents must therefore combine at the liquid surface. It should be pointed out that the potential of a positive ion and an electron separated by about 100 Å with a liquid surface between, is of order 1600 K, which is much greater than the potential preventing the positive ion from leaving the liquid, so that such an explanation of the steady current is energetically favourable.

Finally it is necessary to explain the general form shown in figures 9.1 and 9.5, of the temperature dependence of the apparent

positive ion current $I_{c2}$ crossing the liquid surface. Between 4.2 K and 3.8 K there is a very sharp fall in current. This can only be due to a genuine flow of positive ions across the surface, falling with decreasing temperature, in a manner similar to that of the negative ion discussed in chapter 6, but with a considerably larger energy barrier. The subsequent increase in current with falling temperature will not be due to positive ions but to photoelectronsand will be caused by an increase in the thermalization range $x_o$ with decreasing vapour density, such that more and more photoelectrons will be able to escape from the collector surface. When the vapour density is very low, almost all of the photoelectrons will escape from the metal surface and this will give rise to a more or less constant current, as observed.

## SUMMARY

The thesis has covered several problems associated with the production and properties of ions in liquid Helium. First, a vortex refrigerator was designed and built in order to extend the experimental temperature range down from 1.2K to 0.8K. Second, the production of ions and their properties in cells where the source and collector were immersed in the liquid was studied. Third, an investigation was carried out on possible ion currents in Helium films, and fourthly, an investigation was carried out on the passage of ions across the liquid-vapour interface, when the source was immersed and the collector was in the vapour.

A vortex refrigerator was constructed and its operation and properties were examined. It has been found that greater cooling capacities were obtained as the refrigerating capillary diameter increased, but that greater pumping powers were required to produce this. The final temperature reached by the fridge chamber for zero heat input was roughly independent of the fridge capillary diameter, but depended on the temperature of the bath.

The temperature and field dependence of the positive and negative ion currents extracted from an $\alpha$-source immersed in the liquid has been measured. It was observed that for low fields at high temperatures the positive ion current extracted was larger than the negative one, while at low temperatures and high fields, the negative ion current was greater than the positive one. Above about 1.4K, both the positive and negative ion currents extracted in a constant field (for fields $>$ 50 volts $cm^{-1}$) were independent of temperature, while below 1.4K a transition occurred.

to a temperature-dependent region where a decrease in temperature resulted in an increase in current. The temperature dependence is not fully understood, since the explanation of Gaeta is shown to be unsatisfactory and the suggestion of Cope and Gribbon on ion trapping by vortices is shown to be inadequate in accounting for all the results. A suggestion for the future is that measurement of the recombination coefficient of ions in the liquid at different fields and in the presence of vorticity might or might not confirm Cope and Gribbon's suggestion that vorticity can affect ionic recombination. It might also be useful to extend the constant field-temperature measurements to lower temperatures than were obtainable in the present apparatus, since the resulting form of the temperature dependence might shed some light on its origin.

An energy barrier was found to inhibit the passage of negative ions from the liquid into the vapour, in agreement with other workers, in particular Bruschi et al,and Schoepe and Probst. The latter authors have suggested that the energy barrier is present only in the superfluid state, but an argument is presented which makes the suggestion doubtful. There is little agreement among the various groups of workers on the magnitude and field dependence of the energy barrier, and a possible explanation of this is presented as a result of the observation of the present work that the magnitude of the energy barrier depends upon three parameters. These are;

(i) the potential applied to the grid (in a triode), or to the source (in a diode),

(ii) the position of the liquid surface between the grid,or the source, and the collector, and

(iii) the geometry of the ion cell.

Each ion cell used in the present work incorporated an electrode which was positioned so as to collect any ions which flowed via the Helium film. However, a large fraction of the negative ion current collected on this electrode has been shown to derive from transmission across the surface. The real negative ion film currents were very small, being slightly greater on a perspex substrate than on a glass one. No real positive ion film currents were detected. That the ions experience great difficulty in moving in the Helium film is interpreted as a result of the combination of the large image potential binding the ion to the substrate and the intrinsic roughness of the substrate.

As a consequence of the inability of negative ions to leak away via the Helium film, a layer of charge is thought to establish itself below the free surface as the temperature was reduced, such that the potential of the surface increased with falling temperature until it had adopted the potential of the grid or source. This generally caused the appearance of a large current across the surface due to dielectric breakdown in the vapour. There are no reports in the literature on the breakdown potential of gaseous Helium at temperatures below 4.2K and some preliminary measurements of this have been carried out in the present work. While the values of the breakdown voltages obtained are not very accurate, they do at least confirm Paschen's law within the experimental error. A more systematic study of the breakdown potential of Helium vapour at low temperatures would be useful.

At all temperatures it was found possible to detect what

appeared to be a current of positive ions crossing the liquid surface. This was completely unexpected since there have been no reports of such behaviour in the literature. However, the effect has been shown to be due to photoemission from the surface of the collecting electrode above the liquid surface caused by the uv radiation emitted by ionic recombination in front of an α-source immersed in the liquid.

## APPENDIX 1

The author is indebted to J. G. M. Armitage
for the following calculation

### The Derivation of Equation 5.(7)

Consider a diode cell immersed in liquid Helium consisting of a source of ions and a collector separated by a distance d on the x axis, the source and collector being located in the y,z plane. Let the potential on the collector be $V_o$ volts and its position be x = d, while the potential on the source is zero and its position is x = o.

If the current in the diode is J when the ionic mobility is $\mu$, then

$$J = n e \mu \frac{dV}{dx} , \qquad (1)$$

where n is the number density of ions of charge e. Poisson's equation is

$$\frac{d^2V}{dx^2} = - \frac{ne}{\varepsilon_o} . \qquad (2)$$

Eliminating n from equations (1) and (2) and solving for the potential V(x) yields

$$V = \pm \frac{\varepsilon_o \mu}{3J} \left[ A - \frac{2J}{\varepsilon_o \mu} x \right]^{3/2} + C , \qquad (3)$$

where A and C are the constants of the integration, and the positive sign is taken when dealing with negative ions, while the negative sign is taken with positive ions.

The assumption is then made that the current which is extracted from the source depends upon the square root of the field at the source. That is,

$$J = B \left(\frac{dV}{dx}\right)^{1/2}_{x=o} , \tag{4}$$

where B is some constant.

A further assumption is made concerning the low temperature current. That is, for a given field, there is a maximum current $J_o$ which can be extracted from the source at low temperatures. Also, in this low temperature limit, the space charge should be small due to high mobility, so it is expected,

$$\frac{dV}{dx} = \left(\frac{V_o}{d}\right)_{T \to 0} .$$

so that $$J_o = B \left(\frac{dV}{dx}\right)^{1/2}_{\substack{x=o \\ T \to 0}}$$

$$= B \left(\frac{V_o}{d}\right)^{1/2} \tag{5}$$

Eliminating the constant B from equations (4) and (5), yields

$$J = J_o \left(\frac{dV/dx}{Vo/d}\right)^{1/2} . \tag{6}$$

Equation (6) then becomes one of the boundary conditions on the solution (3). The other boundary conditions are that V = o at x = o, and that at V = $V_o$ at x = d. At x = o,

$$C = \frac{\varepsilon_o \mu}{3J} (A)^{3/2} .$$

Applying equation (6),

$$A = \left(\frac{J}{J_o}\right)^4 \left(\frac{V_o}{d}\right)^2 .$$

The final boundary condition then yields the final solution:

$$V_o = \pm \frac{\varepsilon_o \mu}{3J} \left(\frac{J}{J_o}\right)^6 \left(\frac{V_o}{d}\right)^2 \left[\left\{1 - \frac{2J}{\varepsilon_o \mu} \left(\frac{d}{V_o}\right)^2 \left(\frac{J_o}{J}\right)^4 d\right\}^{3/2} - 1\right] \quad (7)$$

In order to make this equation more tractable, the variables $\alpha$ and $\beta$ will be introduced, where

$$\alpha = -\frac{J}{\varepsilon_o \mu} d \left(\frac{d}{V_o}\right)^2 \left(\frac{J_o}{J}\right)^4 , \text{ and}$$

$$\beta = \left(\frac{J}{J_o}\right)^2 .$$

Equation (7) may now be written:

$$1 = \frac{\beta}{3\alpha} \left[(1 + 2\alpha)^{3/2} - 1\right] .$$

Solving for $\alpha$ yields the final variation of current J with mobility $\mu$ for a given cell dimension d and collector voltage $V_o$, assuming an experimentally determined value of $J_o$, this is,

$$-\frac{16d^3}{\varepsilon_o V_o^2} \cdot \frac{J}{\mu} = (9 - 12\beta^2) + \sqrt{81 - 216\beta^2 + 192\beta^3 - 48\beta^4} .$$

## APPENDIX 2

### The potential of an ion in a region of surface charge

Consider a disc of radius r and with uniform surface charge density $\sigma$. The total charge on the surface is then $\pi r^2 \sigma$. Now add a small element of area dS and with the same surface charge density to the outside of the disc. The potential of this system may then be written as

$$\frac{(\pi r^2 \sigma)\ (\sigma\, dS)}{4 \pi \varepsilon_o\, r} .$$

If now, more and more elements are added till the disc of charge has increased in radius to R then the total energy of the system of charges is U where

$$U = \int \frac{(\pi r^2 \sigma)\ (\sigma\, dS)}{4 \pi \varepsilon_o\, r}$$

$$= \int_0^{2\pi} \int_0^{R} \frac{(\pi r^2 \sigma) \cdot \sigma \cdot r\, d\theta\, dr}{4 \pi \varepsilon_o\, r}$$

Since the element of area $dS = r\, d\theta\, dr$.

So that $$U = \frac{\pi R^3 \sigma^2}{6 \varepsilon_o}$$

Now the surface charge density is given by

$$\sigma = \frac{Ne}{\pi R^2}$$

where N is the total number of charges present.

Thus the average energy per charge in the surface is

$$\frac{U}{N} = \bar{u} = \frac{R\sigma e}{6\varepsilon_o}$$

# APPENDIX 3

## Re-analysis of the data in chapter 7

It was noted in chapter 7 that the current $I_{c1}$ , collected on the "film" collector C1, below about 1.4K exhibited a temperature-dependent fall similar to that observed for the transmission current $I_{c2}$ . It was therefore assumed that a substantial fraction of $I_{c1}$ was derived from transmission through the liquid surface and was not in fact due to the passage of negative ions through the film. On this assumption, a new current I has been calculated from the relevant data, where

$$I = I_{c1} + I_{c2} ,$$

and has been found to display a temperature dependence below about 1.4K according to

$$I \propto e^{-\phi_E/kT} ,$$

where $\phi_E$ is the slope of the current versus reciprocal temperature curve corresponding to the applied field E. $\phi_E$ has previously been interpreted as the actual energy barrier which the negative ion must surmount in its excursion from the liquid into the vapour. It was discussed in section 6.4 that the measured values of $\phi_E$ should be related to the zero field value $\phi_o$ by the relation,

$$\phi_o = \phi_E + 2\sqrt{AeE'} , \qquad (1)$$

where E' is the electric field inside the liquid. At relatively high temperatures E' will be equal to the applied electric field E, and on both sides of the liquid surface the fields will be equal. At low temperatures however, where the current I has substantially fallen, E' will be almost zero, while the field in the vapour, $E_v$ ,

will have increased to $\frac{d_{gc}}{d_{lc}} \cdot E$ , where $d_{gc}$ and $d_{lc}$ are the distances from the grid (or source) to the collector C2 and from the liquid surface to the collector C2 respectively. On this basis, three values of $\phi_o$ have been calculated from each new measurement of $\phi_E$ using three different values for the electric field E' in the expression (1). These fields are:

1. The applied field E, relevant when there is no permanent distribution of charge below the free surface.
2. Half the applied field E. This was an attempt at a more realistic value of the field inside the liquid when the current I is a rapidly varying function of temperature, and the surface has adopted some new potential due to the formation of a layer of surface charge.
3. The field in the vapour $\frac{d_{gc}}{d_{lc}} \cdot E$ , at low temperatures when the surface has adopted the grid (or source) potential.

From the values of $\phi_o$ calculated in this way, the most consistent from cell to cell was found to be that which employed the field 2 above in the expression (1). These values of $\phi_o$ have been listed along with their corresponding values of $\phi_E$ and field E in the tables A to D for the glass triode 7.1(b), the glass diode 7.1(d), and for two positions of the liquid surface in the perspex triode 7.1(a). It should be pointed out that the addition of the current $I_{c1}$ to the transmission current $I_{c2}$ generally had the effect of reducing the value of the slope $\phi_E$.

It may be seen from the tables that in almost all cases the field dependence of the values of $\phi_E$ is only apparent at the higher fields, as was already noted in chapter 7 for those values of $\phi_E$ calculated from the transmission current $I_{c2}$ alone. It is interesting that a careful examination of the results of Schoepe and Probst, shown in figure 6.2, reveals that the slopes of their results corresponding

to the lowest two fields used by them, yield values which in no way substantiate the field dependence observed at the higher fields.

The remeasured values of $\phi_E$ display a dependence on liquid level between the grid and collector, as was observed in section 7.5 for those values of $\phi_E$ measured from $I_{c2}$ alone. This is shown for the two applied fields of 160 volts $cm^{-1}$ and 100 volts $cm^{-1}$ in the perspex triode in table E.

There would appear to be no significant difference between the results obtained in glass and in perspex-walled cells, although the statement made in section 7.8(e) that the observed energy barriers are only meaningful in the particular circumstances in which they were measured, would still appear to be correct. The conclusion to be drawn from the large variation in the values of $\phi_E$ therefore, must be that the method of measuring the temperature-dependence of the transmission current as a means of determining the zero field value of the energy barrier presented to an ion in the liquid by the surface is wholly unsatisfactory. In other words, the exponential fall in current is only indicative of an energy barrier and does not necessarily reflect its absolute magnitude.

In a recent paper, Schoepe and Rayfield (1971 - Z.Naturforsch, 26a,1392) have shown that experiments on the trapping times of negative ions held below the free surface provide the most accurate indication of the zero field barrier $\phi_o$ , and they have in fact remarked that it is not possible to determine the actual surface barrier from the temperature-dependence of the emission current.

Glass Triode 7.1(b)

| Applied Field E | Measured $\phi_E$ | $\phi_o = \phi_E + 2\sqrt{AeE/2}$ |
|---|---|---|
| 160 volts $cm^{-1}$ | 24 $\pm$ 2 K | 31 $\pm$ 2 K |
| 100 volts $cm^{-1}$ | 26 $\pm$ 2 K | 33 $\pm$ 2 K |
| 20 volts $cm^{-1}$ | 29 $\pm$ 2 K | 32 $\pm$ 2 K |

TABLE A

Glass Diode 7.1(d)

| Applied Field E | Measured $\phi_E$ | $\phi_o = \phi_E + 2\sqrt{AeE/2}$ |
|---|---|---|
| 160 volts $cm^{-1}$ | 23 $\pm$ 2 K | 32 $\pm$ 2 K |
| 130 volts $cm^{-1}$ | 24 $\pm$ 2 K | 32 $\pm$ 2 K |
| 100 volts $cm^{-1}$ | 26 $\pm$ 2 K | 33 $\pm$ 2 K |
| 70 volts $cm^{-1}$ | 21 $\pm$ 2 K | 27 $\pm$ 2 K |
| 50 volts $cm^{-1}$ | 20 $\pm$ 2 K | 25 $\pm$ 2 K |
| 20 volts $cm^{-1}$ | 19 $\pm$ 2 K | 22 $\pm$ 2 K |
| 10 volts $cm^{-1}$ | 21 $\pm$ 2 K | 23 $\pm$ 2 K |

TABLE B

Perspex Triode 7.1(a)

Liquid surface 4mm above grid and 11mm below collector C.2

| Applied Field E | Measured $\phi_E$ | $\phi_o = \phi_E + 2\sqrt{AeE/2}$ |
|---|---|---|
| 200 volts $cm^{-1}$ | 24 $\pm$ 2 K | 34 $\pm$ 2 K |
| 160 volts $cm^{-1}$ | 27 $\pm$ 2 K | 36 $\pm$ 2 K |
| 130 volts $cm^{-1}$ | 29 $\pm$ 2 K | 37 $\pm$ 2 K |
| 100 volts $cm^{-1}$ | 28 $\pm$ 2 K | 35 $\pm$ 2 K |
| 70 volts $cm^{-1}$ | 26 $\pm$ 2 K | 32 $\pm$ 2 K |
| 20 volts $cm^{-1}$ | 26 $\pm$ 2 K | 29 $\pm$ 2 K |

TABLE C

Perspex Triode 7.1(a)

Liquid surface 13mm above grid and 2mm below collector C.2

| Applied Field E | Measured $\phi_E$ | $\phi_o = \phi_E + 2\sqrt{AeE/2}$ |
|---|---|---|
| 160 volts $cm^{-1}$ | 22 $\pm$ 2 K | 31 $\pm$ 2 K |
| 100 volts $cm^{-1}$ | 24 $\pm$ 2 K | 31 $\pm$ 2 K |
| 70 volts $cm^{-1}$ | 29 $\pm$ 2 K | 35 $\pm$ 2 K |
| 50 volts $cm^{-1}$ | 21 $\pm$ 2 K | 26 $\pm$ 2 K |
| 10 volts $cm^{-1}$ | 23 $\pm$ 2 K | 25 $\pm$ 2 K |

TABLE D

Liquid level dependence of $\phi_E$ in Perspex Triode 7.1(a)

| E = 160 volts $cm^{-1}$ | |
|---|---|
| Height of liquid level above grid | Measured $\phi_E$ |
| 4 mm | 27 $\pm$ 2 K |
| 10 mm | 25 $\pm$ 2 K |
| 13 mm | 22 $\pm$ 2 K |

| E = 100 volts $cm^{-1}$ | |
|---|---|
| Height of liquid level above grid | Measured $\phi_E$ |
| 4 mm | 28 $\pm$ 2 K |
| 10 mm | 26 $\pm$ 2 K |
| 13 mm | 24 $\pm$ 2 K |

TABLE E

## REFERENCES


J. F. Allen and H. Jones, (1938) Nature, London, 141,243.

J. F. Allen and A. D. Misener, (1938) Nature, London, 141,75.

P. W. Anderson, (1966) Quantum Fluids (D. F. Brewer, Ed.) p. 146, (North Holland Publ. Co. Amsterdam).

K. R. Atkins, (1959) Phys. Rev. 116,1339.

K. R. Atkins, (1959) Liquid Helium, Cambridge University Press.

B. Bertman and T. A. Kitchens, (1968) Cryogenics 8,36.

A. Bianconi and B. Maraviglia (1969) J. Low Temp. Phys. 1,201.

L. Bruschi, B. Maraviglia and F. E. Moss (1966) Phys. Rev. Lett. 17,682.

L. Bruschi, B. Maraviglia and P. Mazzoldi (1966) Phys. Rev. 143,84.

G. Careri, U. Fasoli and F. S. Gaeta (1960) Nuovo Cimento 15,774.

G. Careri, S. Cunsolo and P. Mazzoldi (1961) Phys. Rev. Lett. 7,151.

G. Careri (1961) Prog. Low Temp. Phys. (C. J. Gorter, ed.) vol. 111 p. 58 (North Holland Pub. Co. Amsterdam).

M. W. Cole and M. H. Cohen (1969) Phys. Rev. Lett. 23,1238.

J. Cope and P. W. F. Gribbon (1970) J. Phys. (C) 3,472.

S. Cunsolo, G. Dall'Oglio, B. Maraviglia and M. V. Ricci (1968) Phys. Rev. Lett. 21,74.

S. Cunsolo (1961) Nuovo Cimento, 21,76.

J. G. Daunt and K. Mendelson (1939) Nature, London, 143,719.

R. J. Donnelly (1967) Experimental Superfluidity, (University of Chicago Press).

E. Fallou, J. Galland and B. Bouvier (1970) Cryogenics, 10,142.

R. P. Feynman (1954) Phys. Rev. 94,262.

R. P. Feynman (1955) Progress in Low Temp. Phys. (C. J. Gorter, ed.) Vol. 1 p. 17, (North Holland Publ. Co. Amsterdam).

R. P. Feynman and M. H. Cohen (1956) Phys. Rev. 102,1189.

F. S. Gaeta (1962) Nuovo Cimento, 26,1173.

A. N. Gerritsen (1948) Physica, 14,407.

E. F. Hammel, W. E. Keller and R. H. Sherman (1970) Phys. Rev. Lett. 24,712.

H. R. Harrison and B. E. Springett (1971) Phys. Lett. 35A,73.

F. L. Hereford and F. E. Moss (1966) Phys. Rev. 141,204.

M. C. Hetzler and D. Walton (1968) Rev. Sci. Instr. 39,1656.

K. Hiroike, N. R. Kestner, S. A. Rice and J. Jortner (1965) J. Chem. Phys. 43,2625.

G. Jaffé (1913) Ann. d. Physik, 42,303.

J. Jortner, N. R. Kestner, S. A. Rice and M. H. Cohen (1965) J. Chem. Phys. 43,2614.

P. L. Kapitza (1938) Nature, London, 141,74.

P. L. Kapitza (1941) J. Phys. USSR, 5,59.

W. H. Keesom and G. E. MacWood (1938) Physica, 5,737.

W. E. Keller (1969) Helium 3 and Helium 4, (Plenum Press, New York).

H. A. Kramers (1952) Physica, 18,665.

M. Kuchnir, P. R. Roach and J. B. Ketterson (1970) J. Low Temp. Phys. 3,183.

L. Landau (1941) J. Phys. USSR, 5,71.

L. Landau (1947) J. Phys. USSR, 11,91.

J. L. Levine and T. M. Saunders (1967) Phys. Rev. 154,138.

F. London (1938) Nature, London, 141,643.

H. London (1938) Nature, London, 142,612.

B. Maraviglia (1967) Phys. Lett. 25A,99.

L. Meyer and F. Reif (1958) Phys. Rev. 110,279.

L. Meyer and F. Reif (1960) Phys. Rev. 119,1164.

J. F. Olijhoek, W. M. Van Alphen, R. De Bruyn Ouboter and K. W. Taconis (1967) Physica, 35,483.

D. G. Onn and M. Silver (1971) Phys. Rev. A 3,1773.

L. Onsager (1949) Nuovo Cimento Suppl., 6,2249.

O. Penrose and L. Onsager (1956) Phys. Rev. 104,576.

G. W. Rayfield and F. Reif (1963) Phys. Rev. Lett. 11,305.

G. W. Rayfield and W. Schoepe (1971) Phys. Lett. 34A,133.

W. Schoepe and K. Dransfeld (1969) Phys. Lett. 29A,165.

W. Schoepe and C. Probst (1970) Phys. Lett 31A,490.

H. J. Seguin and R. W. Leonard (1966) Rev. Sci. Instr. 37,1743.

J. E. Simmons and R. B. Perkins (1961) Rev. Sci. Instr. 32,1173.

F. E. Simon (1950) Physica, 10,753.

W. T. Sommer (1964) Phys. Rev. Lett. 12,271.

F. A. Staas, K. W. Taconis and W. M. Van Alphen (1961) Physica, 27,893.

F. A. Staas and A. P. Severijns (1969) Cryogenics, 9422.

C. M. Surko and F. Reif (1968) Phys. Rev. 175,229.

P. M. Sutton (1960) Progress in Dielectrics, 2,113.

D. J. Tanner (1966) Phys. Rev. 152,121.

L. Tisza (1938) Nature, London, 141,913.

W. M. Van Alphen, G. J. Van Haasteren, R. De Bruyn Ouboter and K. W. Taconis (1966) Phys. Lett. 20,474.

W. Vermeer, W. M. Van Alphen, J. F. Olijhoek, K. W. Taconis and R. De Bruyn Ouboter (1965) Phys. Lett. 18,265.

J. Wilks (1967) Liquid and Solid Helium, Oxford University Press.

R. L. Williams (1957) Can. J. Phys. 35,134.

R. Williams, R. S. Crandall and A. H. Willis (1971) Phys. Rev. Lett. 26,7.

M. A. Woolf and G. W. Rayfield (1965) Phys. Rev. Lett. 15,235.